ISTANBUL TECHNICAL UNIVERSITY ★ GRADUATE SCHOOL OF SCIENCE ENGINEERING AND TECHNOLOGY

AN INVESTIGATION ON BEHAVIOR OF BURIED PIPELINES SUBJECTED TO TRANSVERSE PERMANENT GROUND DEFORMATION

M.Sc. THESIS

Hasan Emre DEMİRCİ

Department of Civil Engineering

Soil Mechanics and Geotechnical Engineering Programme

May 2014

ISTANBUL TECHNICAL UNIVERSITY ★ GRADUATE SCHOOL OF SCIENCE ENGINEERING AND TECHNOLOGY

AN INVESTIGATION ON BEHAVIOR OF BURIED PIPELINES SUBJECTED TO TRANSVERSE PERMANENT GROUND DEFORMATION

M.Sc. THESIS

Hasan Emre DEMİRCİ
(501111305)

Department of Civil Engineering

Soil Mechanics and Geotechnical Engineering Programme

Thesis Advisor: Doç. Dr. Musaffa Ayşen LAV

May 2014

İSTANBUL TEKNİK ÜNİVERSİTESİ ★ FEN BİLİMLERİ ENSTİTÜSÜ

YANAL KALICI ZEMİN DEFORMASYONLARINA MARUZ GÖMÜLÜ BORULARIN DAVRANIŞLARI ÜZERİNE BİR İNCELEME

YÜKSEK LİSANS TEZİ

Hasan Emre DEMİRCİ
(501111305)

İnşaat Mühendisliği Anabilim Dalı

Zemin Mekaniği ve Geoteknik Mühendisliği Programı

Tez Danışmanı: Doç. Dr. Musaffa Ayşen LAV

Mayıs 2014

Hasan Emre Demirci, a **M.Sc.** student of ITU **Institute of / Graduate School of.....** student ID **501111305**, successfully defended the **thesis/dissertation** entitled "**AN INVESTIGATION ON BEHAVIOR OF BURIED PIPELINES SUBJECTED TO TRANSVERSE PERMANENT GROUND DEFORMATION**", which he prepared after fulfilling the requirements specified in the associated legislations, before the jury whose signatures are below.

Thesis Advisor :	**Doç. Dr. Musaffa Ayşen LAV** İstanbul Technical University	.....
Jury Members :	**Doç. Dr. Abdullah GEDİKLİ** İstanbul Technical University	.....
	Doç. Dr. Ayşe EDİNÇLİLER Boğaziçi University	.....

Date of Submission : 2 May 2014
Date of Defense : 28 May 2014

To my family,

FOREWORD

I would like to express my great gratitude and sincere thanks to my thesis advisor Assoc. Prof. Dr. Musaffa Ayşen LAV, for her continued inspiration, support and invaluable guidance during my study.
I thank the members of thesis defense committee Assoc. Prof. Dr. Abdullah GEDIKLI and Assoc. Prof. Dr. Ayşe EDINCLILER for their assistance in reviewing and editing my manuscript. I also would like to thank to my research assistant colleagues Mustafa KARAMAN and Paulina BAKUNOWICZ for dedicated support during my thesis study.
My special thanks go to Assoc. Prof. Dr. Kutlu DARILMAZ for his inspiring discussions and comments about finite element model.
I am grateful to my family for their support and endless encouragement. Lastly, my gratitude also due to my special friend Magdalena KOLODZIEJ, whose continuous support helped me to finish this thesis. Thanks to all.

May 2014

Hasan Emre DEMİRCİ
Reseach Assistant

TABLE OF CONTENTS

Page

ABBREVIATIONS

PGD	**:** Permanent Ground Deformation
δ	**:** Amount of PGD Movement
δ_{cr}	**:** Critical Displacement
W	**:** Width of PGD Zone
L	**:** Longitudinal Length of the PGD Zone
a_c	**:** Critical Acceleration
δ_{SL}	**:** Newmark Displacement
I_a	**:** Arias Intensity
M	**:** Earthquake Magnitude
δ_f	**:** Fault displacement
L_a	**:** Anchor Length
K_1	**:** Lateral Soil Coefficient
P_{uplift}	**:** The Uplift Force per Unit Length
LSI	**:** Liquefaction Severity Index
FEM	**:** Finite Element Method
R_f	**:** Reduction Factor
W_{cr}	**:** Critical width of liquefied soil

LIST OF TABLES

Page

LIST OF FIGURES

Page

AN INVESTIGATION ON BEHAVIOR OF BURIED PIPELINES SUBJECTED TO TRANSVERSE PERMANENT GROUND DEFORMATION

SUMMARY

The past eartquakes showed that the pipelines are threatened by permanent ground deformation. A lot of significant damages occurred in pipelines due to the permanent ground deformation (PGD) caused by earthquakes. To predict behavior of pipeline subjected to external loading caused by earthquake induced PGD is essential in design to reduce the risk of accident, injury and material loss. Finite element method is one of the useful methods to predict behavior of pipeline subjected to PGD.

In this study, the behavior of pipeline subjected to transverse PGD is investigated parametrically for various wall thickness, diameter and steel type of pipe, type and width of PGD zone, the amount of PGD, PGD patterns, angle of friction angle of backfill and burial depth of pipe using ABAQUS. Beam elements were used to model pipe. The pipe-soil interaction was modeled by axial and lateral connector elements which have nonlinear behavior. Transverse PGD is applied to end point of connector elements in PGD zone. Spatially distributed PGD was calculated by using the equation proposed by O'Rourke (1989).

Maximum and minimum bending moments of pipe and maximum pipe displacements were obtained from finite element element analyses results. The variation of pipe moments and pipe displacements depending on pipe diameter, the wall thickness of pipe, steel type, type and width of PGD zone, the amount of PGD, the angle of friction of backfill and burial depth of pipe were observed.

It is concluded that the thinner wall correspond to the more flexible pipe behavior. The more rigid pipe displace less than more flexible one. However, bending moments increase with increased pipe rigidity. The width of PGD zone significantly influences the behavior of pipeline subjected to transverse PGD. The pipe behaves like a stiff pipe for narrow PGD zone. On the other hand, the pipe behaves like a flexible pipe for large PGD zone. PGD patterns which can be divided into two groups such as spatially distributed and localized abrupt PGD have a significant effects on pipe behavior. The maximum and minimum pipe moment occurs at the center and margins of PGD zone for spatially distributed PGD. On the other hand, the pipe moments at the center and margins of PGD zone are nearly zero for localized abrupt PGD.

YANAL KALICI ZEMİN DEFORMASYONLARINA MARUZ GÖMÜLÜ BORULARIN DAVRANIŞLARI ÜZERİNE BİR İNCELEME

ÖZET

Türkiye, Asya ile Avrupa arasında bir geçit konumunda bulunmasından ötürü birçok doğalgaz boru hattını üzerinde bulundurmaktadır. Aynı zamanda Türkiye depremsellik açısından çok riskli bir bölgede yer almaktadır. Bu iki koşulun aynı zamanda mevcut olmasından dolayı doğalgaz boru hatlarının güvenliğinin sağlanması önem arz etmektedir. Geçmiş depremler boru hatlarının kalıcı zemin hareketleri tarafından tehdit altında bulunduğunu göstermiştir. Depremler sonucunda oluşan kalıcı zemin deformasyonları nedeniyle boru hatlarında önemli birçok hasar oluşmuştur. Maddi ve yaşamsal kaza riskini azaltmak amacıyla deprem nedeniyle oluşan kalıcı zemin deformasyonlarına maruz gömülü boru hatlarının davranışlarının incelenmesi gerekmektedir. Sonlu elemanlar yöntemi kalıcı zemin deformasyonlarına maruz boruların davranışını incelemek için yararlı olan yöntemlerden biridir.

O'Rourke ve Tawfik (1983), 1971 yılında meydana gelen San Fernando depreminde oluşan yanal kalıcı zemin deformasyonlarını incelemişlerdir. Hamada ve O'Rourke (1992), 1964 yılında meydana gelen Niigata depreminde oluşan yanal kalıcı zemin deformasyonlarını incelemişlerdir. Yapılan bu çalışmalar sonucunda iki tip yanal kalıcı zemin deformasyonuna rastlanmış olup, gözlenen bu yanal kalıcı zemin deformasyonları dağılı yayılı kalıcı zemin deformasyonu ve bölgesel ani kalıcı zemin deformasyonu olarak sınıflandırılmışlardır. Dağılı yayılı kalıcı zemin deformasyonları sıvılaşmaya bağlı oluşan kalıcı zemin deformasyonu durumlarında, bölgesel ani kalıcı zemin deformasyonları ise toprak kayması durumlarında gözlemlenmektedir.

O'Rourke (1988), Suzuki ve diğerleri (1988), Kobayashi ve diğerleri (1989), O'Rourke (1989) dağılı yayılı kalıcı zemin deformasyonlarını modelleyebilmek amacıyla farklı bağıntılar önermişlerdir. Önerilen bu bağıntılarda maksimum kalıcı zemin deformasyonu, kalıcı zemin deformasyonu bölgesinin merkezinde oluşmaktadır. Kalıcı zemin deformasyonu bölgesinin sınırlarında ise kalıcı zemin deformasyonu değerleri sıfırdır.

Bu çalışmada yanal kalıcı zemin deformasyonlarına maruz boru hatlarının davranışı, farklı boru et kalınlığı, çelik boru tipi, boru çapı, kalıcı zemin deformasyonu tipi ve genişliği, kalıcı zemin deformasyonu miktarı, boruyu çevreleyen zeminin içsel sürtünme açısı, borunun gömülü derinliği için parametrik olarak ABAQUS programı yardımıyla incelenmiştir.

Sonlu elemanlar modellerinde boru et kalınlığının, yanal kalıcı zemin deformasyonlarına maruz gömülü boru davranışına etkisinin incelenebilmesi için diğer parametreler sabit tutularak boru et kalınlığı 0.002m-0.008m arasında değişen değerlerden seçilmiştir.

Boru çapının yanal kalıcı zemin deformasyonuna maruz gömülü boru davranışına etkisinin incelenebilmesi için diğer tüm parametreler sabit tutulmuş, boru çapı 0.5m-1.0m arasında değerlerden seçilmiştir.

Boruyu çevreleyen zeminin kayma mukavemeti açısının kalıcı zemin deformasyonlarına maruz gömülü boru davranışına etkisini inceleyebilmek açısından zemin kayma mukavemeti açısı sırasıyla 25^0, 30^0 ve 35^0 olarak seçilmiştir.

Gömülü boru derinlikleri sonlu elemanlar modellerinde 0.6m, 0.8m, 1.0m ve 1.2 m olarak seçilmiş olup, farklı gömülü derinliklerdeki gömülü boruların yanal kalıcı zemin deformasyonları altındaki davranışı incelenmiştir.

Maksimum yanal kalıcı zemin deplasmanı değerleri 1.3m, 3.0m ve 5.0m olarak seçilmiş olup, farklı zemin deformasyonları altında gömülü boru davranışı incelenmiştir.

Yanal kalıcı zemin deformasyonu bölgesi genişliği 10m, 30m ve 50m olarak sonlu elemanlar modellerinde dikkate alınmıştır. Farklı yanal kalıcı zemin deformasyonu değerleri için yanal kalıcı zemin deformasyonlarına maruz gömülü boru davranışı incelenmiştir.

Boru çelik sınıfının, yanal kalıcı zemin deformasyonlarına maruz gömülü boruların davranışına etkisini inceleyebilmek açısından sonlu elemanlar modellerinde dört farklı çelik tipi kullanılmıştır. Bu çelik boru tipleri X-42, X-52, X-60 ve X-70 tipi çelik borulardır.

Literatürde yanal kalıcı zemin deformasyonlarına maruz gömülü borular ve bu gömülü boruların kendisini çevreleyen zeminle olan etkileşimi farklı sonlu elemanlar modelleri kullanılarak modellenmiştir. Liu ve O'Rourke (1997b), Liu ve O'Rourke (1999), O'Rourke ve diğerleri (2003) gömülü boruyu kiriş elemanı olarak, gömülü boru ile boru etrafındaki zeminin etkileşimini ise eksenel ve yanal nonlineer yay elemanlarını kullanarak modellemişlerdir. Takada ve diğerleri (2001), Yoshizaki ve Oguchi (1996), Yoshizaki ve diğerleri (2001), Yoshizaki ve Sakanoue (2004), Karamitros ve diğerleri (2007) boru hattını hibrid model (kiriş+kabuk elemanı) kullanarak, boru ile zemin arasındaki etkileşimi ise nonlineer zemin yaylarını kullanarak modellemişlerdir. Lee (2010), Vazouras ve diğerleri (2010, 2012), Jafarzadeh ve diğerleri (2012), gömülü boruları kabuk elemanı ile boruyu çevreleyen zemini ise katı sürekli ortam ile modellemişlerdir. Zemin davranışını modelleyebilmek için Mohr-Coulomb modelini kullanmışlardır. Boru ile zemin arasındaki etkileşimi teğetsel ve normal temaslarla modellemişlerdir.

Literatürde yapılan çalışmalar incelendiğinde boru elemanın kiriş elemanı, kabuk elemanı ve kiriş ve kabuk elemanının birlikte kullanılması (hibrid model) ile modellenebildiği görülmektedir. Bu çalışma kapsamında boruyu modelleyebilmek için kiriş elemanı kullanılmıştır. Gömülü boru ile boruyu çevreleyen zemin arasındaki etkileşim nonlineer yayların davranışını temsil eden bağlantı elemanları kullanılarak modellenmiştir.

Ramberg ve Osgood (1943) farklı çelik sınıfları için akma sonrası gerilme şekil değiştirme davranışının tanımlanması için bir model önermişlerdir. Bu çalışma kapsamında, çelik boruların akma sonrası davranışı Ramberg-Osgood bağıntısı kullanılarak modellenmiştir. Sonlu eleman modellerinde X-42, X-52, X-60 ve X-70 tipi çelik boru kullanılmıştır.

Literatürde yapılan çalışmalar incelendiğinde gömülü boru ile zemin arasındaki etkileşimin nonlineer yay elemanları ile modellendiği görülmektedir. Bu çalışma kapsamında, boru ve zemin arasındaki etkileşim nonlineer davranışa sahip eksenel ve yanal bağlantı elemanları kullanılarak modellenmiştir. Bağlantı elemanlarının nonlineer davranışının modellenebilmesi için gerekli olan parametreler; maksimum zemin direnci ve maksimum elastik deformasyondur. Bu parametreler ALA (2001)'de önerilen bağıntılar yardımıyla hesaplanmıştır.

Yanal kalıcı zemin deformasyonu, bağlantı elemanlarının uç noktalarına kalıcı zemin deformasyonu bölgesi içinde uygulanmıştır. Yanal yayılı kalıcı zemin deformasyonu dağılımı O'Rourke'nin (1989) önerdiği bağıntı kullanılarak hesaplanmıştır.

Sonlu elemanlar modelinin ankraj noktaları, kalıcı zemin deformasyonu bölgesi sınırlarından 400m ötede seçilmiştir. Ankraj noktaları, eksenel ve eğilme deformasyonlarının sıfıra çok yakın olduğu noktalarda seçilmektedir. 400m'lik bir ankraj mesafesinin sonlu elemanlar modelinin sınır koşullarından etkilenmemesi için yeterli olduğu literatür çalışmalarında görülmektedir. Bağlantı elemanlarının uç noktaları kalıcı zemin deformasyonu bölgesi içinde yassym, kalıcı zemin deformasyonu bölgesi dışında ise ankastre olarak modellenmiştir.

Parça elemanlarının boyutunun seçilmesi sonlu elemanlar analizlerinin gerçeğe yakın sonuçlar verebilmesi açısından büyük önem arzetmektedir. Parça elemanların sayısı arttıkça analiz sonuçları gerçeğe yakın değerlerde olacaktır. Parça elemanlarının sayısının artması aynı zamanda analiz süresini de arttıracaktır. Hem analiz süresinin kısaltılması hem de analiz sonuçlarının yeterli hassaslıkta elde edilebilmesi için optimum bir parça sayısının belirlenmesi gerekmektedir. Optimum parça sayısının seçilmesi için herhangi bir standart bulunmamaktadır. Bu nedenle optimum parça eleman sayısının seçilmesi için ön bir çalışma yapılması gerekmektedir. Bu çalışma kapsamında sonlu elemanlar analizlerinden önce optimum parça sayısının belirlenebilmesi için çalışmalar yapılmıştır. Bu çalışmalar sonucunda optimum parça sayısı belirlenmiş olup, sonlu elemanlar analizlerinde bu parça sayıları kullanılmıştır.

Maksimum ve minimum boru eğilme momenti ve maksimum boru deplasmanları sonlu elemanlar analizleri sonucunda elde edilmiştir. Maksimum ve minimum boru momentlerinin ve maksimum boru deplasmanlarının boru çapına, boru et kalınlığına, çelik boru tipine, kalıcı zemin deformasyonu tipi ve genişliğine, kalıcı zemin deformasyonu miktarına, dolgu malzemesinin içsel sürtünme açısına ve boru gömülü derinliğine bağlı olarak değişimi gözlemlenmiştir. Ayrıca farklı kalıcı zemin deformasyonu bölgesi genişlikleri için boruda oluşan deplasman dağılımları elde edilmiş ve kullanılan kalıcı zemin deplasmanı dağılımı ile boruda oluşan deplasman dağılımları karşılaştırılmıştır.

İnce et kalınlığına sahip boruların daha esnek bir davranışa sahip olduğu sonucu çıkarılmıştır. Rijit borular esnek borulara göre daha az deplasman yapmaktadırlar. Boru rijitliği arttıkça borudaki eğilme momentleri de artmaktadır. Kalıcı zemin deformasyonu bölgesinin genişliği yanal kalıcı zemin deformasyonuna maruz boru davranışını önemli bir şekilde etkilemektedir. Boru dar kalıcı zemin deformasyonu bölgelerinde rijit boru gibi davranmaktadır. Diğer yandan, boru geniş kalıcı zemin deformasyonu bölgelerinde ise esnek boru gibi davranmaktadır. Kalıcı zemin deformasyonu modelleri bölgesel ani kalıcı zemin deformasyonu ve yayılı dağılı zemin deformasyonu olarak ikiye ayrılmaktadır ve boru davranışı üzerinde önemli bir etkiye sahip oldukları görülmektedir. Yayılı dağılı zemin deformasyonu modelinde maksimum ve minimum boru momentleri kalıcı zemin deformasyonu

merkezinde ve sınırlarında oluşmaktadır. Diğer yandan, bölgesel ani kalıcı zemin deformasyonu modelinde ise kalıcı zemin deformasyonu merkezinde ve sınırlarında boru momentleri neredeyse sıfırdır.

1. INTRODUCTION

Pipelines are reliable means that convey water, gas, sewage and other fluids. Because of these missions of pipelines, they have big importance on businesses, economies and life quality of people. Providing protection of pipelines against permanent ground deformation effects caused by earthquake is a significant subject. Especially the performance of gas and oil pipelines requires particular attention due to increasing demand for energy. There is substantial pipeline damage in past major earthquakes, such as 1906 San Fransisco Earthquake, 1933 Long Beach Earthquake, 1952 and 1954 Kern County Earthquakes, 1964 Nigata, 1971 San Fernando, 1979 Imperial Valley Earthquake, 1989 Loma Prieta Earthquake, 1994 Northridge Earthquake, 1999 Duzce Earthquake and 1999 Chi Chi Earthquake. (O'Rourke and Lane, 1989; O'Rourke and Palmer, 1996; Tang, 2000). These earthquakes demonstrated that the permanent ground deformation (PGD) caused by earthquakes generated significant damages on buried pipelines. When the route of pipelines passes through an area where permanent ground deformantion occurred before it is expected that the pipelines will be subjected to high soil loads because of the relative movement between soil and pipeline. It can be sometimes inevitable that must be routed through such vulnerable areas.

The principle form of permanent ground deformation caused by earthquake are observed as landsliding, surface faulting, lateral spreading and seismic settlement. Transverse permanent ground deformation includes landsliding and lateral spreading. O'Rourke and Tawfik (1983), Hamada and O'Rourke (1992) observe two types of transverse PGD as spatially distributed transverse PGD and abrupt transverse PGD. Abrupt transverse PGD generally occurs in landslide cases whereas spatially distributed transverse PGD generally occurs in liquefaction cases.

As Turkey is located on a seismically very active region, natural gas distribution networks all over the country can be under the risk of damage due to permanent ground deformations (PGD) during earthquakes. To predict behavior of pipeline subjected to external loading caused by earthquake induced PGD is essential in

design to reduce the risk of accident, injury and material loss. Finite element method is one of the very useful methods to predict behavior of pipeline subjected to PGD. It is not sufficient to only take into account nonlinear behavior of soil for soil structure interaction problems. While investigating of behavior of pipeline subjected to permanent ground deformation the nonlinear behavior of pipe which has an interaction with soil need to be modeled. Because of these reasons, ABAQUS finite element analysis software was chosen in order to determine response of pipelines subjected to transverse permanent ground deformation. ABAQUS enables to have an accurate calculation by regarding the nonlinearity of materials, geometry and boundaries.

1.1 Purpose of Thesis

The aim of this study is to determine behavior of pipeline subjected to permanent transverse ground deformations. For this aim, the behavior of pipeline subjected to transverse PGD is investigated parametrically for various wall thickness, diameter and steel type of pipe, the amount of permanent ground deformation, angle of internal friction of backfill, type and width of PGD zone using ABAQUS finite element software.

1.2 Organization of Thesis

The thesis includes eight chapters. The contents of each chapter are summarized as follows:

Chapter 2 presents an overview about type of permanent ground deformation caused by earthquake. In this chapter, the calculation of amount of permanent ground deformation for different type of permanent ground deformation was submitted. Furthermore, the effects of permanent ground deformation on buried pipelines are described.

Chapter 3 gives detailed description about response of continuous pipelines to transverse permanent ground deformation. The literature review of finite element methods and finite element models for pipeline buried in non-liquefied soil and pipeline buried in liquefied soil are mentioned in this chapter.

Chapter 4 describes soil-pipe interaction for the pipeline located in non-liquefied soil and the pipeline in liquefied soil, pipe failure modes and pipe failure criterion. Soil-

pipe interaction includes axial soil springs, lateral soil springs and tranverse vertical soil springs. Pipe failure modes involves tensile failure, local buckling and beam buckling. The failure criterion for pipe is described in this chapter.

Chapter 5 includes the procedure for finite element method. The finite element procedure used in ABAQUS is summarized.

Chapter 6 includes finite element analyses of buried pipelines subjected to transverse permanent ground deformation. The literature review for finite element model for pipe and pipe-soil interaction are mentioned. The finite element model for pipe and and pipe-soil interaction are described in this chapter.

Chapter 7 involves analysis results. In this chapter, effects of wall thickness of pipe, pipe diameter, ground displacement, width of PGD zone, angle of internal friction of backfill soil, burial depth of pipe on behavior of pipeline subjected to transverse PGD are investigated. Pipe and ground displacement for different width of PGD zone is obtained in this chapter.

Chapter 8 involves the final conclusions of analysis results.

2. PERMANENT GROUND DEFORMATION CAUSED BY EARTHQUAKE

According to O'Rourke and Liu (1999), the principal type of permanent ground deformation caused by earthquake are landsliding, surface faulting, lateral spreading due to soil liquefaction and seismic settlement. In this section, the situations mentioned above will be defined respectively and the effects of these situations on pipelines will be discussed. The effects of permanent ground deformation on buried pipelines can be investigated by predicting the amount of permanent ground deformation. There are certain empirical relations in order to predict the amount of permanent ground deformation caused by earthquakes. These empirical relations will be mentioned for surface faulting, landsliding and lateral spreading respectively.

2.1 Liquefaction Induced Lateral Spreading

One of the major reasons of devastation during an earthquake is the failure of the ground structure. According to Prakash (1981) the ground may fail due to fissures, abnormal or unequal movements, or loss of strength. The loss of strength in sandy soils may occur when the pore water pressure increases. Because the pore water pressure increases, the interaction between soil grains reduces depending on the decrease in effective stress. The decrease in effective stress causes a reduction in the shear strength. Soil that has lost all shear strength behaves like a viscous fluid. This phenomenon termed as liquefaction and can occur in loose and saturated sands. Liquefaction is most commonly observed near rivers, bays, and other bodies of water (Kramer, 1996).

Liquefaction phenomena can be divided into two main groups: flow liquefaction and cyclic mobility (Kramer, 1996). Flow liquefaction takes place less frequently than cyclic mobility in the field but its effects generally have much more violence. Cyclic mobility can occur under a broader range of soil and site conditions than flow liquefaction on the other hand its effects are generally less severe (Kramer, 1996).

Lateral spread is the most permeative type of ground failure caused by liquefaction. Lateral spreads occur when a loose saturated sandy soil deposit is liquefied because of seismic loading at gentle sloping area. The range of amount of lateral displacement typically can change from a few centimeters to several meters. Lateral spreading can cause significant damage to engineering structures and lifelines (Bartlett and Youd, 1995).

O'Rourke and Pease (1995) illustrate how buried pipelines are affected by settlement caused by post liquefaction consolidation (Fig. 2.1b) and by lateral shear strains (Fig. 2.1c and d).

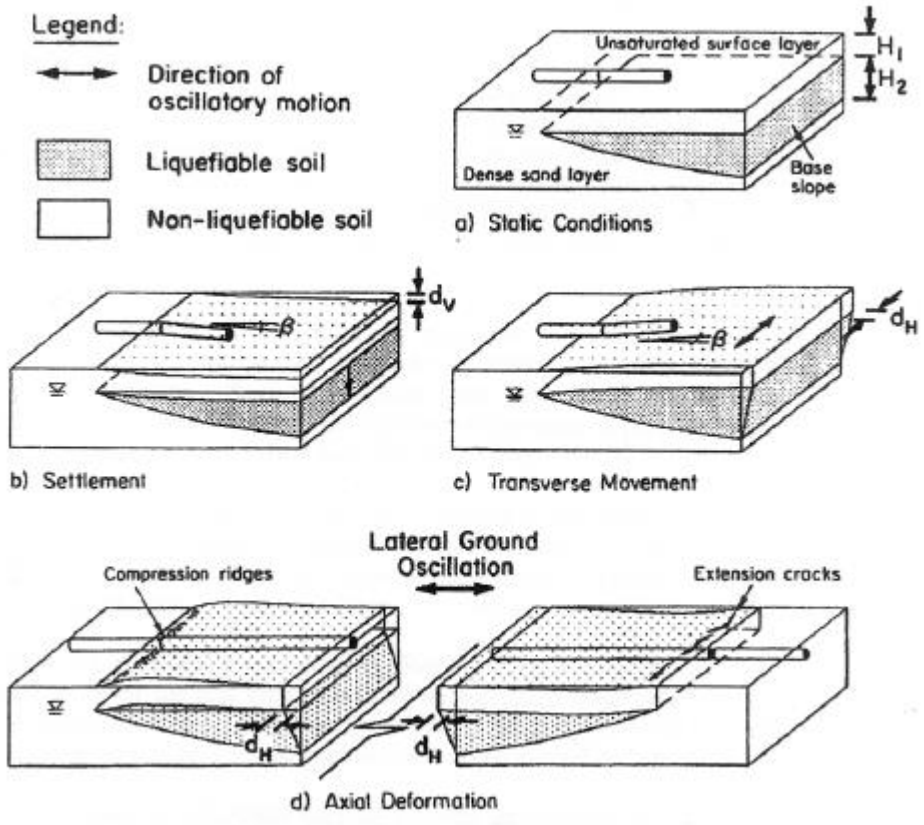

Figure 2.1: Schematic of buried pipeline response to transient displacement at liquefaction site (O'Rourke and Pease, 1995).

Liu and O'Rourke (1999) suggest that characteristics of a lateral spread which affect pipeline response in a horizontal plane are the amount of PGD movement (δ), the transverse width of the PGD zone (W), the longitudinal length of the PGD zone (L), and the pattern or distribution of ground movement across and along the zone. These geometric characteristics of a lateral spread are shown in Figure 2.2. It is so important to predict the amount of permanent ground displacements (δ) associated

with the liquefaction. If the permanent displacement can be predicted, the effects of permanent ground displacement on engineering structures especially pipelines can be estimated. Hamada et al. (1986) proposed an empirical formulation by using horizontal ground displacement vector maps for many locales damaged by lateral spread in the cities of Niigata and Noshiro, Japan during the 1964 Niigata and 1983 Nihonkai-Chubu earthquakes, respectively.

$$D_H = 0.75\sqrt{H_{liq.}} \times \sqrt[3]{\theta} \qquad \textbf{(2.1)}$$

where D_H = horizontal ground displacement in meters; θ=either the gradient of the surface topography or slope of the base of the liquefied layer, whichever is largest, in percent; and $H_{liq.}$= thickness of the liquefied layer in meters.

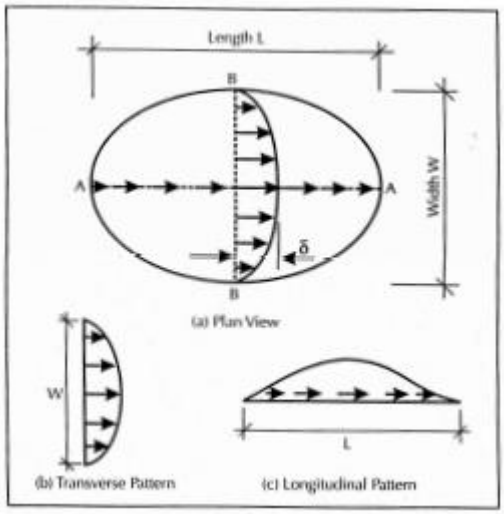

Figure 2.2: Characteristic of lateral spread (Liu and O'Rourke, 1999).

Youd and Perkins (1987) presented an idea of Liquefaction Severity Index (LSI) in order to predict possible ground deformation at a given site. Youd and Perkins obtained a correlation in order to find LSI in terms of earthquake magnitude and distance for the western U.S earthquakes. The correlation is introduced as follows:

$$\log LSI = -3.49 - 1.86 \log R_d + 0.98 M_w \qquad \textbf{(2.2)}$$

Barlett and Youd (1992) found two empirical relations in order to predict the expected amount of PGD due to liquefaction for lateral spreads down gentle ground slopes and lateral spreads at a free face.

The relation for lateral spreads down gentle ground slopes is:

$$\log(\delta+0.01)=-15.787+1.178M-0.927\log R_d-0.013R_d +0.429\log S+0.348\log T_{15}+4.527\log(100-F_{15})-0.922D_{50_{15}} \quad \textbf{(2.3)}$$

The relation for lateral spreads at a free face is:

$$\log(\delta+0.01)=-15.787+1.178M-0.927\log R_d +0.429\log Y+0.348\log T_{15}+4.527\log(100-F_{15})-0.922D_{50_{15}} \quad \textbf{(2.4)}$$

where δ is the permanent horizontal displacement of ground (m), M is the earthquake magnitude, R_d is the epicentral distance (km), S is the ground slopes, Y is the free face ratio, F_{15} is the average fines contents in T_{15} (%), $D_{50_{15}}$ is the mean grain size in T_{15} (mm) and T_{15} is the thickness of saturated cohesionless soils with a corrected SPT value less than 15, (m).

S (ground slopes) and Y (free face ratio) are explained in Figure 2.3.

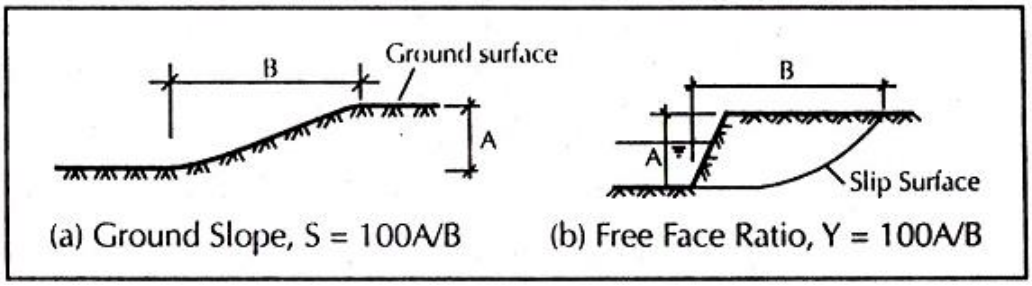

Figure 2.3: Elevation view showing ground slope and free face ratio (O'Rourke and Liu, 1999).

The width and the length of the PGD zone also significantly affect pipe response to PGD. However, there is limited available information about the width and the length of lateral spread zone.

Suzuki and Masuda (1991) presented a relation between the amount of PGD movement and the width of PGD zone for PGD away from a free face by combining 1964 Niigata and 1983 Nihonkai-Chubu earthquakes data. The relation between the amount of PGD movement and the width of PGD zone is given in Figure 2.4.

Barlett and Youd (1992) obtained useful information about the length of the lateral spread zone at a free face. The observed data on the amount of PGD and the length of the lateral spread zone at a free face is shown in Figure 2.5.

It can be concluded that the ground movement decreases while the length of lateral spread zone for free face situation increases. With the aid of Figure 2.4, it can be

observed that the ground displacement is an increasing function of the width of the lateral spread zone for gently sloping ground situations.

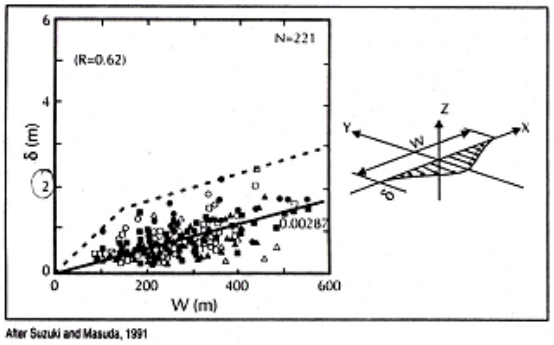

Figure 2.4: Observed data on the amount of PGD and the width of the lateral spread zone away (Suzuki and Masuda, 1991).

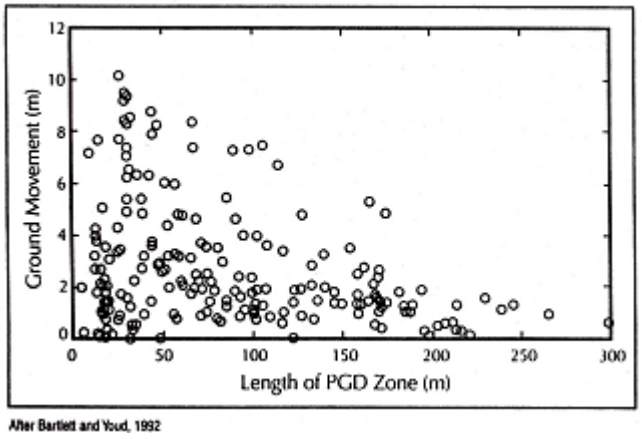

Figure 2.5: Observed data on the amount of PGD and the length of the lateral spread zone at a free face

The variation of permanent ground deformation along the length and across the width of the lateral spread zone influences the response of buried pipelines subjected to PGD. Different PGD pattern for transverse PGD will be discussed in Chapter 3 in detail.

2.2 Landslides

A landslide is a ground movement which involves rockfalls, deep failure of slopes and shallow debris flows which occur in offshore, coastal and onshore environments.

According to Keefer (1984), weakly cemented rocks, residual and colluvial sand, volcanic soils containing sensitive clay, loess, cemented soils, granular alluvium, granular deltaic deposits, more-indurated rocks with prominent or pervasive

discontinuities and granular man-made fill are most susceptible to earthquake-induced landslides.

Varnes (1978) proposed a number of procedures for classification of landslides according to material type (soil or rock), character of movement (disrupted or coherent), and other attributes, such as velocity, water content and depth. According to Keefer (1984), material is classified as rock or soil on the basis of its state prior to landslide initiation. Rock signifies firm intact bedrock. Soil signifies a loose, unconsolidated or poorly cemented aggregate of particles, which may or may not contain organic material. Keefer (1984) divided earthquake induced landslides into three categories as disrupted slides, lateral spreads and flows.

Meyersohn (1991) categorized landslide as slides, rock falls and topples, spread and slump flow based on the types of material involved, soil movements and geometry of soil movement. Landslide can produce different effects on the pipeline depending on the type of landslide. Aboveground pipelines can be damaged by direct impact of falling rocks because of rock fall and rock topple. Rock fall and rock topple have relatively little effect on buried pipelines. The buried pipelines can be adversely affected by earth slump and earth slide.

Pipelines often are threatened by impact and displacement from landslides. Landslides that can affect vary widely in type and in size (Baum et al., 2008). O'Rourke (1998) illustrated principal effects of landslides on buried pipelines according to their orientation (Fig. 2.6).

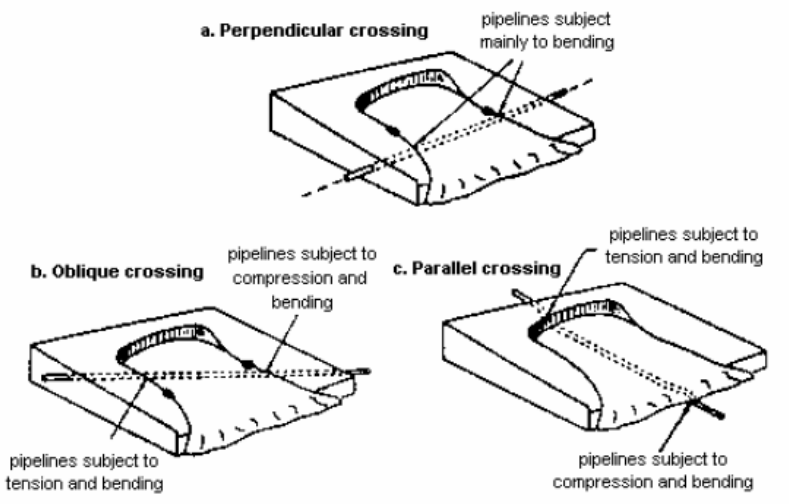

Figure 2.6: Principal effects of landslides on pipelines according to their orientation (O'Rourke, 1998).

As shown Fig. 2.6, the orientation of pipelines with respect to landslides direction is important with regards to determining pipeline strain. In cases where pipelines are placed perpendicular to landslides, pipelines are subjected mainly to bending. Other cases such as oblique crossing and parallel crossing, pipelines are subjected to compression, tension and also bending.

Newmark (1965) proposed a method in order to predict the slope displacements caused by earthquakes. Newmark (1965) produced this method by simulating potential shear failure block to the block resting on an inclined plane (Figure 2.7). According to Newmark (1965), every slope has a critical acceleration that the slope displacements occur when it is exceeded. The critical acceleration can be defined as:

$$a_c = g(FS - 1)\sin\alpha \qquad \textbf{(2.5)}$$

where g is gravitational acceleration, FS is static safety factor, and α is inclination angle of slope.

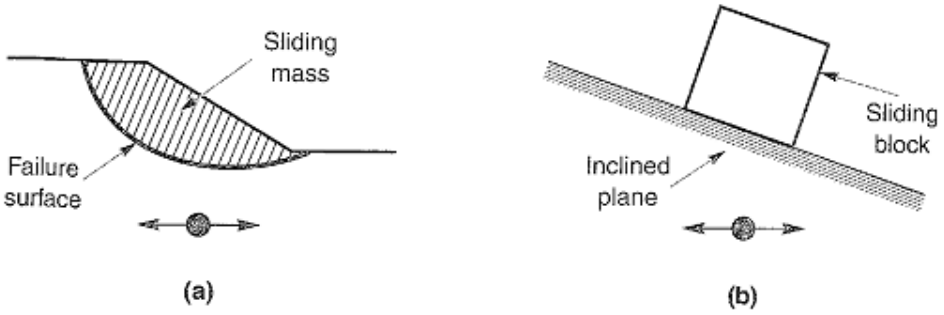

Figure 2.7: Analogy between (a) potential landslide and (b) block resting on inclined plane (Kramer, 1996).

The critical acceleration can also be named as yield acceleration. When the ground acceleration exceeds the yield acceleration of the slope, relative movement of potential shear failure block occurs. The relative movement of block can be obtained by integrating the relative acceleration twice for duration that the yield acceleration is exceeded.

Makdisi and Seed (1978) proposed an approach which is named as simplified seismic displacement method in order to calculate seismic displacement. Their approach is based on a limited number of recorded and modified ground motions. As a result of their studies, they obtained a chart which shows the relation between seismic displacement and k_y/k_{max} for different earthquake magnitude (Figure 2.8).

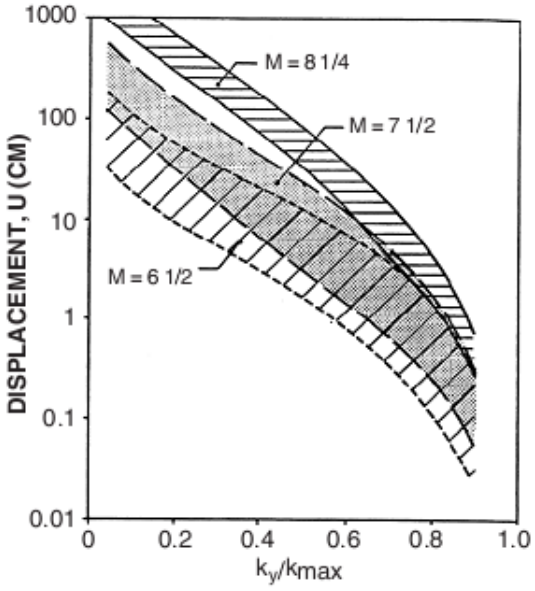

Figure 2.8: Seismic displacement vs k_y/k_{max} and magnitude (Maksidi and Seed, 1978).

Bray et al. (1998) suggested a more comprehensive assessment of the earthquake ground motions, seismic loading and seismic displacement calculations. Bray et al. (1998) combined results of fully nonlinear decoupled one-dimensional dynamic analysis and Newmark rigid sliding block analysis. As a result, they obtained a relation between normalized base linear sliding displacement and k_y/k_{max} (Figure 2.9).

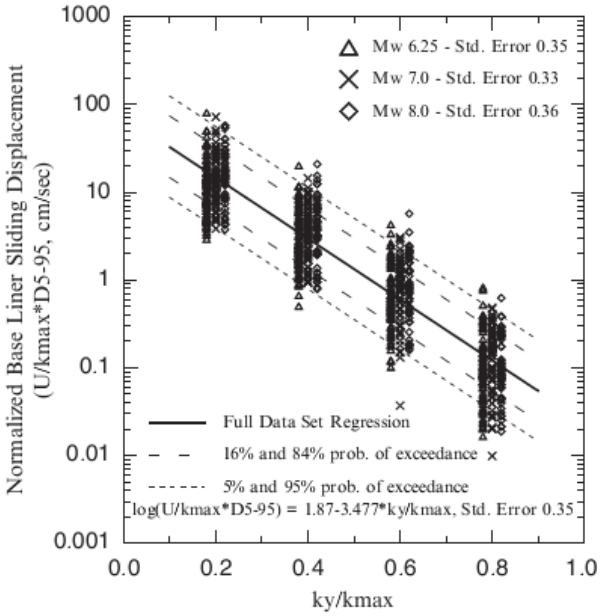

Figure 2.9: Normalized base linear sliding displacements (Bray and Rathje, 1998).

Jibson and Keefer (1993) presented a simplified Newmark method which estimates Newmark displacement as a function of landslide critical acceleration and earthquake shaking intensity. Jibson and Keefer (1993) chose 11 strong motion records in order to calculate Newmark displacement and they found relation between arias intensity and Newmark displacement in the range of 0.02g and 0.4g. The relations between arias intensity and Newmark displacement are given in Figure 2.10 and equation 2.6.

$$\log\delta_{SL} = 1.460\log I_a - 6.642a_c + 1.546 \quad \textbf{(2.6)}$$

The equation 2.6 was updated by using 13 earthquake records by Jibson et al. (1998). The updated equation is given in equation 2.7.

$$\log \delta_{SL} = 1.521\log I_a - 1.993a_c - 1.546 \quad \textbf{(2.7)}$$

where δ_{SL} is Newmark displacement, I_a is arias intensity and a_c is critical acceleration. I_a can be defined as:

$$I_a = \frac{\pi}{2g}\int_0^{\infty}[a(t)]^2\,dt \quad \textbf{(2.8)}$$

Furthermore, Wilson and Keefer (1983) developed a relation between arias intensity and earthquake magnitude (M), source distance (R) in kilometers:

$$\log I_a = M - 2\log R - 4.1 \quad \textbf{(2.9)}$$

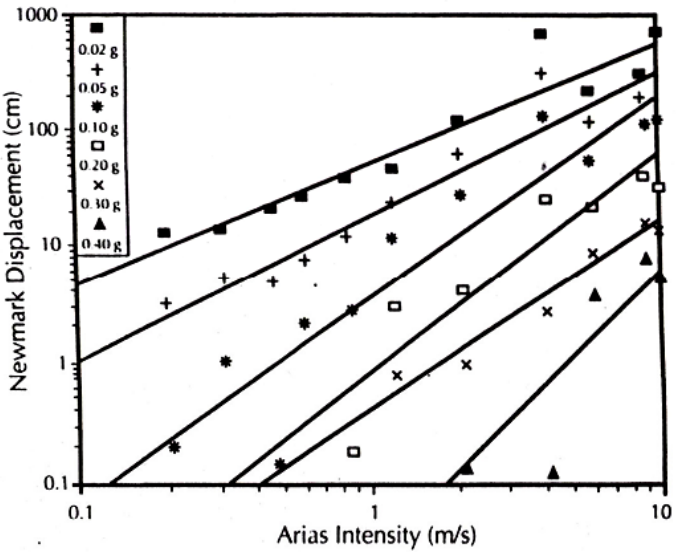

Figure 2.10: Newmark displacements-Arias Intensity (0.002g-0.40g).

2.3 Faulting

Surface faulting is the differential movement of the two sides of a fracture at the Earth's surface according to Hays (1981). There are four types of faulting such as strike slip faulting, normal faulting, reverse faulting and oblique faulting. Kramer (1996) divided faulting movement into two groups such as dip slip movement and strike slip movement. Dip slip movement includes not only normal faulting but also reverse faulting.

According to type of fault, the internal forces in pipelines can be changed. In the strike slip fault the movement is horizontal. The pipes which pass through strike slip fault are exposed to tension or compression depending on the pipe-fault intersectional angle. The movement is vertical in normal and reverse fault. When the fault is normal, the pipes are exposed to primarily in tension. When the fault is reverse, the pipes are exposed to primarily compression.

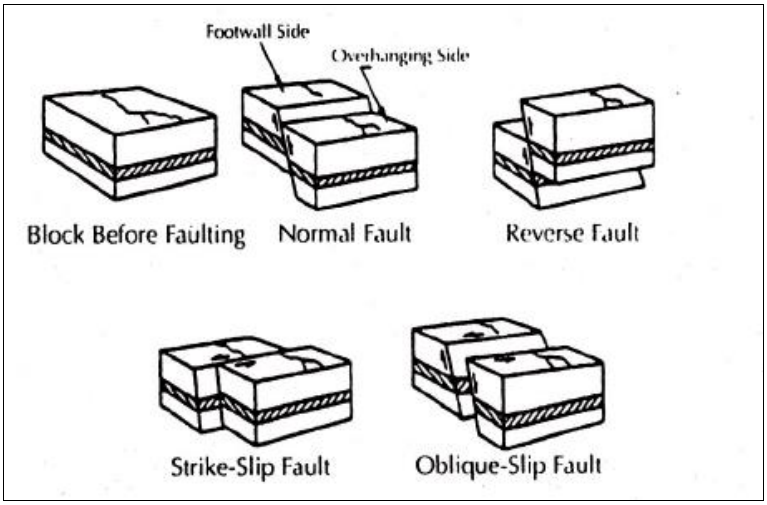

Figure 2.11: Types of surface faulting (Meyersohn, 1991).

The strain in a continuous pipe subject to fault offset relies on the pipe-fault intersectional angle and the amount of the fault offset. Wells and Coppersmith (1994) developed the empirical relationships between earthquake magnitude (M) and fault displacement (δf) for strike-slip fault, normal fault and reverse fault. The empirical relationships between earthquake magnitude and fault displacements are given equation 2.10-2.12.

$$\log \delta_f = -6.32 + 0.90M \text{ for strike-slip fault} \qquad \textbf{(2.10)}$$

$$\log \delta_f = -4.45 + 0.63M \text{ for normal fault} \quad \textbf{(2.11)}$$

$$\log \delta_f = -0.74 + 0.08M \text{ for reverse fault} \quad \textbf{(2.12)}$$

where δ_f is the average fault displacement, in meters, M is the moment magnitude.

Gas and water supply pipeline damage due to ground fault rupture had been observed during past major earthquakes (O'Rourke and Lane, 1989; O'Rourke and Palmer, 1996). More recent earthquakes demonstrated that fault rupture is one of the most violent seismic hazards for gas, electrical and water supply lifelines (Xie et al., 2011). Earthquake-induced ground rupture patterns and ground rupture effects on pipeline are shown in Figure 2.12.

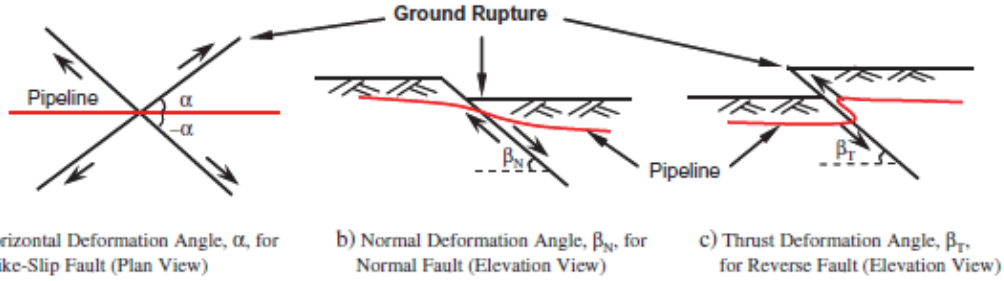

Figure 2.12: Earthquake-induced ground rupture patterns: (a) strike-slip fault, (b) normal fault, and (c) thrust fault (Xie et al., 2011).

For strike slip fault event, compressive stresses mainly occur in the pipeline if pipe-fault intersection angle (α) is negative, on the other hand, tensile stresses mainly occur in the pipeline if pipe-fault intersection angle (α) is positive.

For normal fault event, tensile stresses mainly occur in the pipeline and compressive stresses mainly occur in the pipeline for reverse fault event.

3. RESPONSE OF CONTINUOUS PIPELINES TO TRANSVERSE PGD

Transverse PGD expresses permanent ground movement that is perpendicular to pipe axis. The pipes subjected to transverse permanent ground deformation (PGD) will stretch and bend in order to accord with transverse permanent ground movement. O'Rourke and Tawfik (1983) presented a case history about the pipe failures occurred in 1971 San Fernando earthquake. In this case history, they observed pipe failures that occur due to tensile and compressive failure. Hamada and O'Rourke (1992) investigated transverse permanent ground deformation occurred by 1964 Niigata earthquake.

The response of pipelines subjected to transverse PGD is a function of the amount of PGD (δ), the width of PGD zone (W) and the pattern of ground deformation. O'Rourke and Tawfik (1983), Hamada and O'Rourke (1992) observed two types of transverse PGD as spatially distributed transverse PGD and abrupt transverse PGD (given in Figure 3.1). When PGD zone is wide, the movement at margins of PGD zone matches more or less to a fault offset where the fault pipeline intersection angle is 90^0. Spatially distributed transverse PGD generally occurs in liquefaction cases and its effects on pipelines are lesser than effects of abrupt transverse PGD. Abrupt transverse PGD generally occurs in landslides cases. When the pipeline is subjected to abrupt transverse PGD the damages in pipelines occur at the margins of PGD zone.

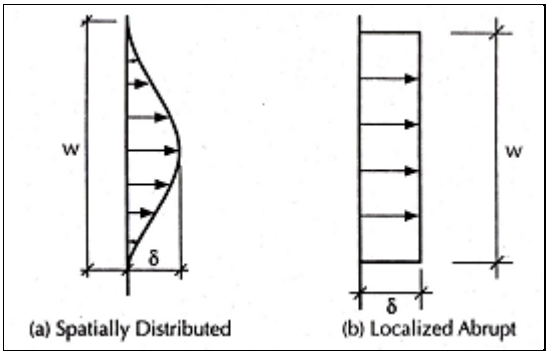

Figure 3.1: Patterns of transverse PGD.

When the pipes are buried directly in liquefied soil the pipes can be subjected to transverse PGD. Because of lateral spreading of liquefied soil, lateral displacement of pipes can occur in the horizontal direction. In addition to this, the pipes may uplift due to buoyancy in the vertical direction. Suzuki (1988) and Takada (1991) indicated some problems that occur due to buoyancy effects during the 1964 Niigata earthquake.

In order to evaluate response of pipelines subjected to spatially transverse PGD the variation of ground displacement along the PGD zone must be determined. Several researchers have proposed different patterns in their analyses (T. O'Rourke et al. 1988; Suzuki et al. 1988; Kobayashi et al. 1989; M. O'Rourke 1989).

T. O'Rourke (1988) predicted the soil deformation with the beta probability density function.

$$y(x) = \delta\left[s / s_m\right]^{r^1-1}\left[(1-s)/(1-s_m)\right]^{\tau-r-1} \qquad 0<s<1 \qquad \textbf{(3.1)}$$

where s is the distance between the two margins of the PGD zone normalized by the width W, s_m is the normalized distance from the margin of the PGD zone to the location of peak transverse ground displacement, δ, while r^1 and τ are parameters of the distribution. T. O'Rourke (1988) used sm=0.5, r^1=2.5 and τ=5.0.

Suzuki et al. (1988) and Kobayashi et al. (1989) predicted the transverse soil deformation with the cosine function raised to a power n.

$$y(x) = \delta \cdot (\cos\frac{\pi x}{W})^n \qquad \textbf{(3.2)}$$

M. O'Rourke (1989) predicted the spatially distributed transverse permanent ground deformation by using the following function:

$$y(x) = \frac{\delta}{2}(1-\cos\frac{2\pi x}{W}) \qquad \textbf{(3.3)}$$

where x is the non-normalized distance from the margin of the PGD zone. When n is equal to 2 in the Suzuki and Kobayashi et al.'s function, M. O'Rourke's function takes the same shape of the Suzuki and Kobayashi et al.'s models.

The maximum soil deformation occurs at the center of PGD zone and the soil deformation is accepted as zero at the margins. These assumptions are valid for all patterns.

3.1 Pipeline Buried in Non-Liquefied Soil

Pipelines generally are buried 1.0m below the ground surface. Therefore ground water level and the liquefied soil layer are both standing below the bottom of the pipe. In this case, the interaction between soil and pipeline is determined by using force-deformation relations used for a pipe in competent non-liquefied soil layer.
In order to understand effects of transverse PGD on pipelines nonlinear finite element approaches have been used. Finite element method can take account of nonlinearity for soil-pipe interaction and nonlinearity for stress-strain behavior of pipe material.

3.1.1 Finite Element Models

Certain researchers (O'Rourke, 1988; Suzuki et al., 1988; Kobayashi et al., 1989; Liu and O'Rourke, 1997) used finite element approaches to evaluate response of buried pipelines subjected to spatially transverse PGD.

O'Rourke (1988) simulated soil deformations with beta probability function. O'Rourke (1988) proposed a model in order to model pipelines subjected to spatially distributed PGD (Figure 3.2). T. O'Rourke (1988) accepts an anchor point where bending strain is lesser than $1x10^{-5}$. The distance between PGD zone margins and anchor points is named as L_a. W value also represents width of PGD zone.

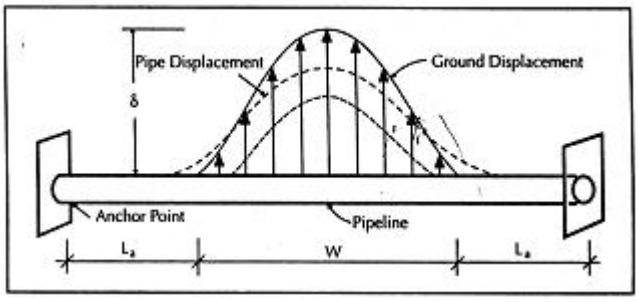

Figure 3.2: Parameters for T. O'Rourke's model.

T. O'Rourke (1988) used X-60 pipe with 0.61 diameter and 0.0095 wall thickness in his model. Furthermore, he accepted burial depth of pipe as 1.5m. T. O'Rourke

(1988) obtained maximum tensile strain and maximum pipe displacement for various widths of PGD zone. He uses 10m, 30m and 50m for width of PGD zone (W) in his model. He observed that the maximum tensile strain occurs when width of PGD is equal to 10m for any maximum ground displacements. Furthermore, T. O'Rourke (1988) changed the soil friction angle for W=30m and he observed that the width of PGD zone affected the magnitude of pipe strains much more than the soil properties do.

Suzuki et al. (1988) predicted the pattern of transverse ground displacements by the cosine function raised to the n power. When n is equal to zero the pattern of transverse ground displacements represents abrupt transverse PGD. On the other hand, the pattern of transverse ground displacements represents spatially distributed transverse PGD when n is equal to one or greater than one. Suzuki et al.'s physical model has similar properties with T. O'Rourke's model. However, PGD pattern and the anchored length in Suzuki et al.'s physical model are different from T. O'Rourke's model. Suzuki et al. defended that the axial and flexural deformations at the anchor point must not occur so the anchored length must be long enough not to occur axial and flexural deformations at the anchor point. Due to this reason, Suzuki et al.'s model is much larger than that in the T. O'Rourke (1988) model.

Suzuki et al. (1988) used X-52 grade steel pipe with 0.61m diameter and 0.0127m wall thickness to observe the effects of width of PGD zone on pipelines in their study. Furthermore, they accepted burial depth of the pipe as 1.5m. As a result of their study, tensile and compressive strains are nearly equal to each other for any W and δ values and this demonstrated that the axial strain in the pipe is small. They obtained the maximum pipe strain when the width of PGD zone is equal to 30m. The results obtained for W=30m and W=50m are consisted with T. O'Rourke's results.

Kobayashi et al. (1989) used the same procedure and shape function as Suzuki et al.'s study. They use X-42 grade steel pipe with 0.61m diameter and 0.0095m wall thickness in their study. They obtain the maximum pipe strain when the width of PGD zone is equal to 19m.

Liu and M. O'Rourke (1997b) proposed a finite element model and they used large deformation theory in their model. They model interaction between soil and pipe with nonlinear soil springs and they modeled behavior of pipe material by using

Ramberg-Osgood stress-strain relation. They used beam element to model pipe and used axial and lateral soil spring. The anchored length is determined to have enough length not to occur axial and flexural deformation as in Suzuki et al.'s model so the anchored length is chosen as 400m. The soil surrounding the pipe is assumed loose to moderately dense sand (friction angle $\phi=35^o$ and soil density $\gamma=18.7$ kN/m^3). The burial depth from ground surface to the top of pipe was assumed 1.2m. The peak longitudinal resistance and peak transverse resistance of elasto-plastic soil springs and relative displacement between pipe and soil were determined by using TCLEE Guideline (ASCE, 1984).

Liu and M. O'Rourke (1997b) obtained the maximum tensile and compressive strains in the pipe depending on ground displacement for W=10, 30 and 50m. They used X-52 grade steel pipe with 0.61m diameter and 0.0095m wall thickness in their model. They used ground deformation pattern given in equation 3.3.

Liu and M. O'Rourke (1997) observed that the maximum tensile and compressive strains are largest for W=30m. The same strain values are approximately obtained with Suzuki et al.'s study for W=10, 30 and 50m although different type of steel is used. Moreover, the maximum tensile and compressive strains obtained by Liu and O'Rourke are consisted with T. O'Rourke (1988) results for W=30 and 50m.

Liu and M. O'Rourke (1997) observed that the maximum pipe displacement more or less matches the ground deformation up to a certain critical displacement (δ_{cr}). After the critical displacement, the pipe strain remains constant while the pipe displacement increases more slowly with ground deformation. Moreover, Liu and M. O'Rourke (1997) investigated the parameter affecting the behavior of pipe subjected to transverse PGD. They concluded that:

- Peak tensile and compressive strains are increasing functions of diameter.
- Peak compressive strain is essentially independent of the wall thickness and the steel grade.
- Peak tensile strain is an increasing function of the pipe diameter and the transverse soil spring resistance. It is a decreasing function of the pipe wall thickness, steel grade and to the longitudinal soil spring resistance.

- The critical ground displacement is a decreasing function of steel grade, axial pipe-soil interaction force, pipe wall thickness and pipe diameter. On the other hand, the critical ground displacement is an increasing function of the lateral pipe-soil interaction force and width of the PGD zone.

In summary, the parameter which most strongly affects the tensile strain is the width of the PGD zone, followed by the transverse soil spring resistance, steel grade, pipe diameter, wall thickness, anchor length of the pipe, PGD pattern and longitudinal soil spring resistance.

3.2 Pipeline Buried in Liquefied Soil

The pipelines are generally located above the top of the liquefied soil layer as mentioned previously. When the pipelines are buried in saturated sand such as in a sea bed or at a river bed, the soil layer surrounding the pipeline may liquefy because of strong seismic shaking. The pipelines may move upwards due to buoyancy and the pipelines may deform laterally because of the lateral spreading that is the flow of liquefied soil down a gentle slope. A gas pipe and a sewage pipe with manhole were uplifted out of the ground due to buoyancy in combination with a compressive load caused by longitudinal permanent ground deformation during the 1964 Niigata earthquake according to Suzuki et al. (1988) and Takada (1991).

3.2.1 Horizontal movement

The pipe may deform laterally following the lateral spreading, or move upward due to buoyancy when the pipe is located in the liquefied soil. As a result of strong seismic shaking, the pipeline located in the liquefied soil may be exposed to lateral movement due to the flow of liquefied soil downslope.

Suzuki et al. (1988) studied the behavior of a buried pipe, located in liquefied soil, subject to spatially distributed transverse PGD. The lateral soil coefficient (K_1) for a pipe located in liquefied soil is assumed to be some fraction of the corresponding value (K_2) for non-liquefied soil. Thus, the presence of the liquefied soil is modeled.

Suzuki et al. (1988) obtained a graph which shows the peak pipe strain as a function of the amount of PGD for three different values of the reduction factor. This graph is given in Figure 3.3. Suzuki et al. (1988) observed that a pipe located in liquefied soil

is much less likely to be damaged by spatially distributed transverse PGD as a result of their study. Therefore, for design purpose, it is logical to assume that the pipe subject to spatially distribute transverse PGD is located in non-liquefied soil.

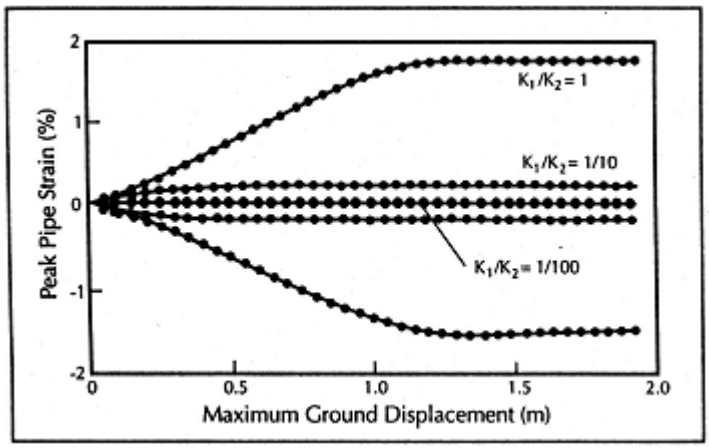

Figure 3.3: Peak pipe strain and amount of PGD for three different values of reduction factor (Suzuki et al., 1988).

3.2.2 Vertical movement

The pipe may uplift due to the buoyancy force occurred by the liquefaction of the soil surrounding a buried pipe. In the literature, several studies have been performed by considering this vertical movement. Yeh and Wang (1985) used a simplified beam-column model for the pipe in order to analyze the dynamic pipe response. They deduced that when the liquefaction of surrounding soil occurs, the dynamic displacement is less than 20% of static pipe displacement.

Cai et al. (1992) performed a series of laboratory tests and they observed pipe response due to soil liquefaction as a result of these laboratory tests. They used two system models in order to observe pipe response due to soil liquefaction. The first model was for a pipeline without a manhole and the other model model was for a pipeline with a manhole. In these tests, only uplifting and shaking response can be observed but lateral response of the pipe was not modeled. They observed that 10% of the static strain due to uplifting was greater than dynamic strain due to shaking.

Hou et al. (1990) used finite element approach in order to analyze the pipe strain due to buoyancy effects. They considered the nonlinearity of both steel material and interaction force at the pipe soil interface outside the liquefied zone. They concluded the uplifting force per unit length, P_{uplift}, acting on the pipe within the liquefied zone as:

$$P_{uplift} = \frac{1}{4}\pi D^2(\gamma_{soil} - \gamma_{contents}) - \pi D t \gamma_{pipe} \quad \textbf{(3.4)}$$

where $\gamma_{soil}, \gamma_{pipe}, \gamma_{contents}$ are the weights per unit volume of liquefied soil, pipe and pipe contents respectively.

Hou et al. (1990) observed a critical width of the liquefied zone, W_{cr}. For the width more than W_{cr}, the pipe strain decreases with the increasing width thereafter while the pipe strain is an increasing function of the width for the width less than W_{cr} (Figure 3.4).

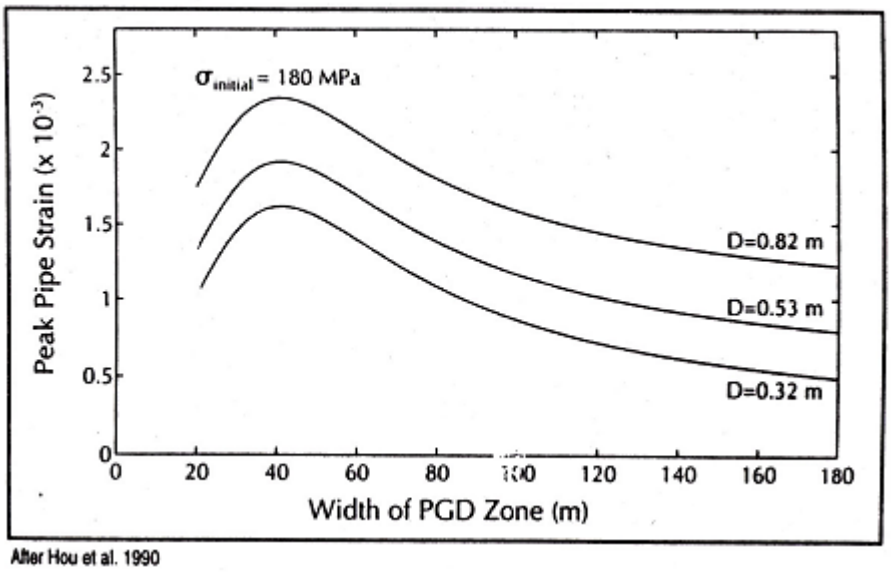

Figure 3.4: Maximum strain vs. width of the liquefied zone (Hou et al., 1990).

3.3 Localized Abrupt PGD

Two patterns of transverse permanent ground deformation were mentioned before. The spatially distributed permanent ground deformation pattern has been discussed. Liu and O'Rourke (1999) studied about localized abrupt permanent ground deformation pattern. They used finite element approach in order to determine response of pipe subject to localized abrupt permanent ground deformation. Liu and O'Rourke (1999) used pipe with 0.61m diameter and 0.0095m wall thickness. The amount of ground movement was δ=1.0m while the width of the permanent ground deformation zone was 50m. The unit weight of soil and the internal friction angle of soil were chosen as $1.8 \times 10^4 N/m^3$ and $\phi = 35^0$ respectively. They concluded that the bending moment is nearly zero over a distance of roughly 20m near the center of the

permanent ground zone. They observed that the continuous pipe behaves as if it was subjected to two separate fault offsets, both having a pipe fault angle of 90^0 in terms of flexure. The pipe axial force near the center depends on the width of the permanent ground deformation zone. The distribution of bending pipe moment and the distribution of axial pipe force are given in Figure 3.5.

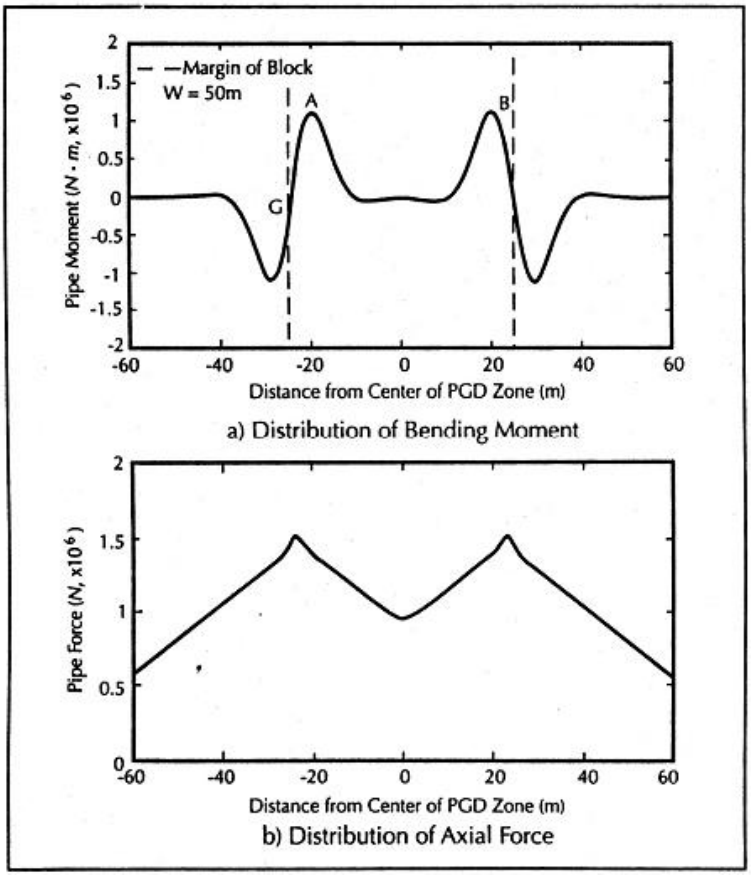

Figure 3.5: Distribution of pipe bending moment and axial force (Liu and O'Rourke, 1999).

4. SOIL-PIPE INTERACTION AND PIPE FAILURE MODES

Buried pipelines are interaction with soil surrounding them. Earthquakes cause that the buried pipelines are damaged because of deformation and forces loaded on them along interactions at the pipe soil interface. When the earthquake occurs, the pipe and the soil surrounding pipe move relatively different from each other. This relative movement induces pipe to become deformed (O'Rourke, M.J., Liu, X., 1999). According to O'Rourke and Liu (1999), the interaction between soil and pipe can be divided into two groups as longitudinal and transverse. In the transverse direction, the interaction between soil and pipe includes horizontal and vertical movement. Furthermore, the vertical component of the interaction between soil and pipe involves upward and downward pipe movement. The interaction between soil and pipe should be divided into two groups with regards to the soil surrounding pipe as the pipelines surrounded by non-liquefied soil, and pipelines located in a liquefied layer (O'Rourke, M.J., Liu, X., 1999).

Despite laboratory tests have demonstrated that at large relative displacement the maximum soil force on pipeline decreases, ALA (2001) proposes an assumption based on that the soil force is constant once it reaches the maximum value.

4.1 The Pipeline Located in Non-liquefied Soil

Trautmann and T. O'Rourke (1983) found a force-deformation relation for horizontal lateral movement as a result of laboratory tests which were performed to determine soil interaction forces for a pipeline surrounded by non-liquefied soil. The ASCE Technical Council on Lifeline Earthquake Engineering (TCLEE) Committee on Gas and Liquid Fuel Lifelines (ASCE, 1984) proposed idealized elasto-plastic models in order to model the interaction between soil and pipe. The elasto-plastic model consists of two parameters. These parameters are the maximum resistance P_u, T_u, Q_u, Q_d in transverse horizontal, axial and transverse vertical directions respectively and the maximum elastic deformation Δ_p, Δ_t, Δ_{qd}, Δ_{qu} respectively (Figure 4.1).

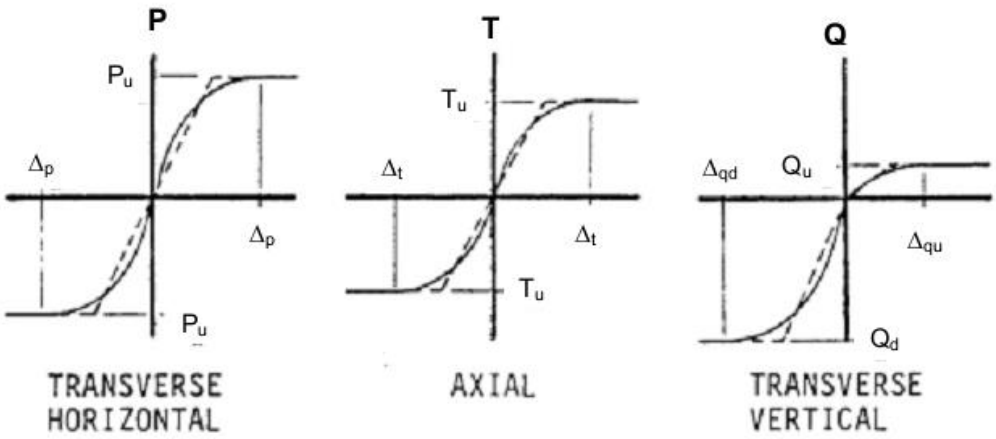

Figure 4.1: Bi-linear soil springs used to represent soil force on pipe (ALA, 2001).

4.1.1 Axial soil springs

Axial spring restraint forces symbolize the skin friction on the cylindrical surface of pipe. Axial spring restraint forces are improved from similar theories as for load transfer at axially loaded pile-soil interface. These forces are attained by integrating shear stresses along the area of contact between pipe and soil. The maximum axial soil force per unit length of pipe can be calculated by using equation 4.1.

$$T_u = \pi D\alpha c + \pi DH\bar{\gamma}\left(\frac{1+Ko}{2}\right)\tan\delta \qquad \textbf{(4.1)}$$

where:

D= pipe outside diameter

c= soil cohesion representative of the soil backfill

H= depth to pipe centerline

$\bar{\gamma}$ = effective unit weight of soil

K_o= coefficient of pressure at rest, K_o=1-sinϕ

α = adhesion factor

α=0.608-0.123c-$\frac{0.274}{c^2+1}+\frac{0.695}{c^3+1}$ where c is in ksf or kPa/100

δ = interface angle of friction for pipe and soil = f×ϕ

ϕ= internal friction angle of the soil

f= coating dependent factor relating the internal friction angle of the soil to the friction angle at the soil-pipe interface.

f values are given Table 4.1 according to various types of external coatings. Furthermore, adhesion factor (α) can be determined with the aid of Figure 4.2.

Table 4.1: Friction factor various external coatings

Pipe Coating	f
Concrete	1
Coal Tar	0.9
Rough Steel	0.8
Smooth Steel	0.7
Fusion Bonded Epoxy	0.6
Polyethylene	0.6

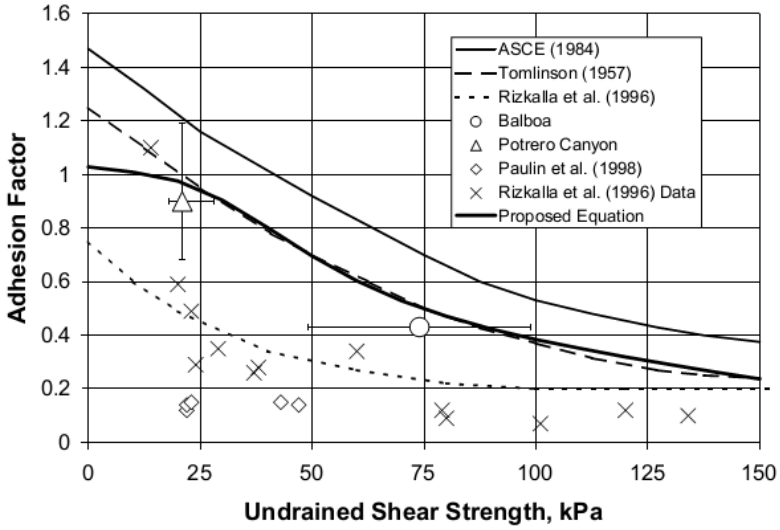

Figure 4.2: Adhesion factor, α (ALA, 2001).

The maximum elastic deformation (Δ_t) values change depending on types of soil surrounding pipe. The maximum elastic deformation for various soil types are given below.

Δ_t = displacement at Tu

= 0.1 inches (3 mm) for dense sand

= 0.2 inches (5 mm) for loose sand

= 0.3 inches (8 mm) for stiff clay

= 0.4 inches (10 mm) for soft clay

4.1.2 Lateral soil springs

Lateral soil springs simulate the resistance of surrounding soils to any horizontal translation of pipeline. Therefore, the mechanisms of soil pipeline interaction are similar with vertical anchor plates or footings moving horizontally relative to the surrounding soils, and thus passive type of earth pressure. The maximum lateral soil force per unit length of pipe can be calculated by using equation below.

$$P_u = N_{ch} cD + N_{qh} \bar{\gamma} HD \qquad \textbf{(4.2)}$$

where:

N_{ch} = horizontal bearing capacity factor for clay (0 for c= 0)

$$N_{ch} = a + bx + \frac{c}{(x+1)^2} + \frac{d}{(x+1)^3} \leq 9$$

N_{qh}= horizontal bearing capacity factor (0 for $\phi = 0^o$)

$N_{qh} = a + b(x) + c(x^2) + d(x^3) + e(x^4)$

D= pipe outside diameter

c= soil cohesion representative of the soil backfill

H= depth to pipe centerline

$\bar{\gamma}$ = effective unit weight of soil

Table 4.2: Nch and Nqh values (ALA,2001).

Factor	ϕ	X	a	b	c	d	e
N_{ch}	0	H/D	6.752	0.065	-11.063	7.119	-
N_{qh}	20	H/D	2.399	0.439	-0.03	$1.059(10)^{-3}$	$-1.754(10)^{-5}$
N_{qh}	25	H/D	3.332	0.839	-0.09	$5.606(10)^{-3}$	$-1.319(10)^{-4}$
N_{qh}	30	H/D	4.565	1.234	-0.089	$4.275(10)^{-3}$	$-9.159(10)^{-5}$
N_{qh}	35	H/D	6.816	2.019	-0.146	$7.651(10)^{-3}$	$-1.683(10)^{-4}$
N_{qh}	40	H/D	10.959	1.783	0.045	$-5.425(10)^{-3}$	$-1.153(10)^{-4}$
N_{qh}	45	H/D	17.658	3.309	0.048	$-6.443(10)^{-3}$	$-1.299(10)^{-4}$

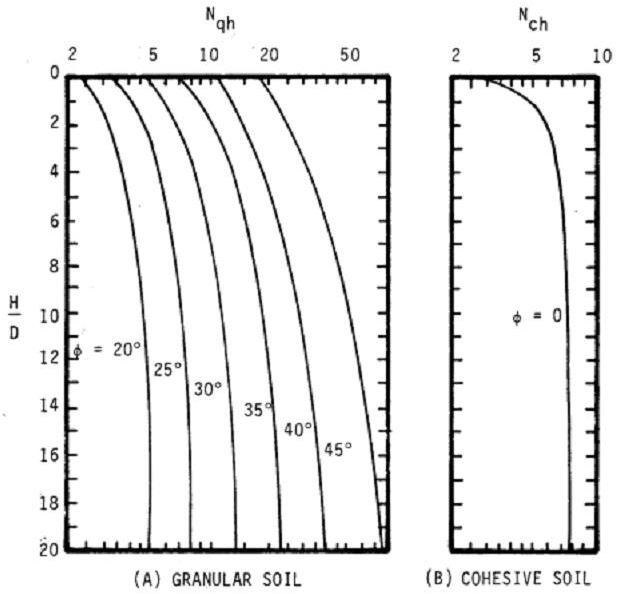

Figure 4.3: Values of N_{qh} and N_{ch} of Hansen 1961 (ALA, 2001).

N_{ch} and N_{qh} values can be determined by using Table 4.2 or Figure 4.3.

Δ_p =displacement at Pu

$= 0.04(H + \frac{D}{2}) \leq 0.10D$ to 0.15D

or;

Δ_p=displacement at Pu

$= (0.07 \sim 0.10)(H + D/2)$ for loose sand

$= (0.03 \sim 0.05)(H + D/2)$ for medium sand

$= (0.02 \sim 0.03)(H + D/2)$ for dense sand

4.1.3 Transverse vertical soil springs

4.1.3.1 Vertical uplift soil springs

The maximum vertical uplift soil force per unit length of pipe can be calculated by using equation below.

$$Q_u = N_{cv} cD + N_{qv} \bar{\gamma} HD \quad \textbf{(4.3)}$$

where:

N_{cv} = vertical uplift factor for clay (0 for c= 0)

N_{qv}= vertical uplift factor for sand (0 for $\phi = 0^o$)

$N_{cv} = 2*(\frac{H}{D}) \leq 10$ applicable for $(\frac{H}{D}) \leq 10$

$N_{qv} = (\frac{\phi H}{44D}) \leq N_q$

$N_q = \exp(\pi \tan\phi)\tan^2(45+\frac{\phi}{2})$

Δq_u = displacement at Q_u

= 0.01H to 0.02H for dense to loose sands < 0.1D

= 0.1H to 0.2H for stiff to soft clays < 0.2D

4.1.3.2 Vertical bearing soil springs

The maximum vertical bearing soil force per unit length of pipe can be calculated by using equation below.

$$Q_d = N_c cD + N_q \bar{\gamma} HD + N_\gamma \gamma \frac{D^2}{2} \quad \textbf{(4.4)}$$

where:

N_c, N_q, N_γ= bearing capacity factors

$N_c = \left[\cot(\phi+0.001)\right]\left(\exp\left[\pi\tan(\phi+0.001)\right]\tan^2(45+\frac{\phi+0.001}{2})-1\right)$

$N_q = \exp(\pi \tan\phi)\tan^2(45+\frac{\phi}{2})$

$N_\gamma = e^{(0.18\phi-2.5)}$

N_q, N_c and N_γ can also be determined by using Figure 4.4.

γ=total unit weight of soil

Δ_{qd}= displacement at Q_d

= 0.1Dfor granular soils

= 0.2Dfor cohesive soils

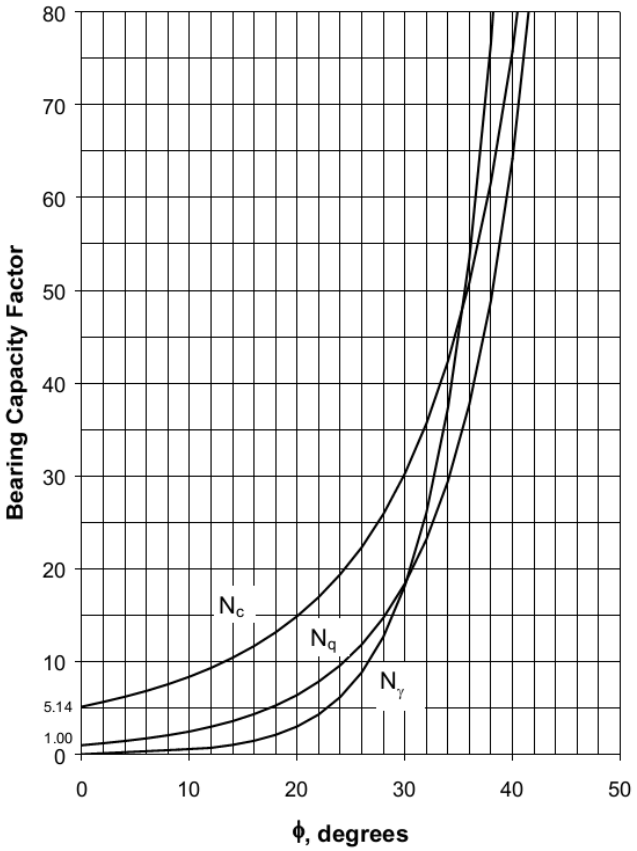

Figure 4.4: Bearing capacity factors (Nq, Nc and N_γ) (ALA, 2001).

4.2 The Pipeline Located in Liquefied Soil

The interaction between pipe and soil for the pipeline located in non-liquefied soil is discussed in previous section. In this section, the interaction between pipe and soil for the pipeline located in liquefied soil will be handled.

Suzuki et al. (1988) and Miyajima and Kitaura (1989) have observed that the pipe response is very sensitive to the stiffness of the equivalent soil springs which represent the interaction between soil and pipe for pipeline located in the liquefied soil as a result of their study.

Takada et al. (1987) proposed an equivalent soil spring for a pipe located in a liquefied soil as a result of their study. They combined experimental data with analytical solutions depending on a beam on an elastic foundation approach in scope of their study. They observed that the equivalent stiffness of liquefied soils varies between 1/1000 and 1/3000 of equivalent stiffness of non-liquefied soil.

Yoshida and Uematsu (1978), Matsumoto et al. (1987), Yasuda et al. (1987) and Tanabe (1988) proposed that the equivalent stiffness varies between 1/100 and 3/100 of the equivalent stiffness of non-liquefied soil.

Miyajima and Kitaura (1991) observed that the stiffness was pertained to effective stress in the liquefied soil and the soil spring constant was an increasing function of effective stress and a decreasing function of excess pore water pressure ratio.

T. O'Rourke et al. (1994) suggested a reduction factor for a pipe or pile subject to tranverse ground displacement for saturated sandy soil as:

$$R_f = \frac{N_{qh}}{K_c} \cdot \frac{1}{0.0055(N_1)_{60}} \tag{4.5}$$

where K_c is the bearing capacity factor for undrained soil and $(N_1)_{60}$ is the corrected SPT value. The reduced stiffness at the pipe-soil interface can be determined by dividing the stiffness for non-liquefied soil to the reduction factor. T. O'Rourke et al. (1994) conclude that the equivalent stiffness ranges from 1/100 to 5/100 of that for non-liqufied soil. Therefore, both transverse and longitudinal stiffness for a pipe located in a liquefied soil can be accepted as 3% of the stiffness for a pipe located in non-liquefied soil.

4.3 Pipe Failure Modes and Failure Criterion

When earthquake occurs, buried pipelines can be damaged because the buried pipelines are exposed to seismic loading. There are three important failure modes for buried pipelines subject to seismic loading. These failure modes are tensile failure, local buckling and beam buckling. Tensile failure occurs due to excessive axial tension along the buried pipeline and local buckling occurs because of excess axial compression and flexural failure. Beam buckling is a failure mode that occurs if the burial depth is shallow and if continuous pipelines are exposed to axial compression. These failure modes will be summarized and failure criterion for these failure modes will be presented.

4.3.1 Continuous pipeline

According to O'Rourke and Liu (1999), the principal failure modes for continuous pipeline with burial depth of about one meter or more are tensile failure and local

buckling. If the burial depth of continuous pipeline is less than about one meter, continuous pipeline may be experienced to beam buckling behavior.

4.3.1.1 Tensile failure criterion

The strain associated with tensile failure is generally well above about 4% (Newmark and Hall, 1975). Beyond the tensile value of 4%, the pipeline is considered to have failed in tension so ultimate tensile value can be considered as 4%.

Tensile failure can be divided into four categories as ductile tensile failure, brittle tensile failure, fatigue failure and bending failure. According to material behavior and loading conditions tensile failure can occur in various forms. If pipe material has a good degree of ductility, the pipe will stretch until ultimate strength of pipe is reached. The brittle tensile failure is opposite of the ductile tensile failure. The pipe material is working properly one moment and the next it has failed. Fatigue failure occurs due to the application of cyclic tensile load.

To understand failures we must understand the behavior of the pipe material. Ramberg and Osgood (1943) proposed a model for description of the post yield stress-strain behavior. The Ramberg Osgood model is given by:

$$\varepsilon = \frac{\sigma}{E}\left[1 + \frac{n}{1+r}\left(\frac{\sigma}{\sigma_y}\right)^r\right] \qquad \textbf{(4.6)}$$

where E is the initial Young's modulus, σ is the uniaxial tensile stress, ε is the engineering strain, σ_y is the apparent yield stress, n and r are Ramberg Osgood parameters. Apparent yield stress, n and r values for various steel types are listed in Table 4.3.

Table 4.3: Ramberg-Osgood for mild steel and X-grade steel.

	Grade-B	**X-42**	**X-52**	**X-60**	**X-70**
Yield Stress (Mpa)	227	310	358	413	517
n	10	15	9	10	5.5
r	100	32	10	12	16.6

4.3.1.2 Local buckling

Local buckling occurs due to axial compression. The axial compression in the pipe causes structural stability broken down. In consequence of a sudden change from a

stable to unstable condition, local instability of pipe wall can occur. Hall and Newmark (1977) performed laboratory tests on thin wall cylinders and they observed that local buckling in a pipe starts at a strain of 1/3 to 1/4 of the theoretical value of:

$$\varepsilon_{theory}=0.6\times t/R \qquad \textbf{(4.7)}$$

4.3.1.3 Beam buckling

Beam buckling generally occurs when the pipelines are buried in shallow trenches and /or backfilled with loose material (O'Rourke and Liu, 1999). Meyersohn (1991) made a study about critical cover depth when the beam buckling of pipelines occurs. Meyersohn (1991) obtained the relationship between critical cover depth and t/D ratio for sands having different relative density. This relationship for Grade B steel and X-60 Steel are given in Figure 4.5.

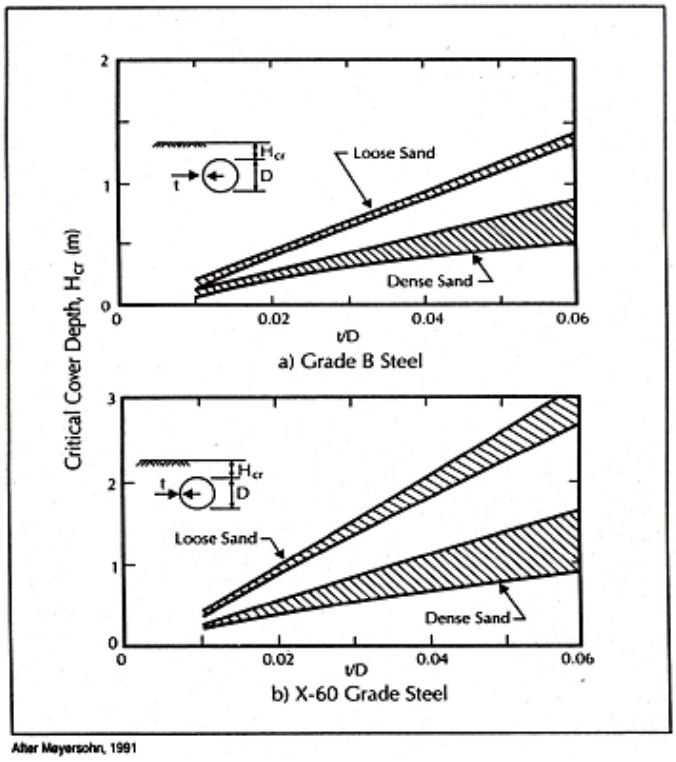

Figure 4.5: Analytical critical depth of pipe for grade B and X-steel (Meyersohn,1991).

If the cover depth is greater than critical depth the buried pipelines would experience beam buckling before local buckling.

5. FINITE ELEMENT METHOD

Finite element method (FEM) is a technique which is used in order to find approximate solution to boundary value problems for differential equation. The finite element method is used for solving physical problems in engineering analysis and design. Bathe (1996) identified the process of finite element analysis which involves five subprocess such as physical problem, mathematical problem, finite element solution, assessment of accuracy of finite element solution of mathematical model and interpretation of results (Figure 5.1).

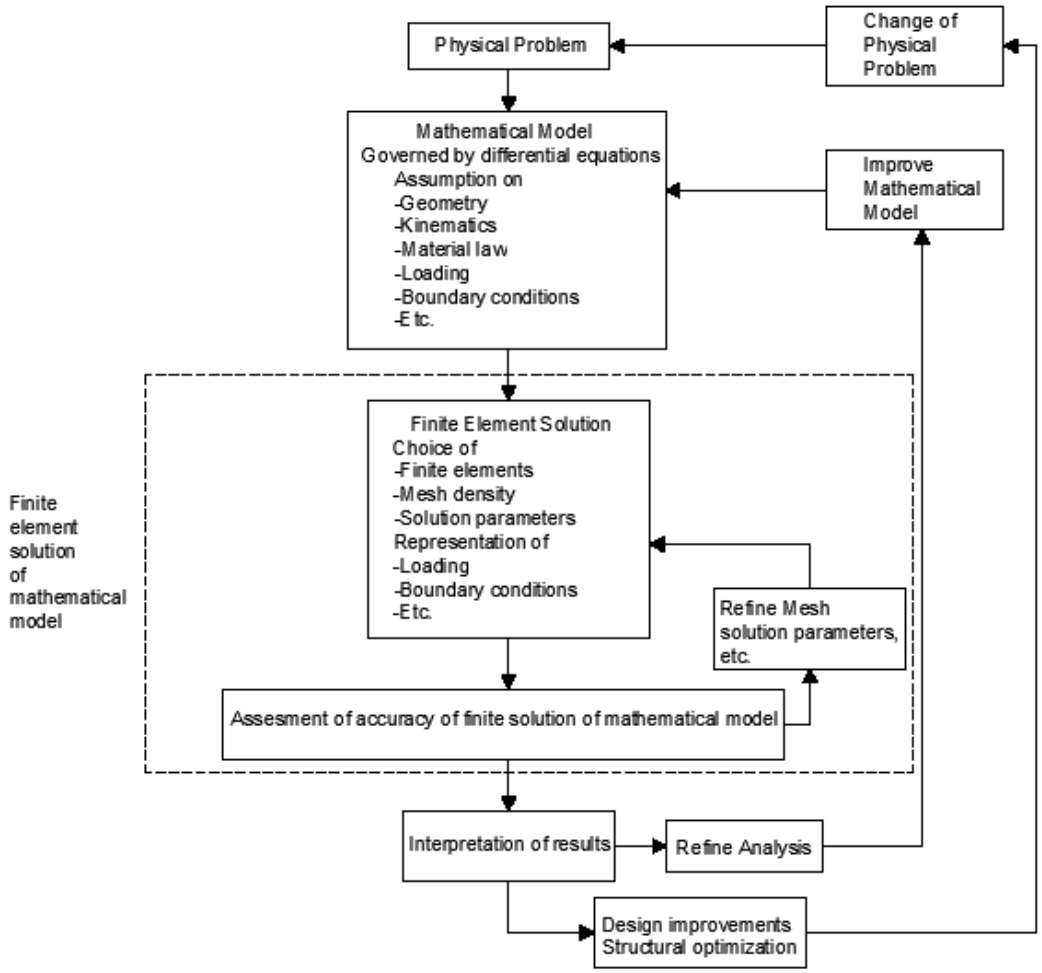

Figure 5.1: The process of finite element analysis (Bathe, 1996).

Firstly physical problem which typically includes an actual structure subjected to certain loads is needed to be formed. Certain assumptions are required to convert physical problem to mathematical model governed by differential equations. Mathematical model involves assumption on geometry, kinematics, material law, loading, and boundary conditions. Mathematical model can be solved by using finite element solution. Because finite element solution technique is a numerical procedure, the accuracy of finite element solution of mathematical model must be evaluated. If the accuracy criteria are not obtained the finite element solution must be repeated with refined solution parameters until the accuracy of finite element solution is reached.

5.1 Non-linear Problems

In linear problems, there is a linear relationship between applied loading and displacement caused by applied load.

$$[K]\{u\}=\{R\} \qquad \textbf{(5.1)}$$

Displacements {u} are linear increasing or decreasing function of the loads {R}. The linearity of equation is valid if three assumptions below are met.

1) The relationship between stress and strain is linear. (Material linearity)

2) Original geometry is accepted as unaffected by displacements which occur as a result of applied loads. (Geometric linearity)

3) The boundary conditions have not any alteration during the loading. (Boundary linearity)

If all three assumptions are not satisfied the relationship between displacements and forces will be non-linear and it will be needed to be performed a non-linear analysis. The stiffness matrix is changing with the displacements and temperatures in non-linear analysis. Because the stiffness matrix is not known until after a solution is obtained the system of equations can not be solved directly. The solution is found by determining the loading as a function of time. Incrementation of time is used to obtain the non-linear response. Therefore the finite element simulation is broken into a number of time increments and at the end of each time increment approximate equilibrium configuration is found (Abaqus 6.12 User's Manual).

5.1.1 General solution procedures for non-linear problems

The equilibrium equation of a system can generally be stated as

$$^{t}\{R\} - {}^{t}\{F\}=0 \qquad \textbf{(5.2)}$$

where $^{t}\{R\}$ is a vector including all externally nodal point forces at time t and $^{t}\{F\}$ is a vector containing internal stresses caused by nodal point forces at time t.

Equation 5.2 must be satisfied for any time and load step t and the current geometry must be in equilibrium. In many cases, the total load is applied in increments and solution is obtained for every increment in load. According to Bathe (1996) and Beer and Watson (1992), there is an solution example for nonlinear problems presented below.

If we assume that the solution at time t is known the solution at time $t+\Delta t$ is required to be find. At time $t+\Delta t$ we have

$$^{t+\Delta t}\{R\} - {}^{t+\Delta t}\{F\} =0 \qquad \textbf{(5.3)}$$

where

$$^{t+\Delta t}\{F\} = {}^{t}\{F\} + {}^{\Delta t}\{F\} \qquad \textbf{(5.4)}$$

$^{\Delta t}\{F\}$ is the increment in nodal point forces caused by the increment of stresses during interval Δt. In finite element analysis $^{\Delta t}\{F\}$ can be calculated from

$$^{\Delta t}\{F\} = {}^{t}[K]\,{}^{\Delta t}\{u\} \qquad \textbf{(5.5)}$$

where $^{t}[K]$ is a tangential stiffness matrix at time t and $^{\Delta t}\{u\}$ is an increment in displacements caused by the increment in nodal point forces. By using equation 4, equation 5 and equation 6 we can obtain

$$^{t}[K]\,{}^{\Delta t}\{u\} = {}^{t+\Delta t}\{R\} - {}^{t}\{F\} \qquad \textbf{(5.6)}$$

and we can have an approximation to the displacements at time $t+\Delta t$

$$^{t+\Delta t}\{u\} = {}^{t}\{u\} + {}^{\Delta t}\{u\} \qquad \textbf{(5.7)}$$

${}^{t}[K]$ changes with time step Δt in a non-linear analysis in order to get a realistic results. If a constant stiffness matrix is assumed throughout time increment Δt there can be significant errors when Δt is not very small.

The repetitive steps for iteration i are

$$ {}^{t}[K]^{i-1}\{u\}^{i} = \Delta\{F\}^{i-1} \tag{5.8} $$

where the increment in the residual force vector is given by:

$$ \Delta\{F\}^{i-1} = {}^{t+\Delta t}\{R\} - {}^{t+\Delta t}\{F\}^{i-1} \tag{5.9} $$

The total displacement at iteration i is:

$$ {}^{t+\Delta t}\{u\}^{i} = {}^{t+\Delta t}\{u\}^{i-1} + \Delta\{u\}^{i} \tag{5.10} $$

${}^{t}[K]$ is the stiffness matrix at the ith iteration and $\Delta\{u\}^{i}$ is the increment in displacement at the ith iteration. This iteration procedure above is named as the Newton-Raphson procedure. The process of solution which is used for a single degree of freedom system is illustrated in Figure 5.2.

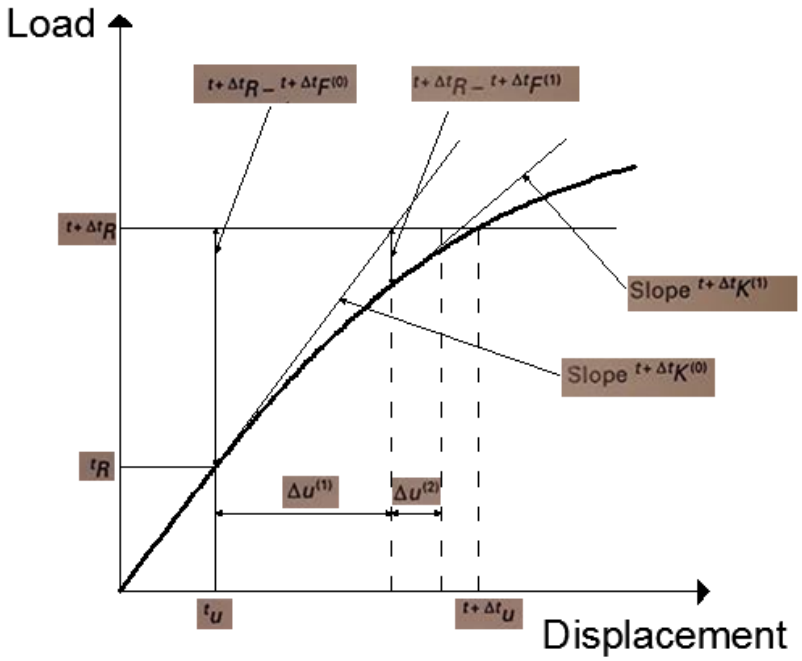

Figure 5.2: Illustration of Newton-Raphson iteration in solution of a single degree of freedom (Bathe, 1996).

The initial conditions in this iteration are ${}^{t+\Delta t}[K]^{(0)} = {}^{t}K$, ${}^{t+\Delta t}\{F\}^{(0)} = {}^{t}F$, ${}^{t+\Delta t}\{u\}^{(0)} = {}^{t}U$. The iteration process is continued until appropriate convergence criteria are satisfied. The use of the iterative solution requires appropriate convergence criteria. Convergence criteria will be discussed in next section.

5.1.2 Convergence criteria

The convergence criteria is used for checking whether the iteration has converged within preset tolerances or whether the iteration is diverging. There are three different convergence tolerances such as $\in_{\mathbf{D}}$, $\in_{\mathbf{F}}$ and $\in_{\mathbf{E}}$. When the convergence tolerances are too loose inaccurate results are obtained, and when the tolerances are too tight, in order to obtain needed accuracy much computational effort is spent.

$\in_{\mathbf{D}}$ is a displacement convergence tolerance and it can be expressed as:

$$\frac{\left\|\Delta U^{(i)}\right\|_2}{\left\|{}^{t+\Delta t}U\right\|_2} \leq \in_D \qquad \textbf{(5.11)}$$

A second convergence criterion ($\in_{\mathbf{F}}$) is gained by measuring the out of balance load vector. Force convergence tolerance can be expressed as:

$$\frac{\left\|{}^{t+\Delta t}R - {}^{t+\Delta t}F^{(i)}\right\|_2}{\left\|{}^{t+\Delta t}R - {}^{t}F\right\|_2} \leq \in_F \qquad \textbf{(5.12)}$$

A third convergence criterion ($\in_{\mathbf{E}}$) can be expressed as:

$$\frac{\Delta U^{(i)T}({}^{t+\Delta t}R - {}^{t+\Delta t}F^{(i-1)})}{(\Delta U^{(1)T}({}^{t+\Delta t}R - {}^{t}F))} \leq \in_E \qquad \textbf{(5.13)}$$

This energy convergence criteria include both forces and displacements.

5.2 Static Analysis

The static analysis is used when inertia effects and time-dependent effects can be neglected. The equilibrium equation in static analysis can be expressed as mentioned below:

$$KU = R \qquad \textbf{(5.14)}$$

K is the stiffness matrix and U is the displacement vector and R is the load vector of finite element system.

There are essentially two different group of methods for the solution of equilibrium equations in static analysis. These are:

1. Direct Solution Methods

- Gauss Elimination
- The LDL^T Solution
- Cholesky Solution

2. Iterative Solution Methods

- The Gauss Seidel Method
- Conjugate Gradient Method with Preconditioning

Direct solution methods are used in most cases but iterative solution methods can be much more effective for large system.

5.3 Dynamic Analysis

The equilibrium equation in dynamic analysis can be expressed as:

$$M\ddot{U}+C\dot{U}+KU=\mathrm{R} \qquad \textbf{(5.15)}$$

M is mass matrix, C is damping matrix, K is stiffnes matrix, R is the vector of externally applied loads. U is displacement vector, $\dot{U}$ is velocity vector and $\ddot{U}$ is acceleration vector.

The solution methods of equilibrium equations in dynamic analysis can be divided into two main group as:

1. Direct Integration Method

- The Central Difference Method
- The Houbolt Method
- The Wilson θ Method
- The Newmark Method

2. Mode Superposition Method
3. Solution of Nonlinear Equations in Dynamic Analysis

- Explicit Integration
- Implicit Integration
- Solution Using Mode Superposition

5.4 Abaqus Fea Program

ABAQUS finite element program is a general-purpose simulation tool and has solution for a wide range of engineering problems including soil-structure interaction problem. ABAQUS has widespread element, material libraries and material constitutive laws.

ABAQUS includes three main analysis software product such as ABAQUS/Standard, ABAQUS/Explicit and ABAQUS CFD. ABAQUS/Standard is a general purpose analysis program in order to solve linear, nonlinear, static and dynamic problems. ABAQUS/Explicit that uses an explicit dynamic finite element formulation is a special purpose analysis program in order to solve linear, nonlinear, static and dynamic problems. ABAQUS/CFD provides advanced fluid dynamics capabilities with extensive support for preprocessing and post processing supplied in ABAQUS/CAE. ABAQUS/CAE supports a graphical environment for pre-processing and post processing. In the scope of this study, Abaqus/Standard software will be focus on since all parametric studies are performed with using Abaqus/Standard.

ABAQUS involves ten modules such as:

- Part (Creation of geometry of physical model)
- Property (Creation of element section, Identification of material data, Assignment section and material properties to the members)
- Assembly (Assemblage of parts to build up the entire structure)
- Step (Creation of steps and selection of analysis method)
- Interaction (Assemblage of parts to build up the entire structure)

- Load (Identification of load and boundary conditions)
- Mesh (Meshing of structure)
- Job (Creation of jobs and submitting for analysis)
- Visualization (Vizualization of results)
- Sketch (Creation of geometry of physical model)

5.4.1 Abaqus/Standard

Abaqus/Standard can perform static and dynamic analysis by regarding nonlinearity of systems. Abaqus/Standard generally uses Newton Raphson method in order to solve nonlinear problems. Abaqus/Standard uses stifness method to solve linear problems. Stifness matrix is required in both cases. (Abaqus Analysis User's Manual)

5.4.1.1 Source of nonlinearity

Nonlinear stress analysis problems include three sources of nonlinearity such as: material nonlinearity, geometric nonlinearity and boundary nonlinearity as mentioned before.

1) **Material nonlinearity:** This nonlinearity exists if the stress-strain relationship between material is not linear.
2) **Geometric nonlinearity:** This nonlinearity can occur due to large displacements, large strains and large rotations. In Abaqus, the geometric nonlinearity can be ignored while defining a problem as a small displacement analysis. Geometric nonlinearity can be considered while defining a problem as a large displacement analysis. (Abaqus Analysis User's Manual)
3) **Boundary nonlinearity:** This nonlinearity can be resulted from contact problems, nonlinear elastic springs, films, radiation multi-point constraints, etc. (Abaqus Analysis User's Manual)

5.4.1.2 Direct linear equation solver in Abaqus/Standard

Linear equation solution is used both in linear and nonlinear analysis. Abaqus/Standard uses the Newton method in nonlinear analysis. The direct linear equation solver in Abaqus/Standard uses a sparse, direct, Gauss elimination method.

5.4.1.3 Iterative equation solver in Abaqus/Standard

The iterative linear equation solver in Abaqus/Standard can be used for linear and nonlinear static, quasi-static, heat transfer and geostatic analysis. The iterative solution technique in Abaqus/Standard is based on Krylov methods employing a preconditioner. The iterative equation solver uses the following strategy:

1) The Krylov method solver iterates on the system of equations constituted by the finite element method while a preconditioner is applied at each iteration.
2) The preconditioner is calculated only once at the beginning of each linear system solve and it is used to accelerate the convergence of the Krylov Method.

Preconditioning is a procedure of an application of transformation, called the preconditioner, that conditions a given problem into a form that is more suitable for numerical solution. Preconditioning is typically related to reducing a condition number of the problem. The preconditioned problem is then usually solved by an iterative method.

6. FINITE ELEMENT ANALYSES OF BURIED PIPELINES SUBJECTED TO TRANSVERSE PGD

It is necessary to understand how buried pipelines behave when they are subjected to external loading in order to reduce the risk of any accident, material loss and injury. Finite element method is very useful to predict behavior of pipeline subjected to permanent ground deformation. There are certain subjects to be regarded when the pipeline subjected to permanent ground deformation is modeled by using finite element method. These subjects are represented below respectively:

- the modelling of the mechanical behavior of the pipeline;
- the modelling of the mechanical response of the soil surrounding the pipeline;
- the modelling of the interaction between the soil and buried pipeline;
- the modelling of the mechanical response of the soil/pipeline contact surface;
- the geometry and orientation of the pipeline;
- the boundary conditions of model;

T. O'Rourke (1988), Suzuki et al. (1988), Kobayashi et al. (1989), and Liu and M. O'Rourke (1997b) evaluate the response of buried pipeline subjected to spatially distributed transverse PGD by using the finite element approach.

Liu and O'Rourke (1997b) model the pipe as beam element and the interaction between pipe and soil is modeled by using both axial and lateral soil springs. The elasto-plastic soil springs are modeled depending on the TCLEE Guideline (ASCE, 1984). The mechanical behavior of the pipeline is modeled with Ramberg Osgood stress-strain relations for the pipe material. The flexural and axial pipe strains are essentially zero at anchor points so the anchor points are modeled as fixed points.

Liu and M. O'Rourke (1999) proposed a model in order to estimate the pipe strain using the ABAQUS finite element program. They model a pipeline subject to strike-slip faulting in their study. The pipeline is modeled as beam element and the

interaction between pipe and soil is modeled with lateral and axial soil springs. The pipeline model is fixed at the point A and this point is 500m away from the pipe-fault intersection point. The pipe-fault intersection point is represented by point O. The unanchored length is long enough not to generate any axial strain and bending strain at point A. Relative movement between the pipe and the surrounding soil does not occur at point D. In order to simulate strike slip fault event all the bases of soil springs which are standing on the left of fault trace are modeled to be fixed. All the bases of lateral soil springs which are standing on the right of the fault trace move a distance of $\delta_f \sin\beta$ in the Y direction and all the bases of axial soil springs move a distance $\delta_f \cos\beta$ in the X direction. Moreover, the mechanical behavior of pipe material is modeled by using the Ramberg Osgood stress-strain relationship and the nonlinear interaction at pipe-soil interface is modeled depending on the TCLEE Guideline (ASCE, 1984). The model for pipeline subject to strike slip faulting is shown in Figure 6.1.

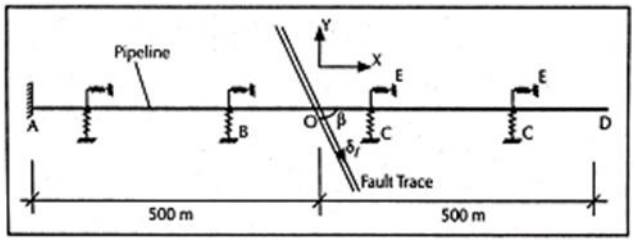

Figure 6.1: Finite element method for pipeline crossing strike-slip fault.

Takada et al. (2001) used a hybrid beam-shell model for FEM analysis by the ABAQUS program. Their analytical model is shown in Figure 6.2. They modeled the part which is between the fixed point and point B as a beam element and assumed that the beam element has only axial elongation.

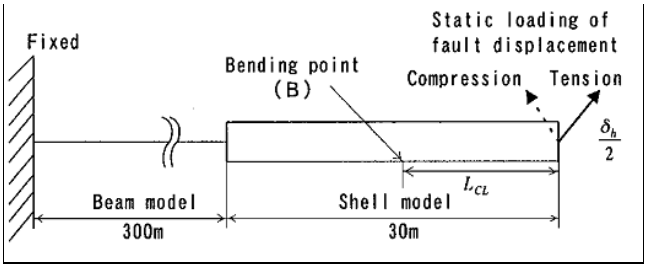

Figure 6.2: Analytical model of pipe (Takada et al., 2001).

The shell elements are used for the part between point B and the fault, which is subjected to section deformation. However, certain length beyond point B is also

modeled by using shell element because the pipe is sliding. Static loading is applied at the pipe-fault crossing point and in the direction of the fault in order to simulate the fault movement.

O'Rourke et al. (2003) have used a set of finite element model in their study. The simplified model for numerical analysis of pipeline subjected to strike slip faulting is shown in Figure 6.3.

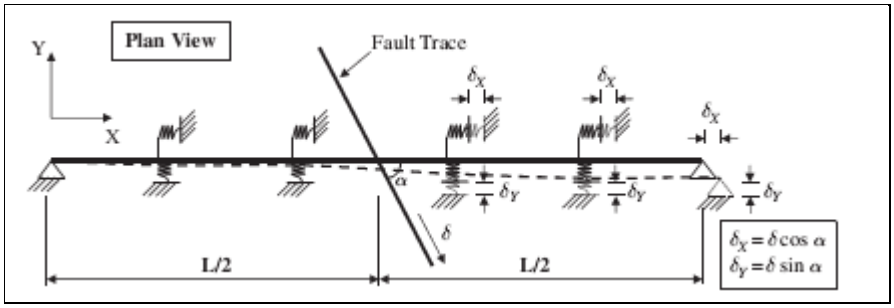

Figure 6.3: Simplified model for numerical analysis of pipeline subjected to strike-slip faulting.

The pipe is modeled by using beam elements while the soil is modeled by using elasto-plastic springs. The corresponding maximum soil spring resistances and yield displacements are used depending on the ASCE Guidelines. The pipe is assumed to be pinned at beginning and end point. The fault offset is simulated by moving the base of all the spring placed on one side of the fault.

Lim et al. (2004) used beam element to model pipe and a series of soil springs to model the interaction between pipe and soil. They developed their model using finite element method based on beam on elastic foundation theory. The slip behavior on the soil-pipeline interface were modeled as elasto-plastic behavior. In order to find soil-pipeline interaction they used the relation between soil stiffness and shear modulus.

Yoshizaki and Oguchi (1996), Yoshizaki et al. (2001) and Yoshizaki and Sakanoue (2004) proposed a modeling technique called hybrid model for simulating a large-scale pipeline and bend response to PGD. Shell elements are used for the bend and neighboring parts where large localized strains occur. The shell elements are linked to beam elements with rigid elements. The soil-pipeline interaction was simulated with discrete spring elements in the longitudinal direction for the beam and in both the longitudinal and circumferential directions for the shell elements.

Karamitros et al. (2007) used hybrid model for the simulation of the pipeline in their study. A part of 50m along both sides of the fault trace was modeled as a cylindrical shell, and the remaining part was modeled as beam elements as shown in Figure 5.4. The shell elements and beam elements were connected with each other by using rigid elements. Each node of the model was connected to axial, horizontal and vertical elasto-plastic soil springs in order to simulate soil-pipeline interaction effects.

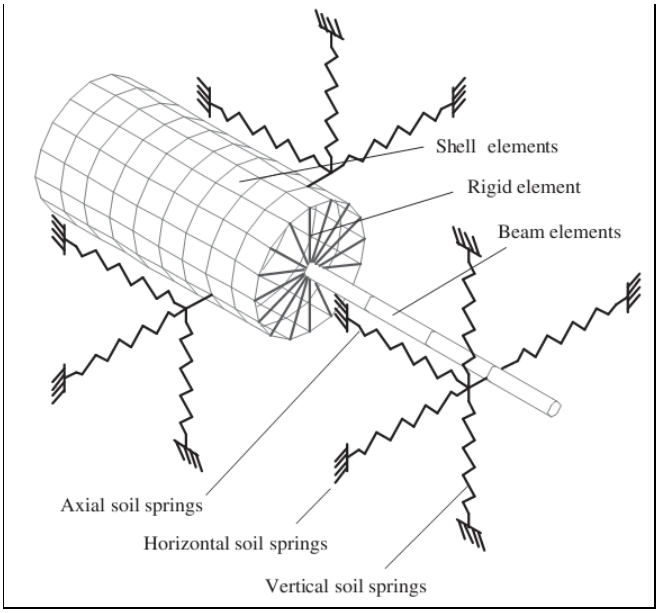

Figure 6.4: Hybrid model for the simulation of the pipeline.

Lee (2010) established practical 3-D model based on the platform of ABAQUS. Whereas shell elements were used to simulate the pipe, the solid continuum elements were used to simulate the soil. In order to define the contacts between the soil and the pipeline tie elements which are types of constraint were used. An elasto-plastic Mohr-Coulomb model was used to simulate soil behavior.

Vazouras et al. (2010, 2012) considered elongated prismatic model where the pipeline is embedded in the soil (Figure 5.5). Brick elements (C3D8R) were used to simulate the surrounding soil and shell elements (S4R) were used to simulate the pipe. An elastic-perfectly plastic Mohr-Coulomb model was considered to model soil behavior. The interaction between soil and pipe was simulated by using contact algorithm. Tangential contact was considered using penalty frictional contact with 0.3 friction coefficient. Normal contact was considered as hard contact with allowing separation of the pipe and soil.

Jafarzadeh et al. (2012) used solid continuum elements to model soil and Mohr-Coulomb behavior model was selected to represent the stresses and strains in soils. The shell elements were used to model the pipe. Tangential contact was used to model the interaction between the pipe and soil by choosing penalty frictional contact (Coulomb frictional formulation) with 0.493 friction coefficient. At the same time, normal contact was used to model the interaction between the pipe and soil by hard contact with allowing separation of surfaces.

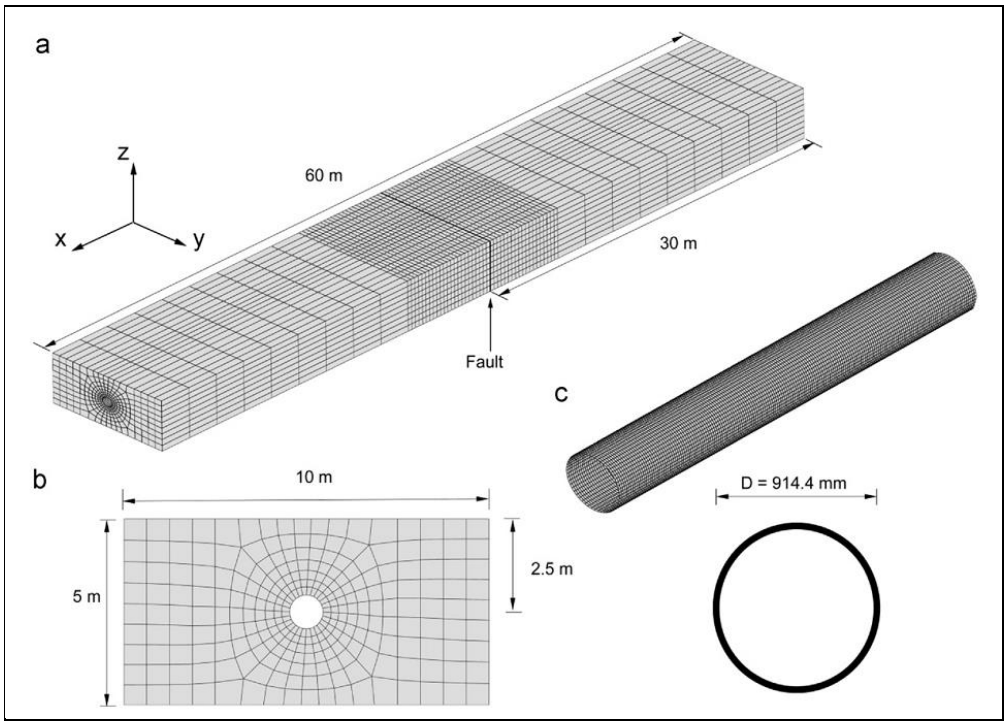

Figure 6. 5: Finite element model of pipeline and soil.

A fine mesh was employed for the central part of pipeline which is close to fault because maximum strain and stresses are expected at this part of the pipeline.

Jafarzadeh et al. (2012) used solid continuum elements to model soil and Mohr-Coulomb behavior model was selected to represent the stresses and strains in soils. The shell elements were used to model the pipe. Tangential contact was used to model the interaction between the pipe and soil by choosing penalty frictional contact (Coulomb frictional formulation) with 0.493 friction coefficient. At the same time, normal contact was used to model the interaction between the pipe and soil by hard contact with allowing separation of surfaces.

6.1 Finite Element Model

When the literature of finite element model of pipelines is researched, it can be seen that the pipe can be modeled as a beam element or a shell element. Moreover, hybrid model that is combination of shell model and beam model can be used to model of pipeline system. In the literature, it can be seen that nonlinear spring element is used for modeling the soil-pipe interaction. On the other hand, the solid continuum model is used for modeling soil behavior, the contact model is used for simulating soil-pipe interaction and the shell element is used for modeling of pipe for 3-D model.

In the scope of this study, the pipe was modeled as a beam element and connector element like nonlinear spring element was used for modeling of soil-pipe interaction. The finite element model of pipeline was generated by using ABAQUS v6.12.

6.1.1 Pipe Model

In this study, four type of steel were used for modeling of pipe. These steel types are X-42, X-52, X-60 and X-70. Elastic and plastic properties of these steels are given in Table 6.1. The plastic properties of steel types such as yield stress and yield strain are calculated with the aid of Ramberg-Osgood relation mentioned in Chapter 4. The beam element was used to model pipe in ABAQUS v6.12. The profile for beam element was chosen as pipe in ABAQUS v6.12. The parameters that were used for pipe profile in the scope of this study are given in Table 6.2 and Table 6.3. The profile parameters are pipe diameter and wall thickness of pipe (Figure 6.6).

Table 6.1: Elastic and plastic properties of different steel types (X-42, X-52, X-60, X-70).

				Ramberg –Osgood Relation	
	Elastic Properties			**Plastic Properties**	
Steel Grade	**Density (kN/m^3)**	**Young's Modulus (kPa)**	**Poisson's Ratio**	**Yield Stress (kPa)**	**Yield Strain**
X-42	78.5	210000000	0.3	310000	0.00215
X-52	78.5	210000000	0.3	358000	0.00310
X-60	78.5	210000000	0.3	413000	0.00348
X-70	78.5	210000000	0.3	517000	0.00323

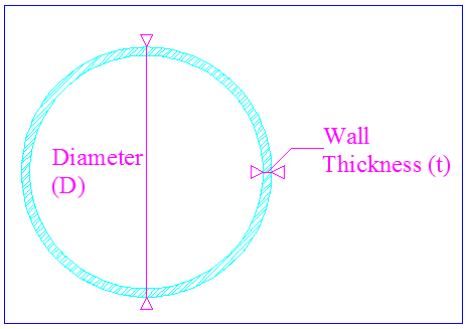

Figure 6.6: The pipe profile

Table 6.2: The parameters used for pipe profile (D=0.61m).

Diameter (D)	Wall Thickness (t)	Moment of Resistance (w)
m	m	m
0.61	0.008	0.00225
0.61	0.007	0.00198
0.61	0.006	0.00170
0.61	0.005	0.00143
0.61	0.004	0.00115
0.61	0.003	0.00086
0.61	0.002	0.00058

Table 6.3: The parameters used for pipe profile (t=0.008m).

Diameter (D)	Wall Thickness (t)	Moment of Resistance (w)
m	m	m
0.5	0.008	0.001497
0.6	0.008	0.002173
0.7	0.008	0.002975
0.8	0.008	0.003902
0.9	0.008	0.004955
1.0	0.008	0.006134

In order to determine the effects of the pipe diameter and the wall thickness of pipe on behavior of pipe subjected to transverse permanent ground deformation these pipe profile parameters were used. The pipe diameter was kept fixed, the wall thickness of pipe was changed for investigating effects of the wall thickness of pipe. On the other hand the pipe diameter was changed, the wall thickness of pipe was kept fixed in order to examine effects of the pipe diameter.

6.2 Pipe-Soil Interaction

In this study, the pipe-soil interaction was modeled by axial and lateral connector elements that simulate soil springs. Because defining nonlinear spring element is not supported ABAQUS/CAE when we define spring that has nonlinear behavior, we used connector element that has spring like elastic behavior. The axial connector elements were linked to pipe with the aid of rigid elements. The rigid elements have very big rigidity so that the rigid element will have very small strain. Therefore, the rigid elements can transfer load from axial connector to pipe effectively. The mechanical properties of rigid element are given Table 6.4. Because it is thought that there will be high stresses in PGD zone, the connector elements are close to each other in PGD zone and in the distance of W/2 from the PGD zone in order to simulate realistic model. The location of connector elements are shown in Figure 6.7.

Table 6.4: Mechanical properties of rigid element

Density (kN/m^3)	Young's Modulus (kPa)	Poisson's Ratio
78	2.00E+16	0.2

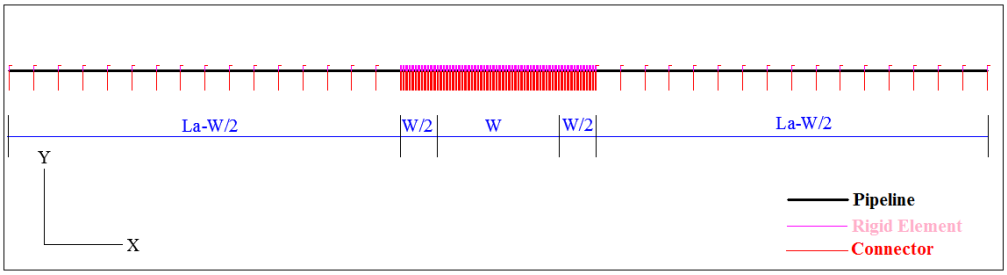

Figure 6.7: The location of connector element

The nonlinear behavior of soil-pipe interaction was simulated by using connector elements. The parameters for the nonlinear behavior of soil-pipe interaction were determined with the aid of equation 4.1 and equation 4.2 in Chapter 4. The maximum resistance and maximum elastic deformation in horizontal transverse (P_u,y_u) and the maximum resistance and maximum elastic deformation in axial (T_u, x_u) for different pipe diameter, different angle of internal friction of backfill surrounding the pipe and different burial depth of pipe are given in Table 6.5, Table 6.6, and Table 6.7.

The maximum elastic deformation is a deformation that the soil reaches its maximum resistance.

Table 6.5: The maximum soil resistance and maximum elastic deformation values for different pipe diameter

			Transverse		Longitudinal	
Angle of Internal Friction	**Diameter (D)**	**Wall Thick. (t)**	**Max. Soil Res. (P_u)**	**Max. El. Def. (y_u)**	**Max.Soil Res. (T_u)**	**Max.El. Def. (x_u)**
^{0}	**(m)**	**(m)**	**(kN/m)**	**(m)**	**(kN/m)**	**(m)**
25	0.61	0.008	61.6	0.13	15.22	0.0038
25	0.61	0.007	61.6	0.13	15.22	0.0038
25	0.61	0.006	61.6	0.13	15.22	0.0038
25	0.61	0.005	61.6	0.13	15.22	0.0038
25	0.61	0.004	61.6	0.13	15.22	0.0038
25	0.61	0.003	61.6	0.13	15.22	0.0038
25	0.61	0.002	61.6	0.13	15.22	0.0038
30	0.61	0.008	88.01	0.1	17.92	0.0038
30	0.61	0.007	88.01	0.1	17.92	0.0038
30	0.61	0.006	88.01	0.1	17.92	0.0038
30	0.61	0.005	88.01	0.1	17.92	0.0038
30	0.61	0.004	88.01	0.1	17.92	0.0038
30	0.61	0.003	88.01	0.1	17.92	0.0038
30	0.61	0.002	88.01	0.1	17.92	0.0038
35	0.61	0.008	135.43	0.06	20.67	0.0038
35	0.61	0.007	135.43	0.06	20.67	0.0038
35	0.61	0.006	135.43	0.06	20.67	0.0038
35	0.61	0.005	135.43	0.06	20.67	0.0038
35	0.61	0.004	135.43	0.06	20.67	0.0038
35	0.61	0.003	135.43	0.06	20.67	0.0038
35	0.61	0.002	135.43	0.06	20.67	0.0038

Table 6.6: The maximum soil resistance and maximum elastic deformation values for different pipe diameter

			Transverse		Longitudinal	
Angle of Internal Friction	**Diameter (D)**	**Wall Thick. (t)**	**Max. Soil Res. (P_u)**	**Max. El. Def. (y_u)**	**Max. Soil Res. (T_u)**	**Max. El. Def. (x_u)**
^{0}	**(m)**	**(m)**	**(kN/m)**	**(m)**	**(kN/m)**	**(m)**
35	0.5	0.008	117.95	0.06	16.94	0.0038
35	0.6	0.008	133.86	0.06	20.33	0.0038
35	0.7	0.008	149.46	0.06	23.72	0.0038
35	0.8	0.008	164.87	0.06	27.11	0.0038
35	0.9	0.008	180.13	0.06	30.50	0.0038
35	1.0	0.008	195.3	0.06	33.89	0.0038

Table 6.7: The maximum soil resistance and maximum elastic deformation values for different burial depth of pipe.

				Transverse		Longitudinal	
Angle of Internal Friction	**Diameter (D)**	**Wall Thick. (t)**	**Burial Depth**	**Max.Soil Res. (P_u)**	**Max. El. Def. (y_u)**	**Max. Soil Res. (T_u)**	**Max. El. Def. (x_u)**
^{0}	**(m)**	**(m)**	**(m)**	**(kN/m)**	**(m)**	**(kN/m)**	**(m)**
35	0.61	0.008	0.6	57.10	0.06	10.34	0.0038
35	0.61	0.008	0.8	81.07	0.06	13.78	0.0038
35	0.61	0.008	1	107.23	0.06	17.23	0.0038
35	0.61	0.008	1.2	135.43	0.06	20.67	0.0038

6.3 PGD zone width, ground displacement and boundary conditions

In this study, the variation of spatially distributed transverse permanent ground deformation is calculated by using O'Rourke (1989) equation. In order to investigate the effects of ground displacement on the pipelines subjected to transverse permanent ground deformation the maximum ground displacement values were taken as 1.3m, 3.0m and 5.0m respectively. Furthermore, widths of PGD zone were taken as 10m, 30m and 50m in order to examine the effects of widths of PGD zone on the pipelines subjected to transverse permanent ground deformation. The anchor length (L_a) was accepted to be equal to 400m as in Liu and M. O'Rourke (1997) finite element model. The anchored length (L_a) is determined to have enough length not to occur axial and flexural deformation. At the same time, the strain that occurs at anchor point is less than $1x10^{-5}$ as in O'Rourke (1998) finite element model. Therefore, it can be seen that there is no boundary effect on the finite element model. The width of PGD zone and the anchored length are shown in Figure 6.8.

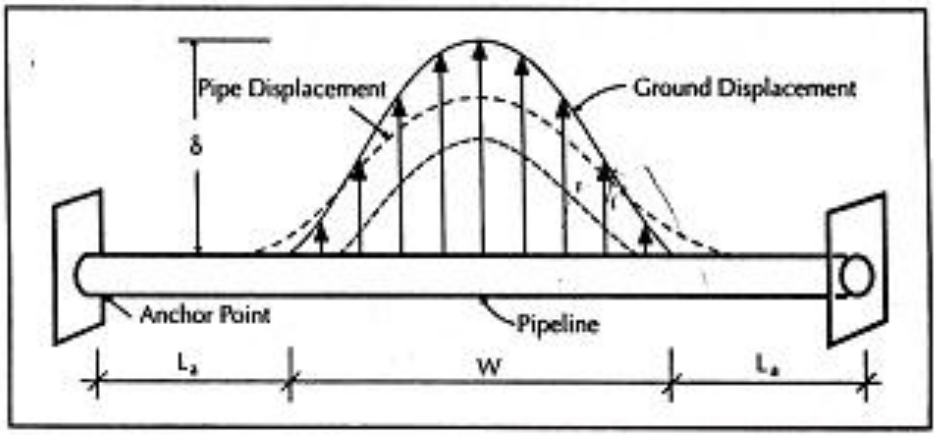

Figure 6.8: The width of PGD zone and the anchored length.

The boundary condition of anchor points is selected as encastre (U1=U2=U3=UR1=UR2=UR3=0). The boundary condition of end point of connector elements which are outside PGD zone is also selected as encastre. The boundary condition of end point of connector elements which are in PGD zone is selected as yasymm (U1=0, U3=0, UR2=0). The boundary conditions are given in Table 5.8. Furthermore, degrees of freedom used in ABAQUS are shown in Figure 6.9.

Table 6.8: The boundary conditions for finite element model.

	U1	**U2**	**U3**	**UR1**	**UR2**	**UR3**	**Boundary Conditions**
Anchor Points	0	0	0	0	0	0	**Encastre**
End point of connectors (I)	0	0	0	0	0	0	**Encastre**
End point of connectors (II)	0	+	0	+	0	+	**Yasymm**

0:Restricted, +:Nonrestricted
(I):outside PGD zone, (II):inside PGD zone

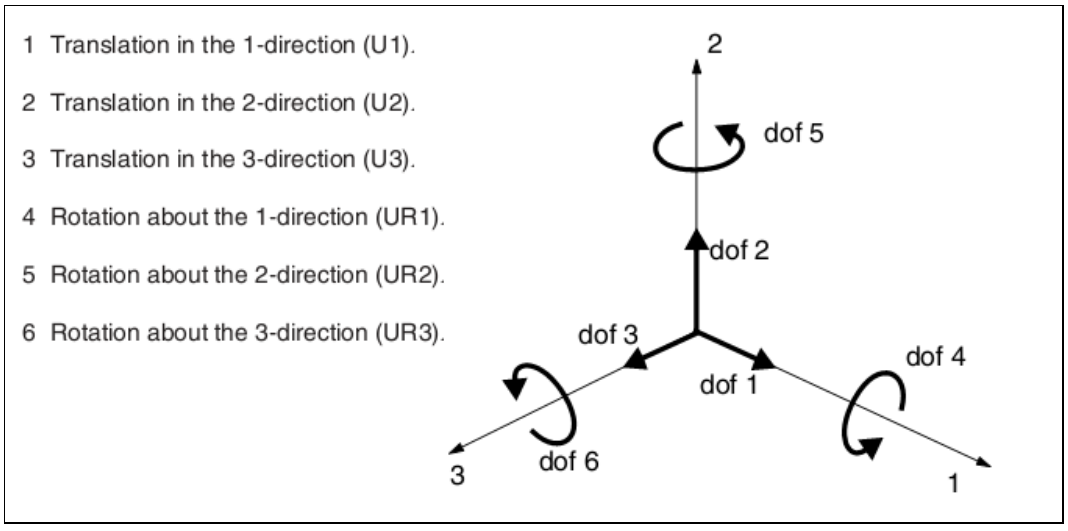

Figure 6.9: Degrees of freedom in ABAQUS.

6.4 Applying the spatially distributed transverse permanent ground displacements to end point of connector elements in PGD zone

There are two steps in the finite element model. The first one is defining boundary conditions, the second one is applying ground displacements to end point of connector element in PGD zone. The spatially distributed transverse permanent ground displacements were calculated as mentioned before.

In the second step, the ground displacements were applied to end point of connector element in PGD zone. The equation used for determining the spatially distributed transverse permanent ground displacement is given in Equation 6.1.

$$y(x)=\frac{\delta}{2}(1-\cos\frac{2\pi x}{W}) \quad \textbf{(6.1)}$$

As seen in Equation 5.1, permanent ground displacement changes with maximum permanent ground displacement (δ), non-normalized distance from the margin of the PGD zone (x) and the width of PGD zone (W). The spatially distributed transverse permanent ground displacements for W=10m and δ=1.3m are given in Table 6.9.

Table 6.9: The spatially distributed transverse permanent ground displacements for W=10m and δ=1.3m.

x	y(x)
0	0.000
0.5	0.032
1.0	0.124
1.5	0.268
2.0	0.449
2.5	0.650
3.0	0.851
3.5	1.032
4.0	1.176
4.5	1.268
5.0	1.300
5.5	1.268
6.0	1.176
6.5	1.032
7.0	0.851
7.5	0.650
8.0	0.449
8.5	0.268
9.0	0.124
9.5	0.032
10.0	0.000

6.5 Mesh Study

The size of mesh element has an great importance for the quality of analysis because increasing the density of the meshed elements gives accurate results. Selecting the optimal number of mesh elements for providing the accuracy of analysis is a difficult problem. There is no standard in order to determine optimum mesh number for the accuracy of analysis. In order to determine the best adaptable mesh number, h-refinement was used. h-refinement is a technique that finds the adaptive mesh size of elements by subdividing the elements into smaller ones (Lo et al., 2010). In this

study, the approximate global size of meshed element which is ranged from 4 meters as a coarse mesh to 0.1 meters as a fine mesh were used. The number of mesh element and the mesh element size corresponding to number of mesh element are given in Table 6.10. The fine mesh provides more accurate results than coarse mesh but at the same time with the increasing the density of meshed elements the analysis time will increase.

Table 6.10: The number of mesh element and mesh element size.

Number of Mesh Element	Mesh Element Size (m)
200	4
264	3
432	2
832	1
1664	0.5
3320	0.25
8304	0.1

Furthermore, p-refinement was also used in this study. The p-refinement is a technique that is performed by changing to higher order polynomial interpolations. The hp-refinement method which is a technique combined with h-refinement and p-refinement. The hp-refinement provides good quality of finite element by decreasing the anticipated errors of results. In Figure 5.4a-c, the Mises stresses and maximum bending strains were obtained for different number of mesh element. It is concluded that the Mises stress and maximum bending strain values converge a certain value. It is observed that quadratic polynomial interpolation converge an accurate value more rapidly than linear interpolation. As a result of this mesh study, 1 m of approximate global size (832 number of mesh element) was found adequate in order to have accurate finite element analysis result. In this mesh study, X-70 steel pipe with D=0.61m was used. The burial depth of the pipe was chosen as 1.2m. The maximum ground displacement was chosen as 1.3m. The widths of PGD zone were chosen as 10m, 30m and 50m respectively. The pipe was assumed to be surrounded by loose to moderately dense sand whose friction angle and density are 35^0 and 18 kN/m^3. Figure 6.10a. demonstrates that the variation of Mises stresses and maximum bending strain with number of mesh element when the width of PGD zone is equal to 10m. Figure 6.10b demonstrates that the variation of Mises stresses and maximum bending strain with number of mesh element when the width of PGD zone is equal to 30m. Figure 6.10c demonstrates that the variation of Mises stresses and maximum

bending strain with number of mesh element when the width of PGD zone is equal to 50m.

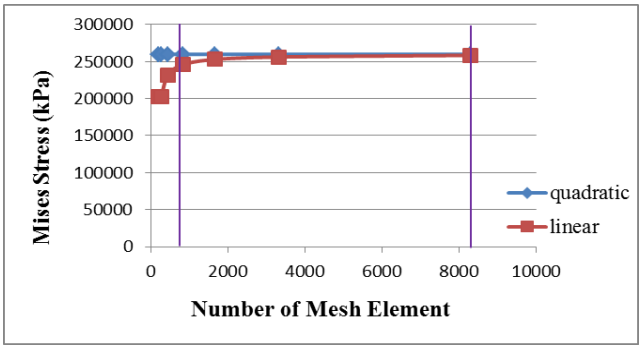

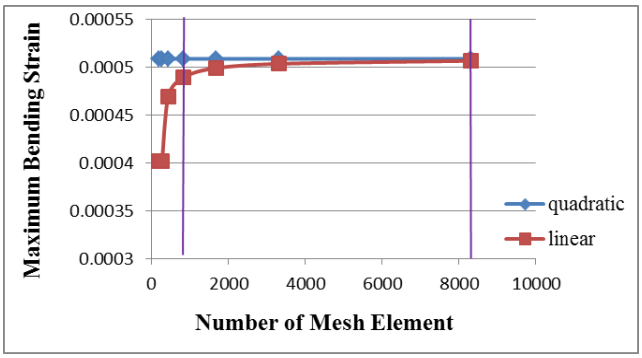

(a)

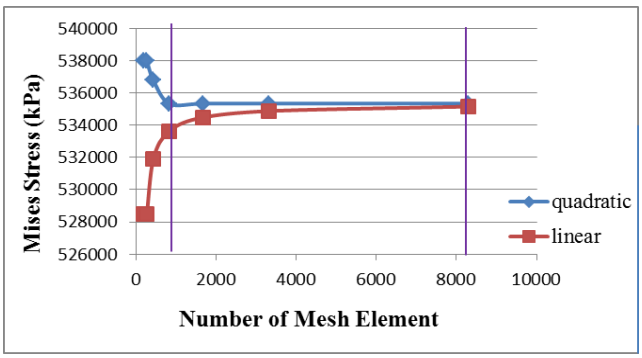

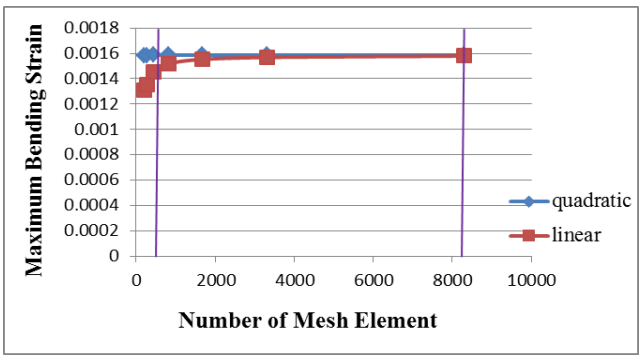

(b)

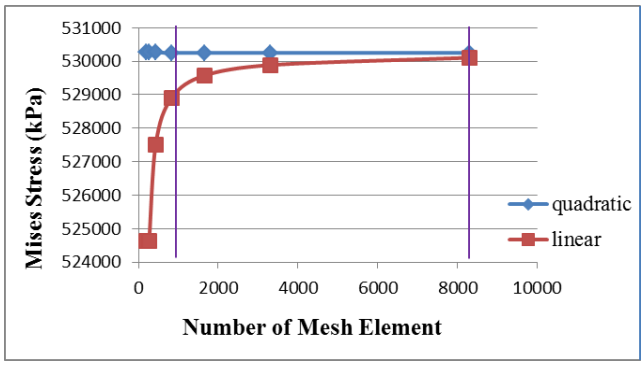

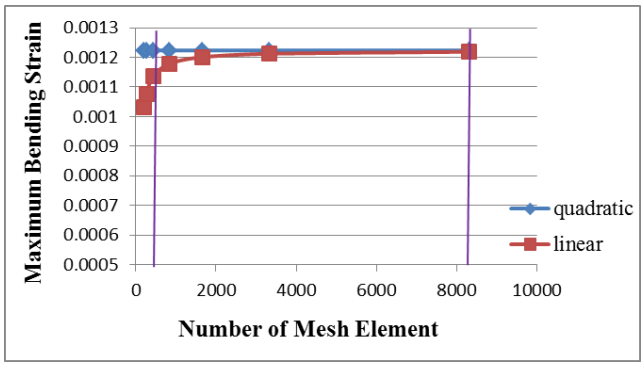

(c)

Figure 6.10: The variation of Mises stresses and maximum bending strains with the number of mesh element (a) W=10m, (b) W=30m, (c) W=50m.

7. ANALYSIS RESULTS

7.1 Effects of Wall Thickness of Pipe on Behavior of Pipeline Subjected to Transverse PGD

The different grade steel pipe with D=0.61m is used for analysis. The burial depth of the pipe is chosen as 1.2m. The maximum ground displacement and the width of PGD zone are chosen as 1.3m, 30m respectively. The pipe is assumed surrounded by loose to moderately dense sand whose angle of internal friction and density are 35^0 and 18 kN/m^3. The variation of maximum pipe displacement for different steel grades depending on wall thickness of pipe is shown in Figure 6.1. X-70 steel pipe has the smallest maximum pipe displacement at the same wall thickness. As seen in Figure 6.1, the pipes behave like a flexible pipe at the small wall thickness value whereas the pipes start to behave like a stiff pipe when the wall thickness of pipes increases. For example, X-70 steel pipe behaves like a flexible pipe up to 0.004 values of wall thickness. After this wall thickness value, the pipe starts to behave like a stiff pipe.

The variation of maximum pipe moment for different steel grades depending on wall thickness of pipe is shown in Figure 6.2. As seen in Figure 6.2, X-70 has the greatest maximum moment capacity. When the steel grade changes from X-42 to X-70 the maximum pipe moment increases at the same wall thickness. The values of maximum moment change with the wall thickness of pipe linearly.

The variation of minimum pipe moment which is referred as maximum negative pipe moment for different steel grades depending on wall thickness of pipe is shown in Figure 6.3. As seen in Figure 6.3, X-70 has the greatest minimum moment capacity. When the steel grade changes from X-42 to X-70 the minimum pipe moment increases at the same wall thickness. The values of minimum moment change with the wall thickness of pipe linearly as in maximum pipe moment.

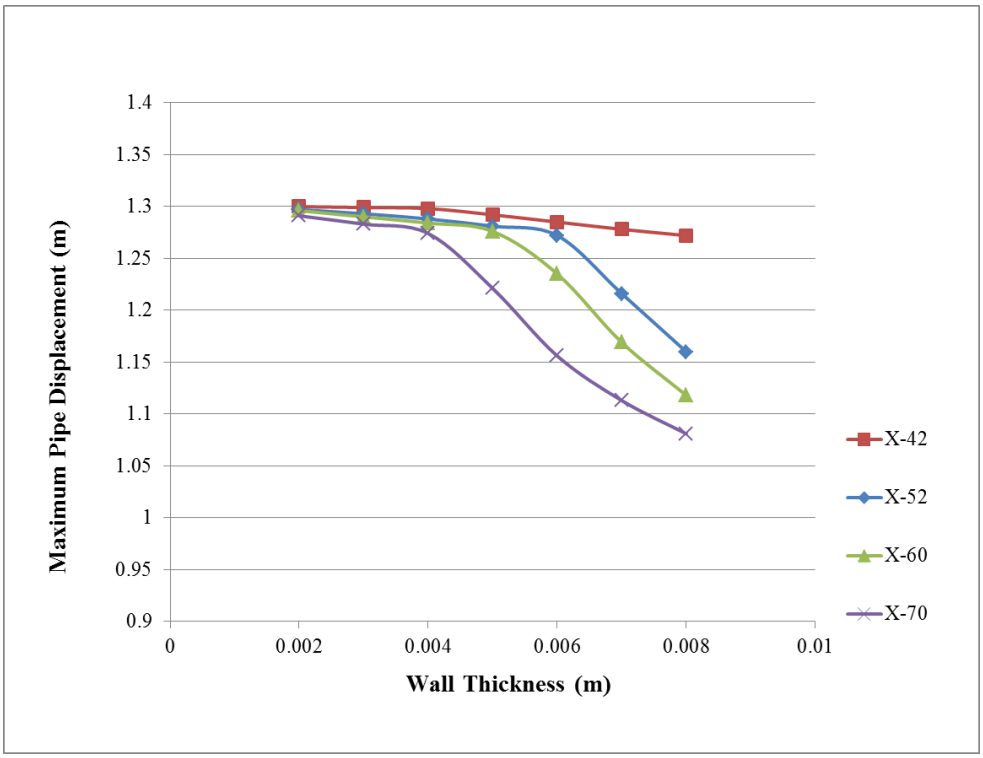

Figure 7.1: The variation of maximum pipe displacement for different steel grades depending on wall thickness of pipe (D=0.61m, W=30m, δ=1.3m, Hc=1.2m)

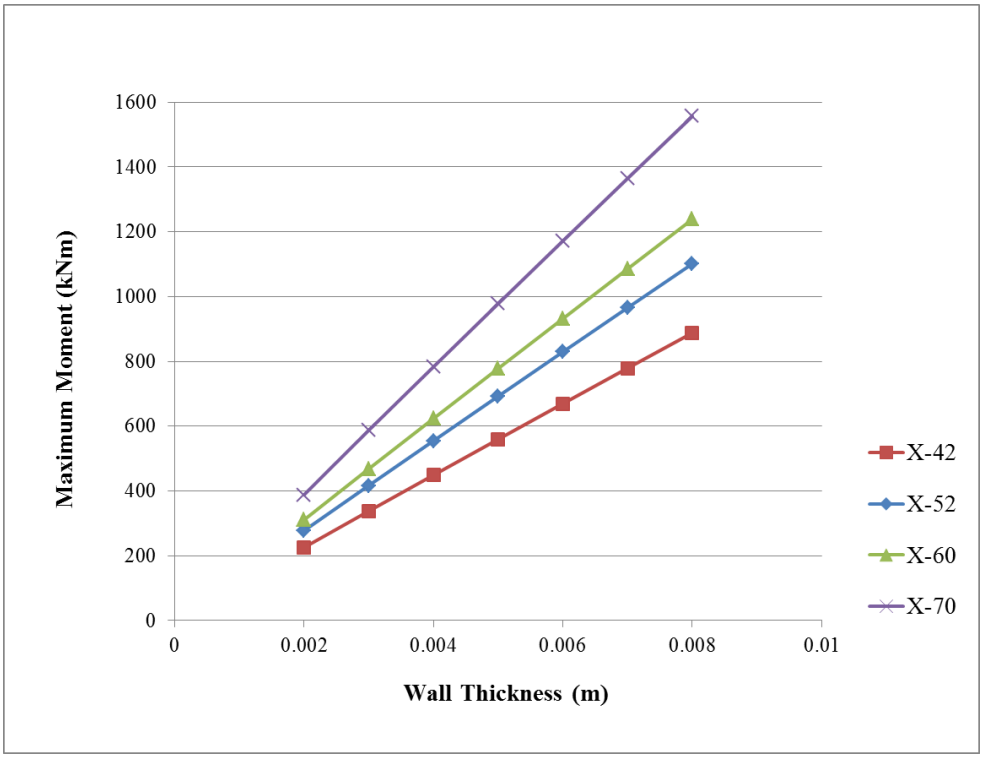

Figure 7.2: The variation of maximum pipe moment for different steel grades depending on the wall thickness of pipe (D=0.61m, W=30m, δ=1.3m, Hc=1.2m)

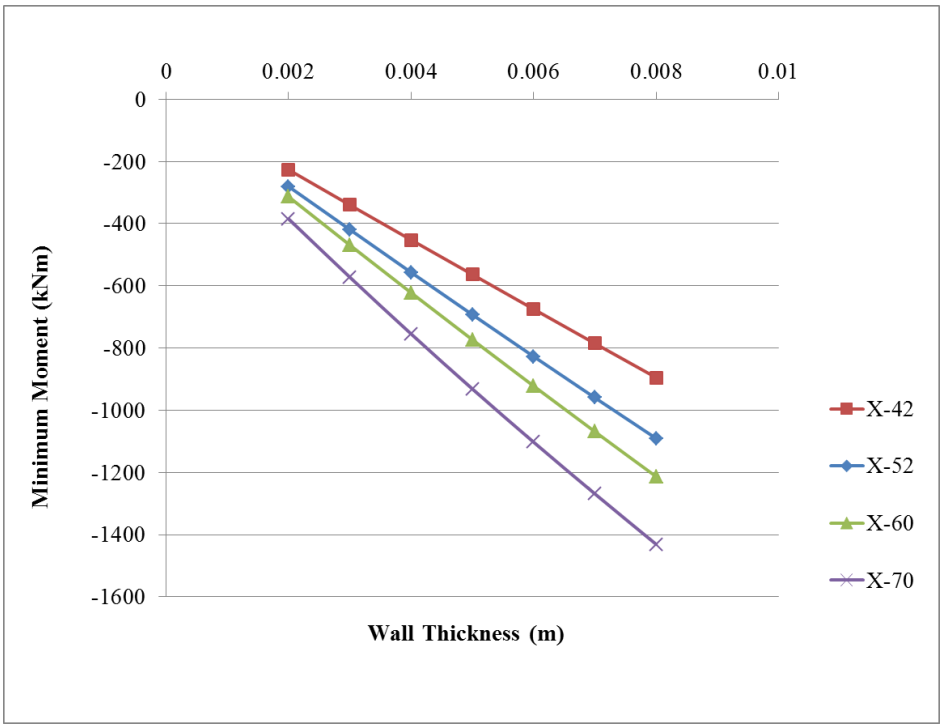

Figure 7.3: The variation of minimum pipe moment for different steel grades depending on the wall thickness of pipe (D=0.61m, W=30m, δ=1.3m, Hc=1.2m)

7.2 Effects of pipe diameter on behavior of pipeline subjected to transverse PGD

The different grade steel pipe with t=0.008m is used for analysis. The burial depth of the pipe is chosen as 1.2m. The maximum ground displacement and the width of PGD zone are chosen as 1.3m, 30m respectively. The pipe is assumed surrounded by loose to moderately dense sand whose angle of internal friction and density are 35^0 and 18 kN/m^3. The variation of maximum pipe displacement for different steel grades depending on pipe diameter is shown in Figure 7.4. X-70 steel pipe has the smallest maximum pipe displacement at the same pipe diameter. When the pipe diameter increases the values of maximum pipe displacement for all type of steel pipe (X-42, X52, X60, X70) approaches each other. For example, at the point that pipe diameter is equal to one meter the values of maximum displacement is nearly the same.

The variation of maximum pipe moment for different steel grades depending on pipe diameter is shown in Figure 7.5. As seen in Figure 7.5, X-70 has the greatest maximum moment capacity. When the steel grade changes from X-42 to X-70 the

maximum pipe moment increases at the same pipe diameter. The values of maximum moment change with the pipe diameter parabolically.

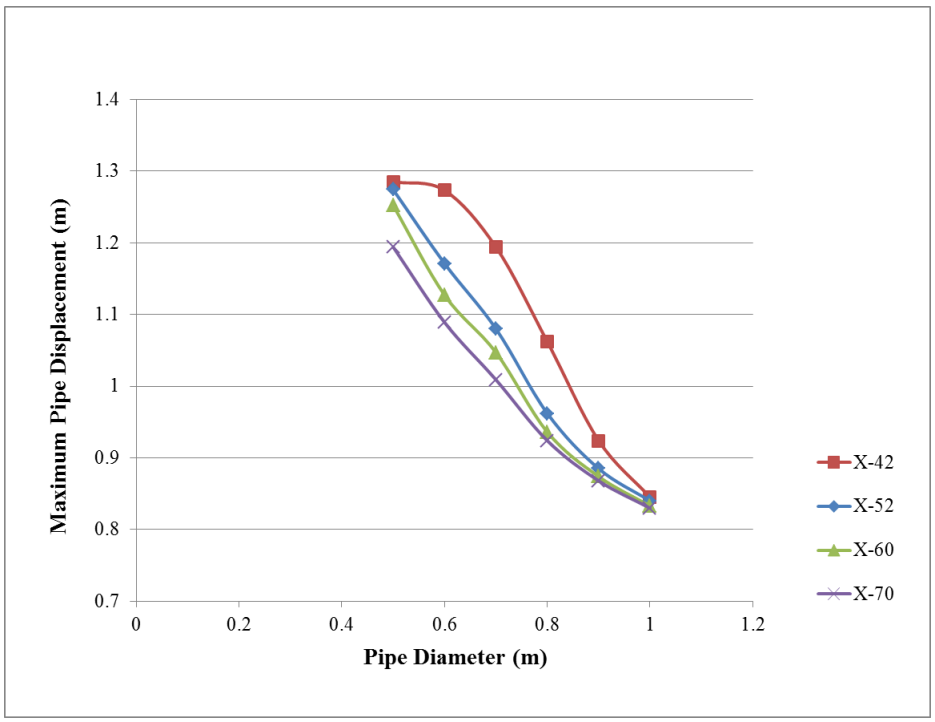

Figure 7.4: The variation of maximum pipe displacement for different steel grades depending on pipe diameter (t=0.008m, W=30m, δ=1.3m, Hc=1.2m)

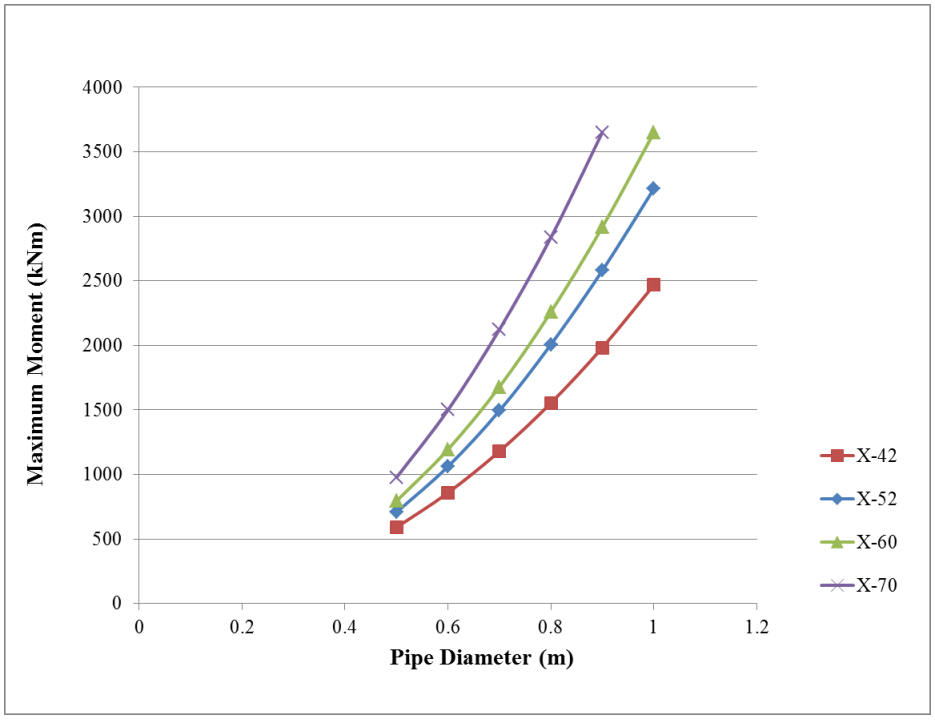

Figure 7.5: The variation of maximum pipe moment for different steel grades depending on pipe diameter (t=0.008m, W=30m, Hc=1.2m).

The variation of minimum pipe moment for different steel grades depending on pipe diameter is shown in Figure 7.6. As seen in Figure 7.6, X-70 has the greatest minimum moment capacity. When the steel grade changes from X-42 to X-70 the minimum moment in pipes increases at the same pipe diameter. The values of minimum moment change with the pipe diameter parabolically.

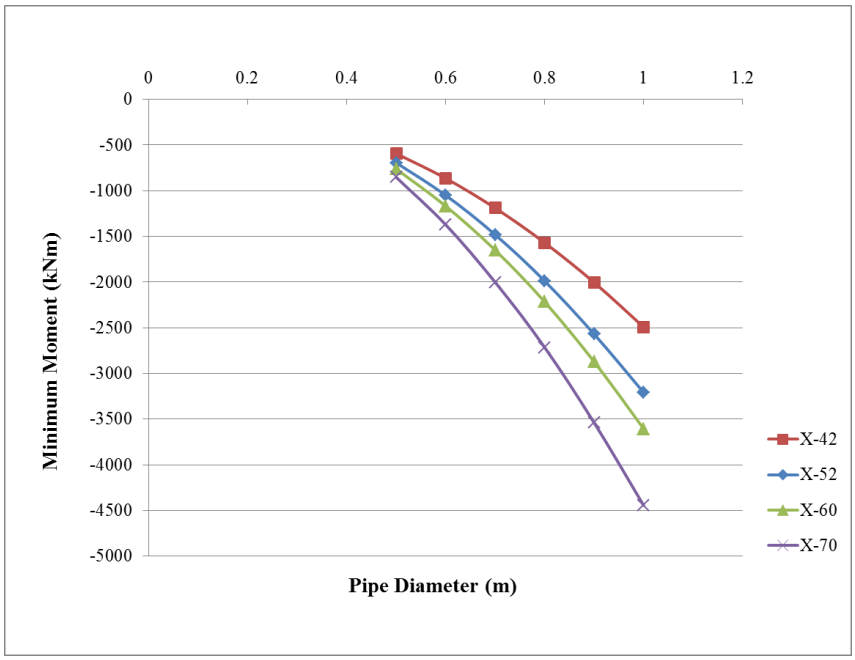

Figure 7.6: The variation of minimum pipe moment for different steel grades depending on pipe diameter (t=0.008m, W=30m, δ=1.3m, Hc=1.2m)

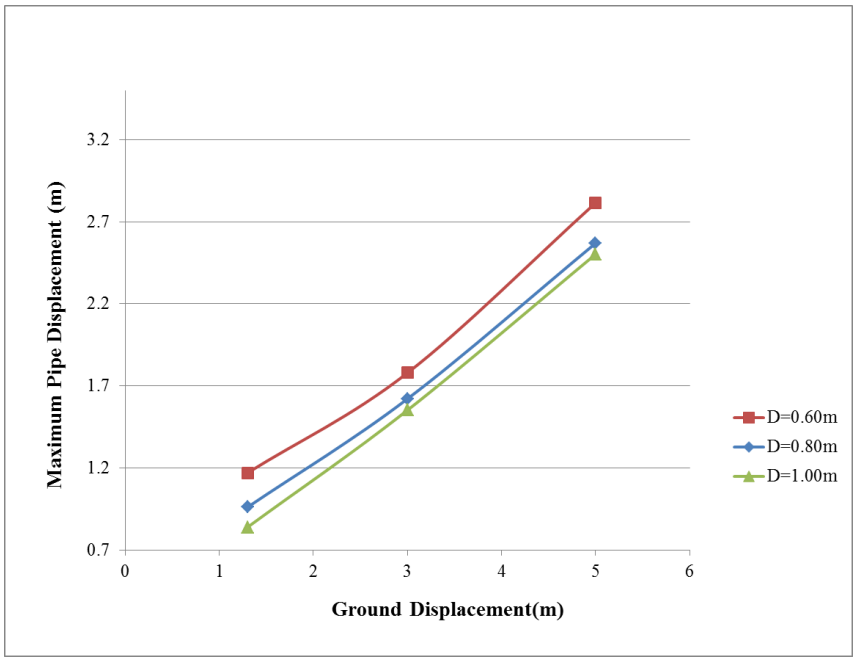

Figure 7.7: The variation of minimum moment for different steel grades depending on pipe diameter (t=0.008m, W=30m, Hc=1.2m).

The variation of maximum pipe displacement according to ground displacement depending on pipe diameter is shown in Figure 7.7. When the ground displacement increases, maximum pipe displacement also increases at the same wall thickness and pipe diameter. Because pipe diameter increases, the bending rigidity of pipe increases. Therefore, the maximum pipe displacement values decreases with an increase in the pipe diameter when the maximum ground displacement increase. When the pipe diameter and the maximum ground displacement increase the values of maximum pipe displacement for all type of steel pipe (X-42, X52, X60, X70) approaches each other.

7.3 Effects of ground displacement on behavior of pipeline subjected to transverse PGD

The different grade steel pipe with D=0.61m, t=0.008m is used for analysis. The burial depth of the pipe is chosen as 1.2m. The width of PGD zone is chosen as 30m. The pipe is assumed surrounded by loose to moderately dense sand whose angle of internal friction and density are 35^0 and 18 kN/m^3. The variation of maximum pipe displacement for different steel grades depending on ground displacement is shown in Figure 7.8.

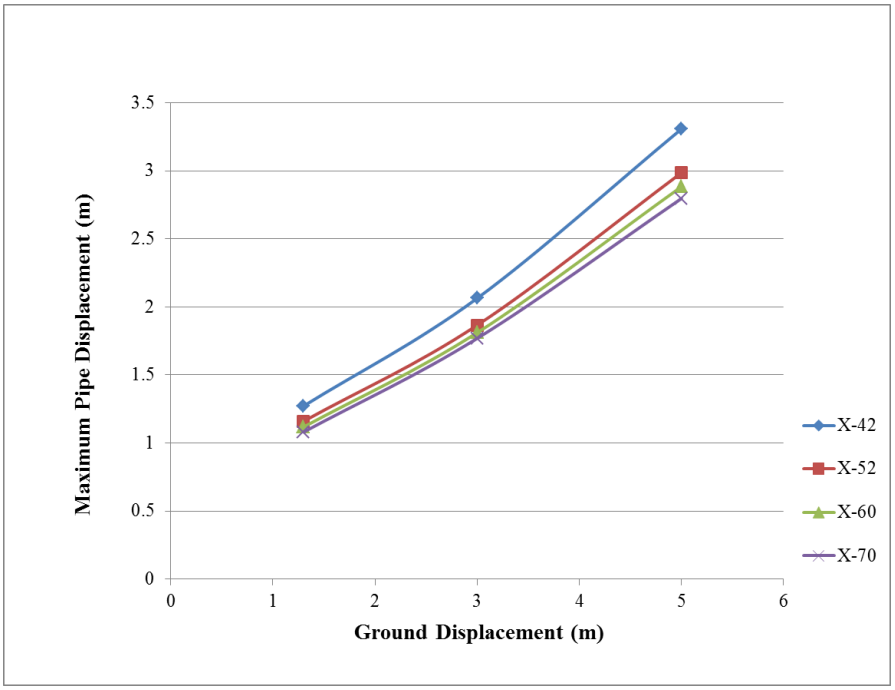

Figure 7.8: The variation of maximum pipe displacement for different steel grades depending on ground displacement (D=0.61m, t=0.008m, W=30m, Hc=1.2m).

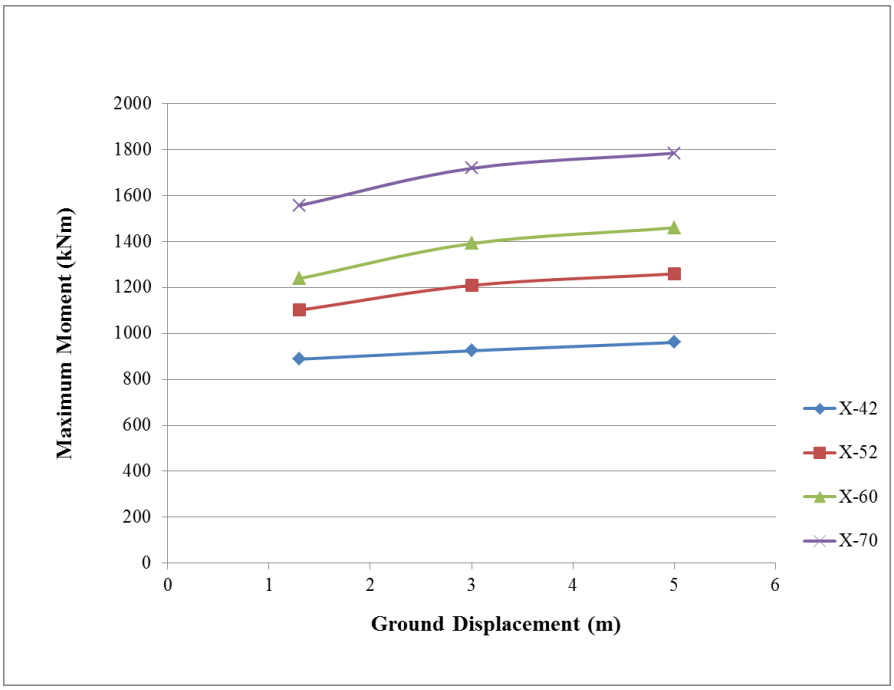

Figure 7. 9: The variation of maximum pipe moment for different steel grades depending on ground displacement (D=0.61m, t=0.008m, W=30m, Hc=1.2m).

The maximum pipe displacement increases with an increase in ground displacement. X-42 has the greatest maximum pipe displacement and the other steel grades (X-52, X-60, X-70) have nearly the same maximum pipe displacement at the same ground displacement. X-70 steel pipe has the least maximum pipe displacement at the same ground displacement. The variation of maximum pipe moment for different steel grades depending on ground displacement is shown in Figure 7.9. Maximum moment increase with an increase in the ground displacement and maximum moment converge to a value when the ground displacement increases.

The greatest maximum moment occurs in X-70 steel pipe. The least maximum moment occurs in X-42 steel pipe. The incline of maximum moment curve decreases with an increase in ground displacement.

The variation of minimum pipe moment for different steel grades depending on ground displacement is shown in Figure 7.10. Minimum moment increase with an increase in the ground displacement and minimum moment converge to a value when the ground displacement increases. The greatest minimum moment occurs in X-70 steel pipe. The least minimum moment occurs in X-42 steel pipe. The incline of minimum moment curve decreases with an increase in ground displacement.

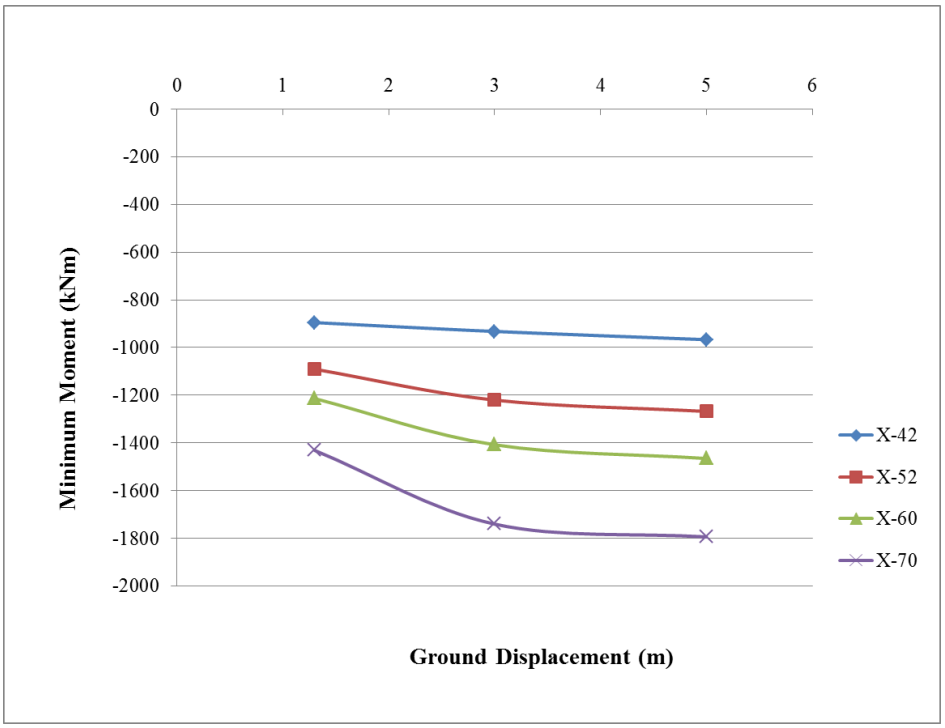

Figure 7.10: The variation of minimum pipe moment for different steel grades depending on ground displacement (D=0.61m, t=0.008m, W=30m, Hc=1.2m).

7.4 Effects of width of PGD zone on behavior of pipeline subjected to transverse PGD

X-70 grade steel pipe with D=0.61m, t=0.008m is used for analysis. The burial depth of the pipe is chosen as 1.2m. The pipe is assumed surrounded by loose to moderately dense sand whose angle of internal friction and density are 35^0 and 18 kN/m^3. The widths of PGD zone are chosen as 10m, 30m and 50m. The maximum ground displacements are chosen as 1.3m, 3.0m and 5.0m. Figure 7.11 demonstrates the variation of the maximum pipe displacement for different width of PGD zone depending on ground displacement. In this figure, when the width of PGD zone is equal to 50m the pipe behaves like a flexible pipe. When the width of PGD zone decreases the pipe behaves like a stiff pipe at the same ground displacement. The maximum ground displacement and the maximum pipe displacement fit each other up to a certain ground displacement. This ground displacement is named as critical ground deformation. Figure 7.12, Figure 7.13 and Figure 7.14 shows the variation of the maximum pipe displacement for different width of PGD zone depending on the wall thickness of pipe. The pipe behaves like a flexible pipe at all values of wall thickness and ground displacement when the PGD zone is equal to 50m. The pipe

behaves like a flexible up to that the ground displacement is equal to 1.1m for that PGD zone is equal to 30m. When the width of PGD zone is equal to 10m the pipe behaves like a stiff pipe for all ground displacement value and for all the wall thickness value. Because of an increase in the wall thickness, the maximum pipe displacement decreases for all ground displacement values.

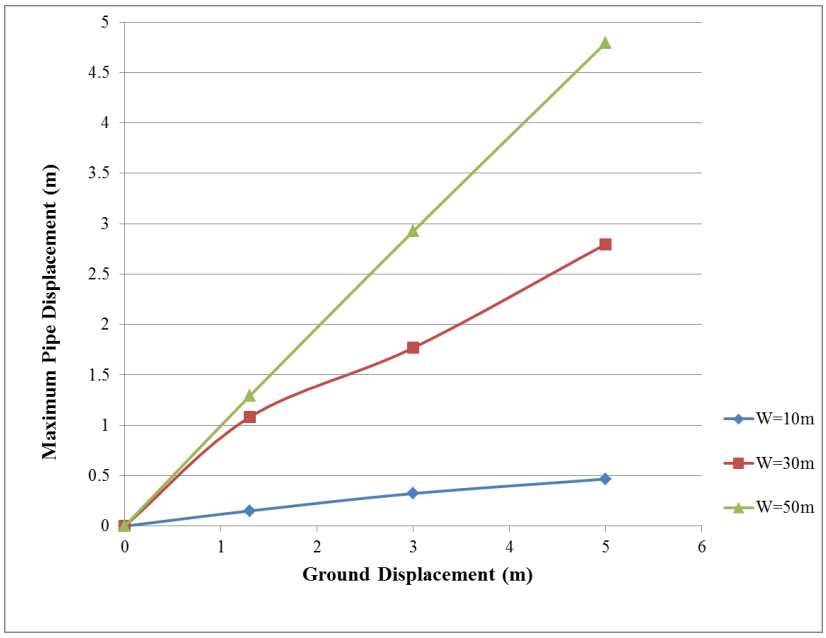

Figure 7.11: The variation of the maximum pipe displacement for different width of PGD zone depending on ground displacement (D=0.61m, t=0.008m, X-70, Hc=1.2m).

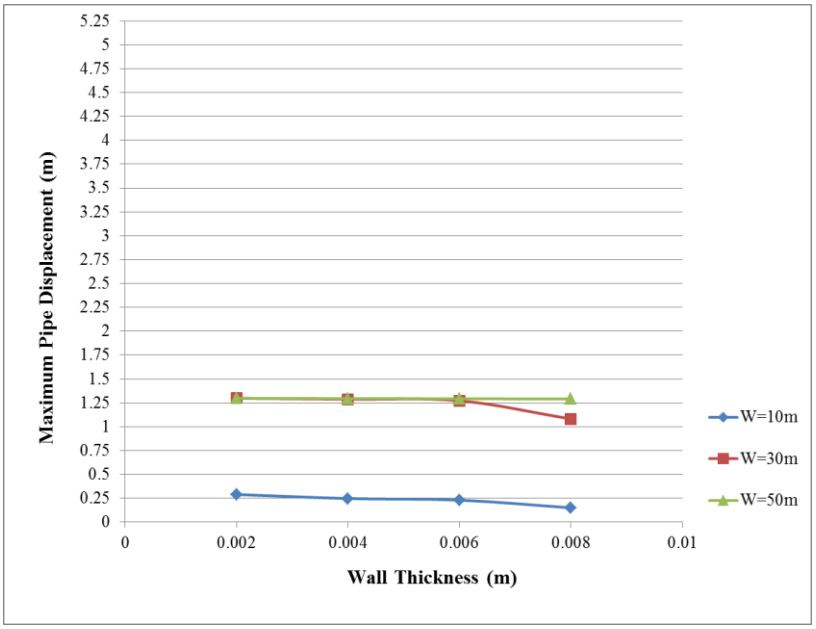

Figure 7.12: The variation of the maximum pipe displacement for different width of PGD zone according to wall thickness of pipe (D=0.61m, δ=1.3m, X-70, Hc=1.2m).

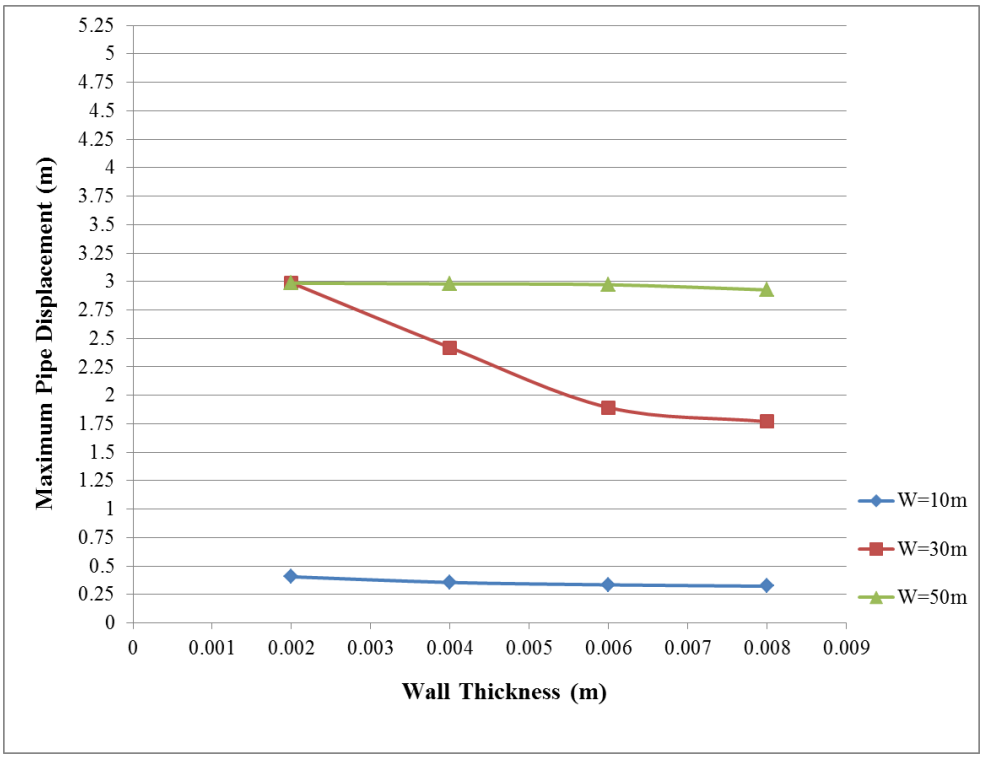

Figure 7.13: The variation of the maximum pipe displacement for different width of PGD zone depending on wall thickness of pipe (D=0.61m, δ=3.0m, X-70, Hc=1.2m).

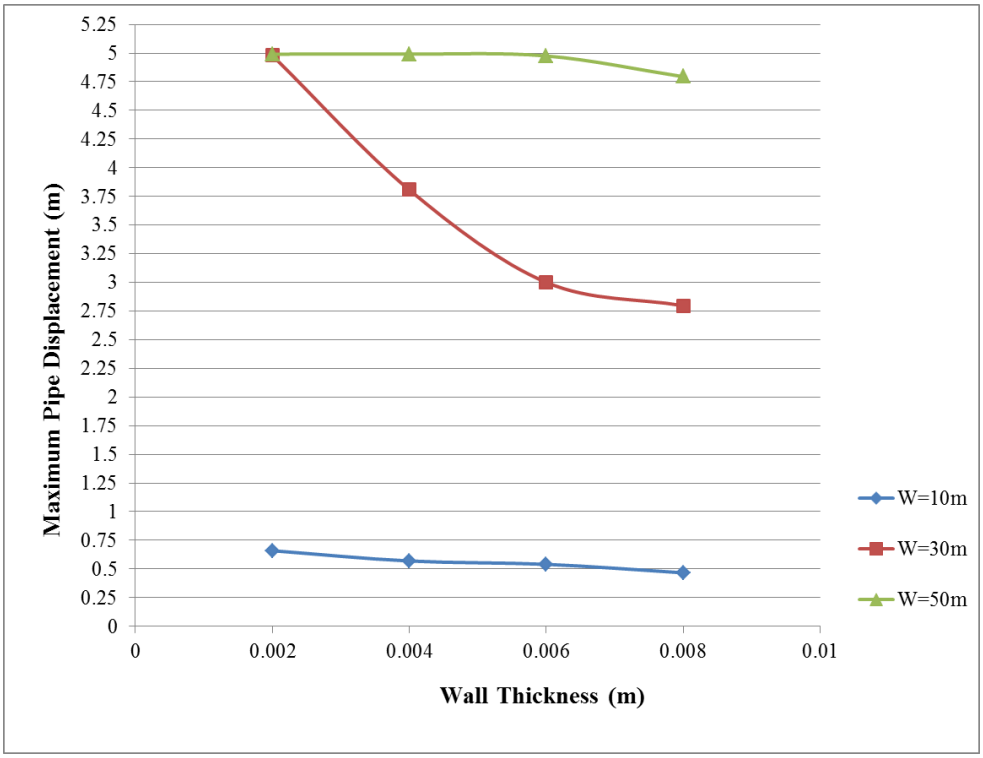

Figure 7.14: The variation of the maximum pipe displacement for different width of PGD zone depending on wall thickness of pipe (D=0.61m, δ=5.0m, X-70, Hc=1.2m).

7.5 Effects of angle of internal friction of backfill soil on behavior of pipeline subjected to transverse PGD

X-70 grade steel pipe with D=0.61m is used for analysis. The burial depth of the pipe is chosen as 1.2m. The maximum ground displacement and the width of PGD zone are chosen as 1.3m, 30m respectively. The angle of internal friction of backfill values are chosen as 25^0, 30^0 and 35^0. Figure 7.15 shows the variation of the maximum pipe displacement for different angle of internal friction of backfill depending on wall thickness of pipe. When angle of internal friction of backfill increase the maximum pipe displacement increases at the same wall thickness. Figure 7.16 and Figure 7.17 show the variation of the maximum and minimum pipe moment for different angle of internal friction of backfill depending on ground displacement. The maximum pipe moment is nearly the same at the same wall thickness of pipe. Therefore, the change of angle of internal friction of pipe does not affect the maximum pipe moment when the ground displacement is equal to 1.3m and when the width of PGD zone is equal to 30m. On the other hand, the change in the angle of internal friction angle causes the increase in the minimum pipe moment.

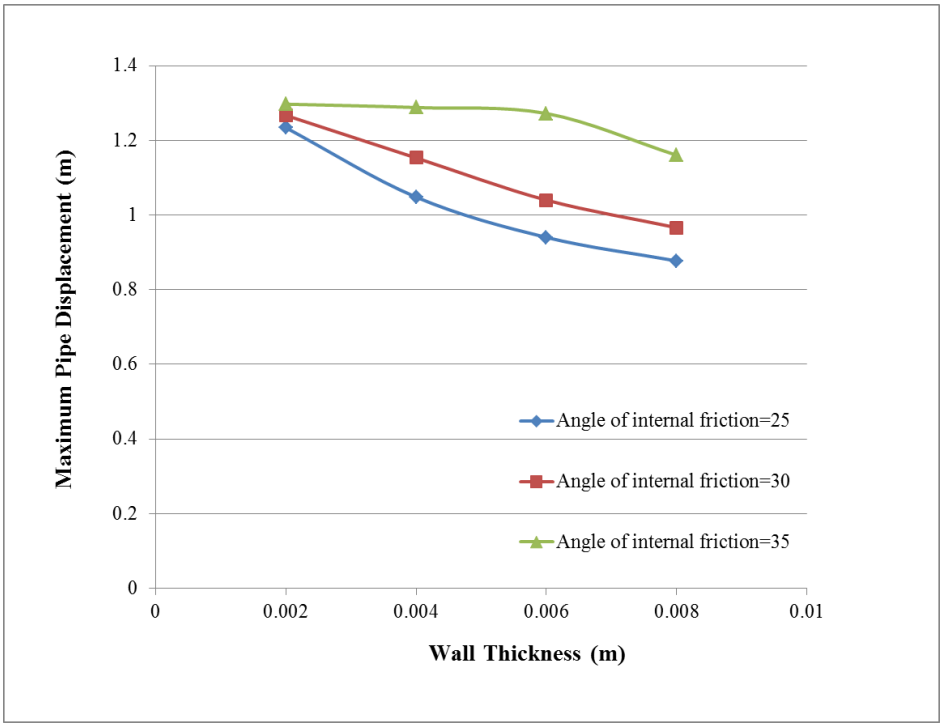

Figure 7.15: The variation of the maximum pipe displacement for different angle of internal friction of backfill depending on wall thickness of pipe (D=0.61m, δ=1.3m, W=30m, X-70, Hc=1.2m).

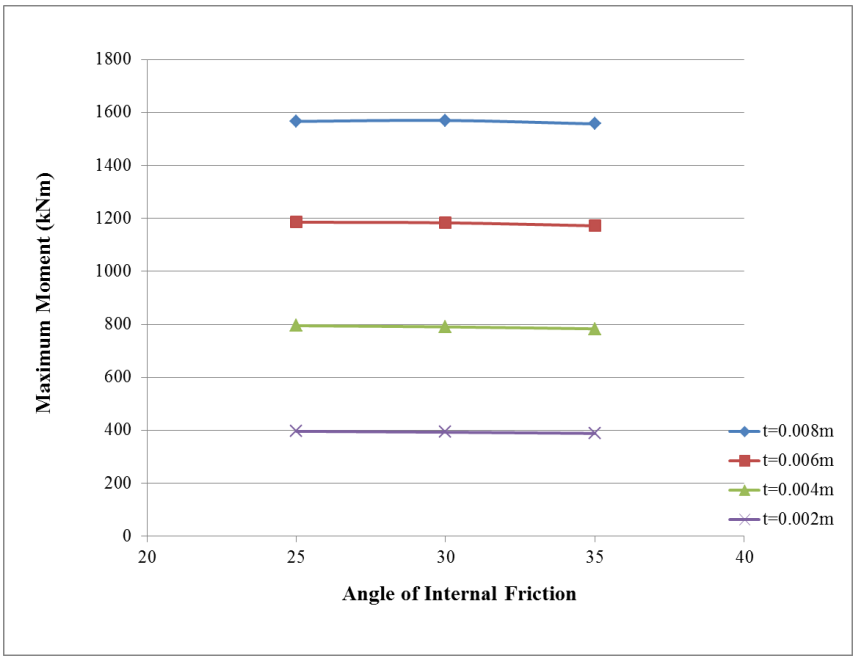

Figure 7. 16: The variation of the maximum moment for different angle of internal friction of backfill according to ground displacements (D=0.61m, W=30m, X-70, Hc=1.2m).

Figure 7.18 demontrates the variation of the maximum displacement for different angle of internal friction of backfill depending on ground displacements. Due to an increase in the angle of internal friction of backfill, the maximum pipe displacement increases for all ground displacement values.

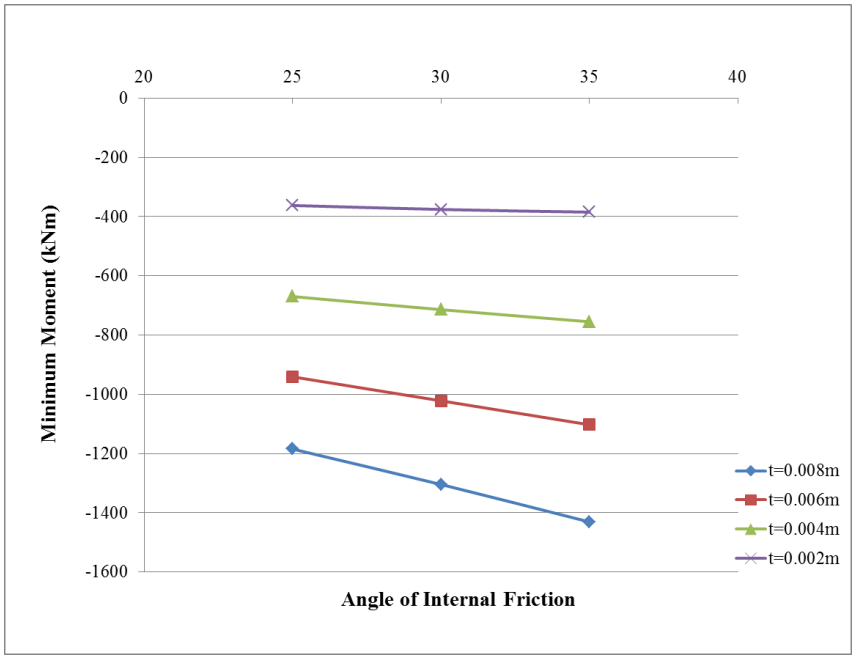

Figure 7. 17: The variation of the minimum moment for different angle of internal friction of backfill depending on wall thickness of pipe (D=0.61m, δ =1.3m, W=30m, X-70, Hc=1.2m).

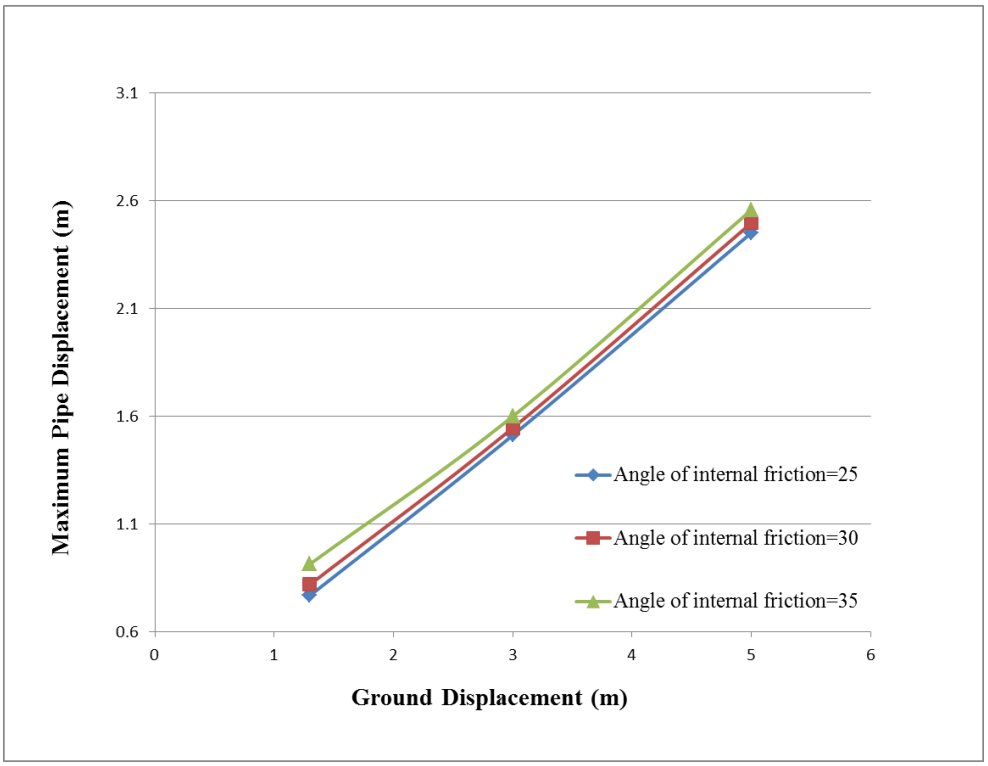

Figure 7.18: The variation of the maximum displacement for different angle of internal friction of backfill depending on ground displacements (D=0.61m, W=30m, X-70, Hc=1.2m).

7.6 Effects of burial depth of pipe on behavior of pipeline subjected to transverse PGD

X-70 grade steel pipe with D=0.61m, t=0.008m is used for analysis. The width of PGD zone is chosen as 30m. The pipe is assumed surrounded by loose to moderately dense sand whose friction angle and density are 35^0 and 18 kN/m^3. The variation of maximum pipe displacement for different ground displacement depending on the burial depth of pipe is shown in Figure 7.19. When the burial depth of pipe increases the maximum pipe displacement increases. The maximum pipe displacement changes with the burial depth linearly. Figure 7.20 shows the variation of maximum pipe moment for different angle of internal friction of backfill soil depending on wall thickness of pipe. When the maximum ground displacement is equal to 1.3m the maximum pipe moment decreases with the wall thickness of pipe linearly. The maximum pipe moment decreases with the burial depth of pipe parabolically when the maximum ground displacement is equal to 3.0m and 5.0m. The maximum pipe moment values approach each other when the maximum ground displacement increases.

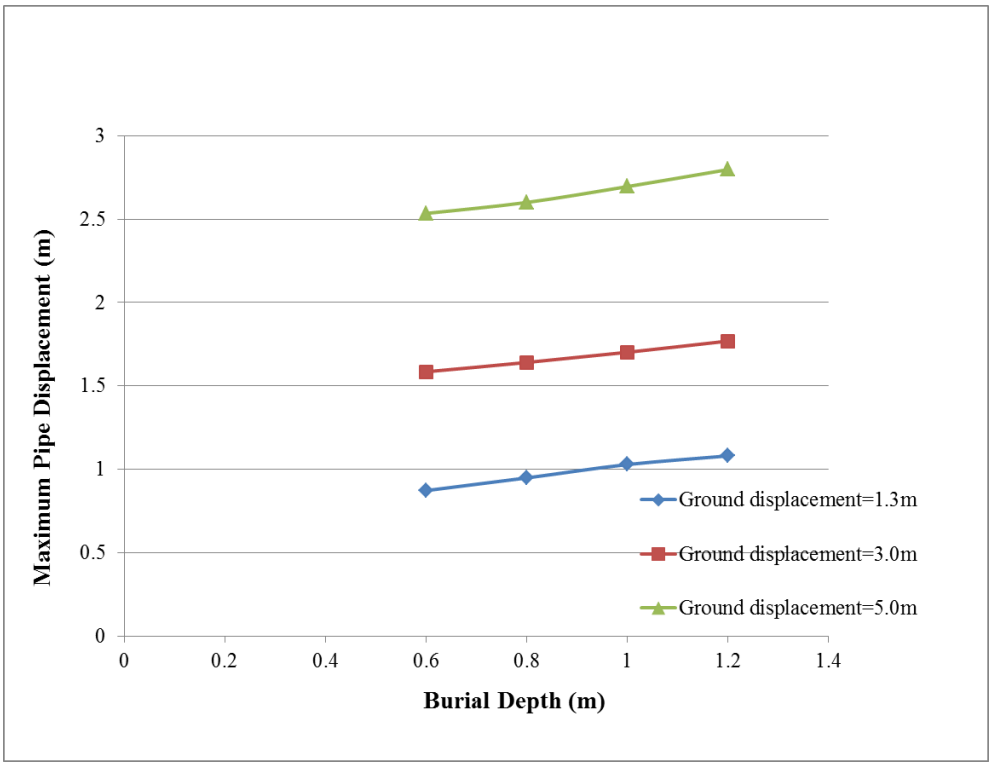

Figure 7.19: The variation of the maximum pipe displacement for different ground displacement depending on burial depth of pipe (D=0.61m, W=30m, X-70, Hc=1.2m).

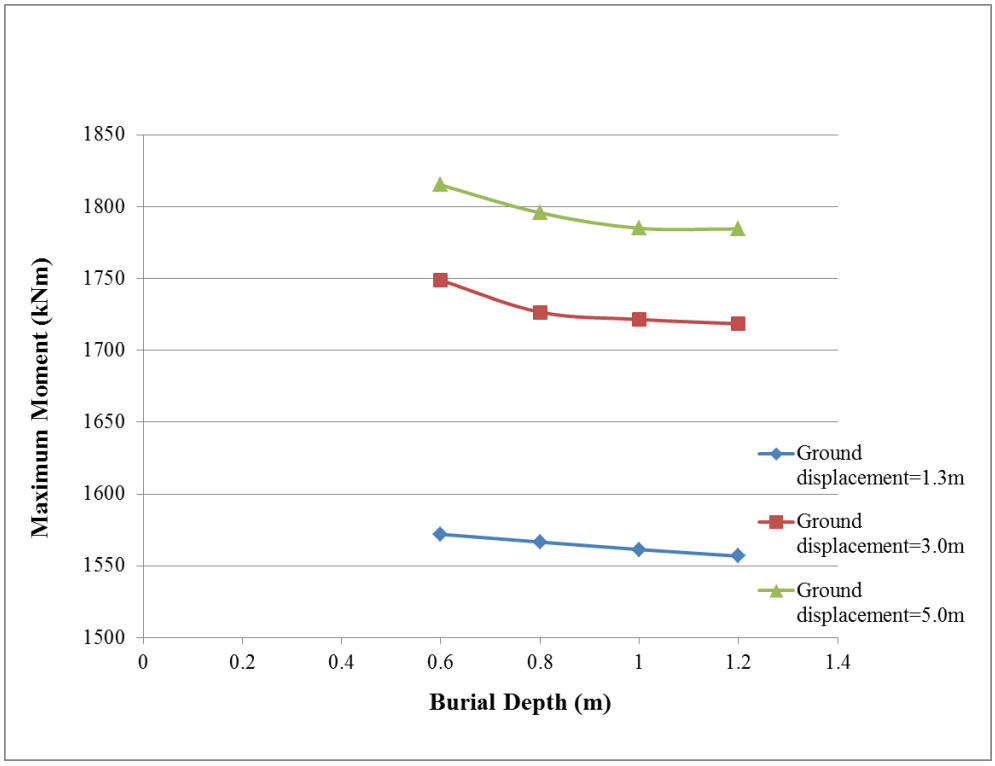

Figure 7.20: The variation of the maximum pipe moment for different angle of internal friction of backfill depending on wall thickness of pipe (D=0.61m, δ=1.3m, W=30m, X-70, Hc=1.2m).

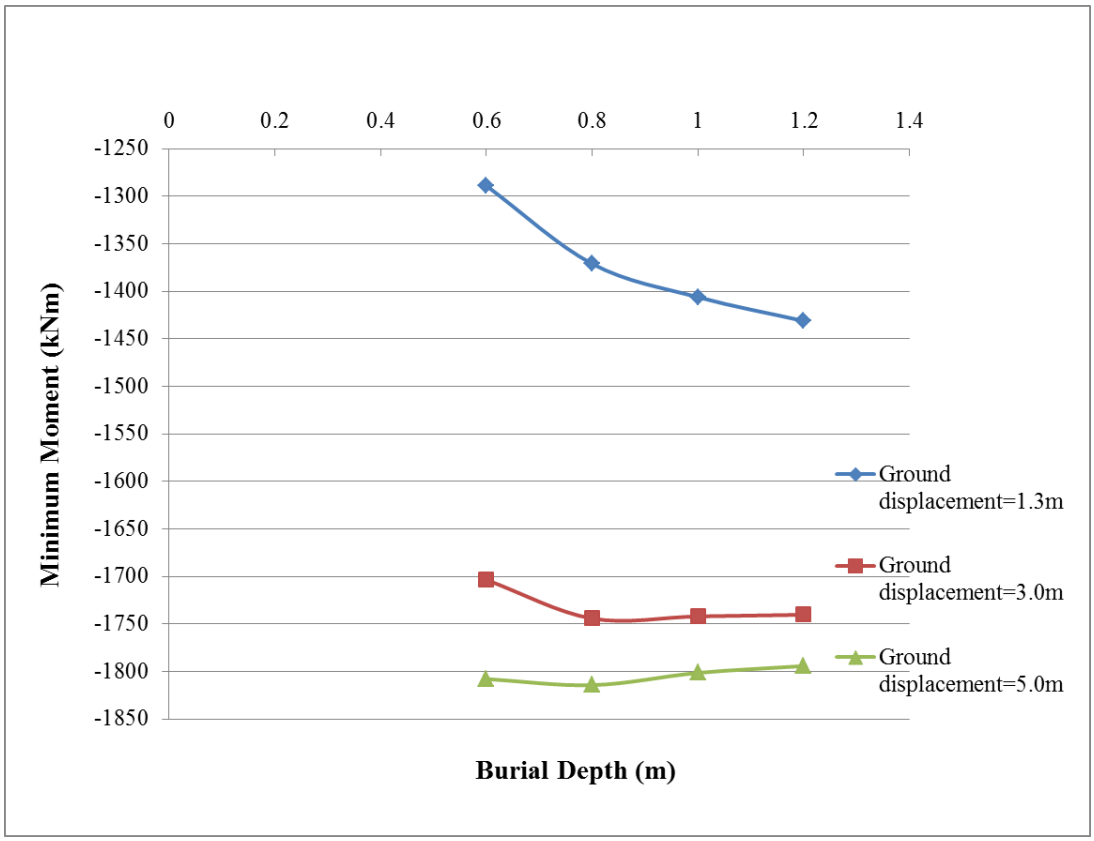

Figure 7.21: The variation of the minimum pipe moment for different angle of internal friction of backfill depending on wall thickness of pipe (D=0.61m, δ=1.3m, W=30m, X-70, Hc=1.2m).

7.7 Pipe and ground displacement for different width of PGD zone

X-70 grade steel pipe with D=0.61m, t=0.008m is used for analysis. The burial depth of the pipe is chosen as 1.2m. The maximum ground displacement is chosen as 1.3m. The pipe is assumed surrounded by loose to moderately dense sand whose friction angle and density are 35^0 and 18 kN/m^3. Ground displacement and pipe displacement caused by ground displacement is shown for different width of PGD zone in Figure 7.22, Figure 7.23 and Figure 7.24. When the width of PGD zone is equal to 10m the pipeline is relatively stiff and the pipe lateral displacement is less than soil. For W=30m and W=50m, the pipeline behaves like a flexible pipe. For these cases, the pipeline is relatively flexible and its lateral displacement is assumed to closely match of the soil. Especially, the pipeline behaves like a flexible pipe for that the width of PGD zone is equal to 50m.

Hetenyi (1946), Vlazov and Leontiev (1966), Gorbunov et al. (1961) and Vesic (1961a,b) proposed a classification system for finite beams according to (λl, $\lambda^* l$, $\lambda_E l$,

λl) a measure of relative flexibility of the beam-soil system. Hetenyi (1946) used λl parameter to classify the finite beams resting on a Winkler medium such as short beams, beams of medium length and long beams. Vlazov and Leontiev (1966) used $\lambda^* l$ parameter to classify the finite beams resting on a two parameter medium such as short beams, beams of intermediate length and long beams whereas Gorbunov et al. (1961) used $\lambda_E l$ parameter in order to classify the finite beams on an elastic soil medium such as short beams, beams of medium length and long beams. Vesic (1961a,b) used λl parameter to classify the finite beams resting on elastic media such as short beams, beams of medium length, moderately long beams and long beams.

The flexural deformations in short beams can be neglected and the short beams satisfy the conditions for the conventional rigid beam analysis of footings. Therefore, the short beam can be treated as an infinitely rigid footing.

Beams of medium length and long beams can be classified as finite flexible beams. Furthermore, long beams have the length of beam which is large enough to neglect effects of end conditioning forces. For long beams, the analytical techniques which are used for the infinite beam can be performed.

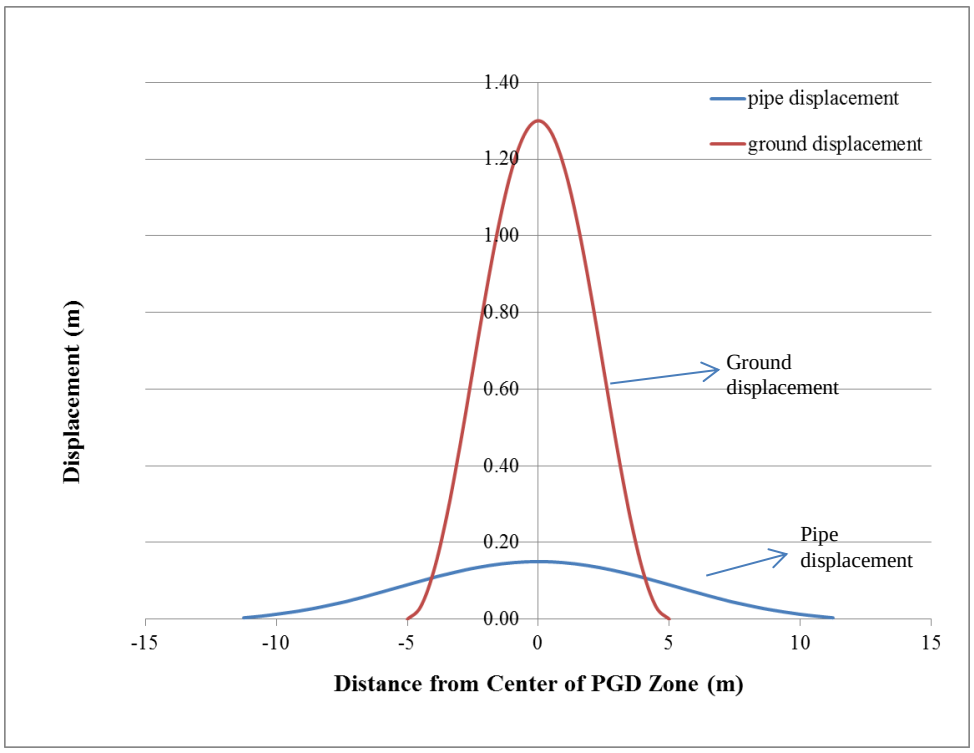

Figure 7.22: Pipe displacement and ground displacement for different width of PGD zone (D=0.61m, 0.008m, δ=1.3m, W=10m, Hc=1.2m, X-70).

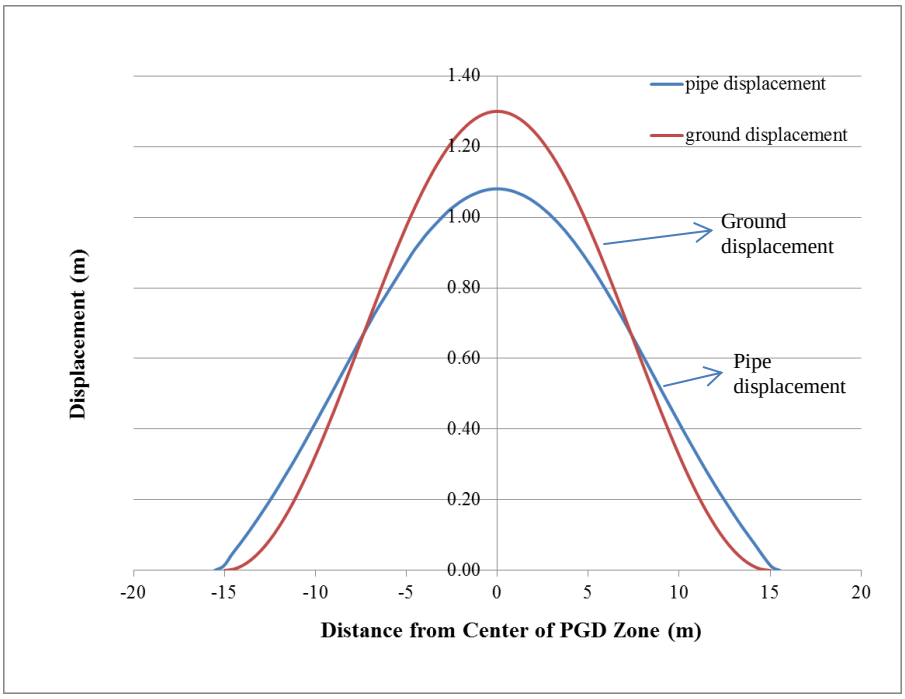

Figure 7.23: Pipe displacement and ground displacement for different width of PGD zone (D=0.61m, 0.008m, δ=1.3m, W=30m, Hc=1.2m, X-70).

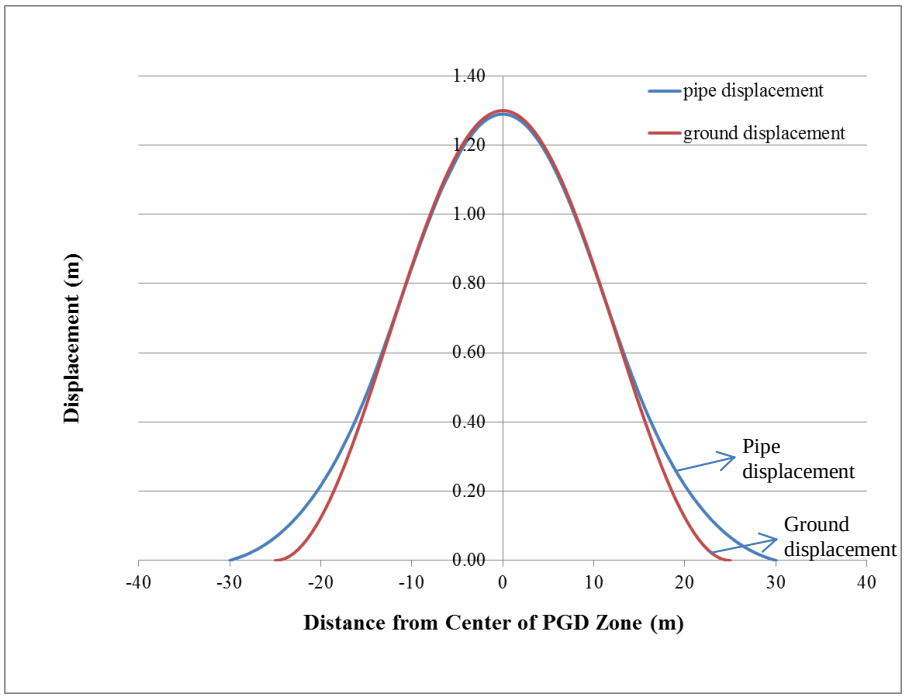

Figure 7.24: Pipe displacement and ground displacement for different width of PGD zone (D=0.61m, 0.008m, δ=1.3m, W=50m, Hc=1.2m, X-70).

The results obtained by finite element analysis correspond to these literature research. When the width of PGD zone increases the pipe starts to behave like a flexible pipe. For narrow PGD zone, the pipe behaves like a rigid pipe.

7.8 Effects of different transverse PGD patterns on behavior of pipeline

Two patterns of transverse PGD are mentioned in chapter 3. These patterns are spatially distributed transverse PGD and localized abrupt PGD. In order to determine the effects of these PGD patterns on continuous pipeline, finite element analysis were performed. In these finite element analysis, the pipe and soil properties are D=0.61m, t=0.0095m, γ_{soil}=18 kN/m^3, ϕ=35^0. The width of the PGD zone (W) is chosen as 30m while the amount of ground movement is chosen as δ=1.3m, δ=3.0m and δ=5.0m, respectively. Figure 7.25 and Figure 7.26 demonstrate the distribution of bending moment and pipe displacement for localized abrupt PGD case. In Figure 7.25, bending pipe moment is essentialy zero over a distance of approximately 10m near the center of PGD zone. The bending pipe moment slightly increases although the ground displacement significantly increases. In Figure 7.26, maximum pipe displacement has a bowl-shaped. When the ground displacement increase the bowl width decreases. For example, the bowl width of pipe displacement is roughly equal to 25m for that ground displacement is equal to 1.3m. On the other hand, the bowl width is approximately equal to 15m for that ground displacement is equal to 5.0m. According to Liu and O'Rourke (1999), continuous pipelines behaves as though it was exposed to two separate fault offsets whose pipe-fault angle is 90.

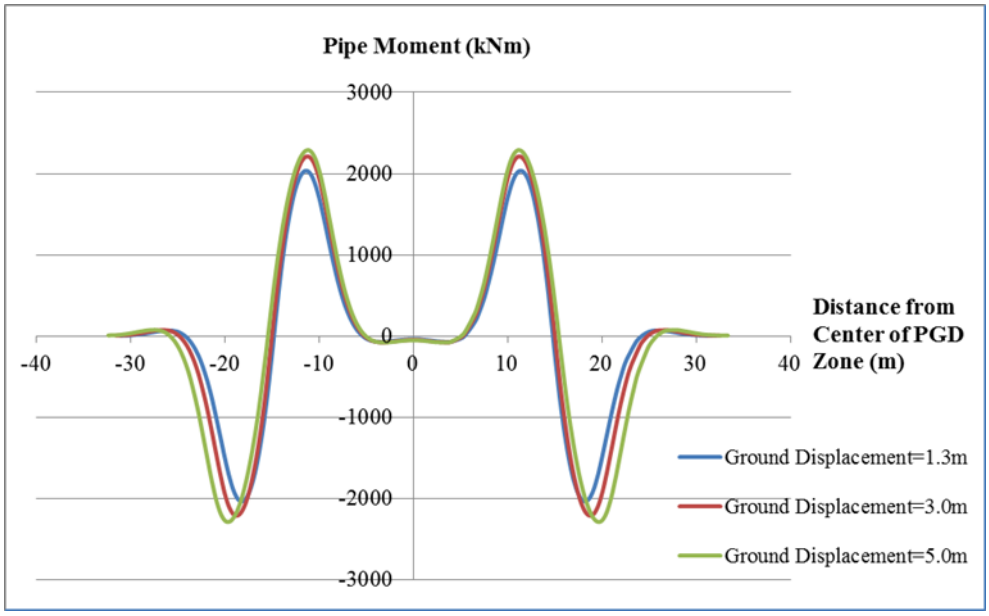

Figure 7.25: Distribution of bending pipe moment.

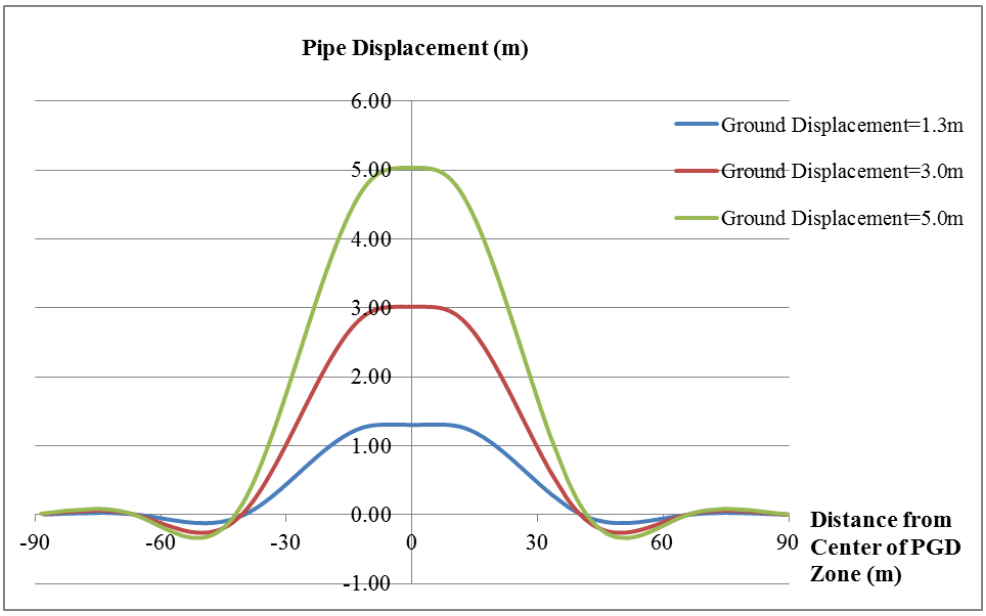

Figure 7.26: Distribution of pipe displacement.

In Figure 7.27 and Figure 7.28 demonstrate the distribution of bending pipe moment and pipe displacement for spatially distributed PGD case. In Figure 7.27, bending pipe moments for all ground displacements reach their maximum values at the center of PGD zone contrary to localized abrupt PGD case. For ground displacement values of 3.0m and 5.0m, the bending moment values are nearly the same. In Figure 7.28, maximum pipe displacements have a curved shape for all ground displacement values.

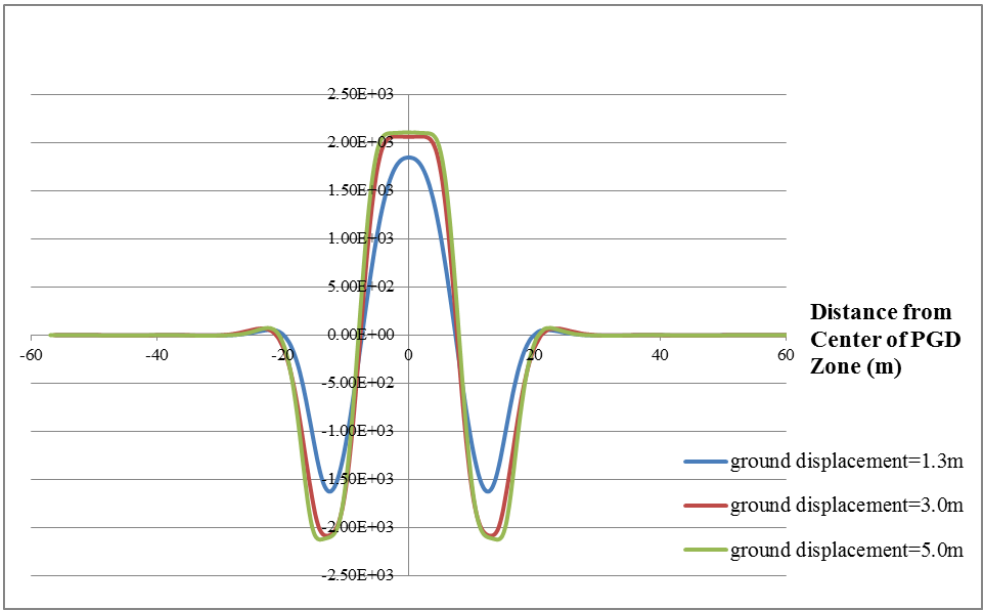

Figure 7.27: Distribution of bending pipe moment.

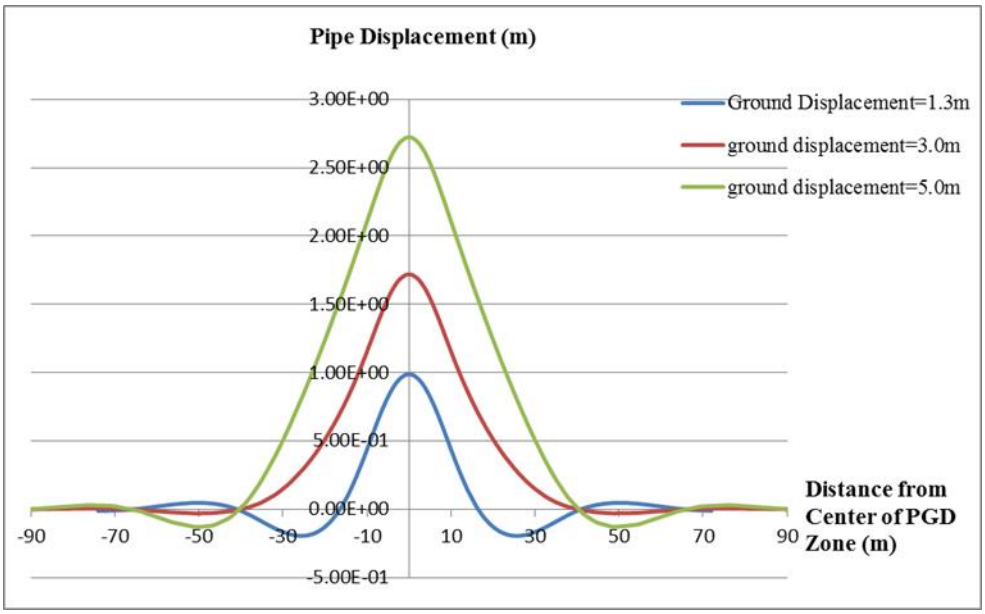

Figure 7. 28: Distribution of pipe displacement.

8. CONCLUSIONS

In this study, finite element analysis were performed to investigate the parameters influencing the behavior of pipeline subjected to transverse permanent ground deformation. For this purpose, a parametric study was carried out by changing parameters such as pipe diameter, wall thickness of pipe, burial depth of pipe, width of PGD zone, PGD patterns, the amount of ground displacement, angle of internal friction of backfill and type of grade steel in finite element model. In consequence of surveying of literature, the pipeline was modeled by using beam element and the interaction between pipeline and soil was modeled with the aid of axial and transverse connector elements. Connector elements simulate the behavior of soil spring elements.

As results of the parametric study, the following subjects were concluded:

- When grades of steel pipe change from X-42 to X-70, the maximum pipe displacement decreases and the pipe moment increases. Therefore, it is concluded that the grades of steel pipe significantly influence the behavior of pipe.
- Since the rigidity of pipe increases due to an increase in wall thickness of pipe, the pipe displacement decreases and pipe moment increases.
- The pipe diameter is one of the profile properties of pipe such as wall thickness. An increase in the pipe diameter contributes to an increase in pipe rigidity. Due to an increase in pipe diameter, the maximum pipe displacement values for different grade steel approach each other. As a result, the types of grade steel have not significant importance with regards to maximum pipe displacement for large pipe diameter. There is parabolic trends between the pipe diameter and pipe moment. Both the maximum pipe moment and the minimum pipe moments increase with the increase in pipe diameter.
- When the amount of transverse permanent ground displacement increases, the maximum pipe displacement also increases. The maximum displacement

values for pipes having large diameters approach each other when the ground displacement increases. Therefore, it can be inferred that the change of ground displacements has more significant influence on maximum pipe displacement than the change of pipe diameter.

- For smaller ground deformation values, the maximum pipe displacements values for different types of grade steel approach each other. Consequently, it can be deduced that the steel grades can be decisive with regards to behavior of pipe for large ground deformations.
- Despite of significant increase in ground displacement maximum and minimum pipe moment does not increase at the same rate. The maximum and minimum pipe moments converge a value that is probably ultimate bending moment of pipe.
- The width of PGD zone has a significant importance on behavior of pipe subjected transverse permanent ground deformation. For a wide width of PGD zone, the pipeline behaves like relatively flexible whereas the pipeline behaves like relatively stiff for a narrow width of the PGD zone.
- The wall thickness of pipe also affects the behavior of pipe subjected to transverse PGD zone. It is observed that the transition from flexible behavior to stiff behavior occurs in the pipe due to the increase of the wall thickness of pipe. On the other hand, the change of pipe behavior is not seen for a width of PGD zone such as 50m although the wall thickness of pipe increases. Therefore, the width of PGD zone has more significant effects on pipe behavior than the wall thickness of pipe.
- The maximum resistance of soil increases with an increase in angle of internal friction. Due to the increase in the maximum resistance of soil, the pipeline begins to behave like relatively flexible.
- The maximum pipe displacement is an increasing function of burial depth of pipe. The maximum pipe moment decreases with an increase in the burial depth. The minimum pipe moment increases with an increase in the burial depth for relatively small ground displacement. The minimum pipe moment remains nearly the same for relatively large ground displacement.

- The behavior of pipeline shows an variation depending on transverse PGD pattern. For spatially distributed PGD, the maximum and minimum pipe moment occurs at the center and margins of PGD zone. On the other hand, the pipe moment at the margins and the center of PGD zone are nearly zero for localized abrupt PGD. The pipeline will have curve-shaped for spatially distributed PGD whereas the pipeline will have a bowl shape for localized abrupt PGD.

8.1 Suggestions for Future Works

In this study, the behavior of pipeline subjected to transverse permanent ground deformation was investigated by differing parameters. The internal forces in pipeline can change depending on the orientation of buried pipelines according to PGD direction . It can be suggested for future works that the behavior of pipeline can be examined based on pipelines according to their orientation. Furthermore, 1D model was used to perform finite element analysis of buried pipelines subjected to transverse permanent ground deformation. In future works, 3D model can be used and the results can be verified with 3D model. As a result, it can be determined whether the usage of 1D model provides reliable results.

REFERENCES

ABAQUS (2012). Getting Started with ABAQUS: Interactive Edition. Version 6.12. Dassault Systèmes Simulia Corp., Providence, RI, USA

ALA (2001). Guideline for the Design of Buried Steel Pipe, ASCE and FEMA

ASCE (1984). Guidelines for the Seismic Design of Oil and Gas Pipeline Systems. Committee on Gas and Liquid Fuel Lifelines of the ASCE Technical Council on Lifeline Earthquake Engineering

Bartlett, S. F., Youd, T. L. (1995). Empirical Prediction of Liquefaction-Induced Lateral Spread, *ASCE Journal of Geotechnical Engineering, **Vol. 121***, No.4

Bartlett, S.F. & Youd, T.L. (1992). Empirical analysis of horizontal ground displacement generated by liquefaction-induced lateral spreads, *Technical Report NCEER-92-0021, National Center for Earthquake Engineering Research*, State University of New York at Buffalo, Buffalo, NY.

Bathe K. J. (1996). Finite Element Procedures.Prentice Hall, Upper Saddle River, New Jersey 07458

Baum, R. L., Galloway, D. L., Harp, E. L. (2008). Landslide and Land Subsidence Hazards to Pipelines, *U.S. Department of the Interior U.S. Geological Survey*, Open-File Report 2008-1164

Beer G. and Watson J.O. (1992). Introduction to Finite and Boundary Element Methods for Engineers

Bray J. D., Rathje E. M., Augello A. J., Merry S. M. (1998). Simplified seismic design procedures for geosynthetic-lined, solid waste landfills. *Geosynthetics International* **5(1–2)**: 203–235

Cai, J., Liu, X., Hou, Z., and Chen, G. (1992). Experimental Research on the Liquefaction Response of Oil Supply Pipeline, *Proceedings of the Second International Symposium on Structural Technique of Pipeline Engineering*, Beijing, pp. 284-291.

Gorbunov-Posadov M. I. And Serebrjanyi, R. V. (1961). Design of structures on elastic foundations, Proc. 5th Int. Conf. Soil Mech. Found. Eng., 643-648.

Hall, W. and Newmark, N. (1977). Seismic Design Criteria for Pipelines and Facilities, *Current State of Knowledge of Lifeline Earthquake Engineering*, ASCE, New York, pp. 18-34.

Hamada, M., Yasuda, S., Isoyama, R., Emoto, K. (1986). Study on liquefaction induced permanent ground displacements, *Association for the Development of Eartquake Prediction in Japan*, Tokyo, Japan

Hamada, M. and O'Rourke, T.D., (1992), Large Ground Deformations and Their Effects on Lifelines, *Japanese Case Studies of Liquefaction and Lifeline Performance During Past Earthquakes, Technical Report NCEER-92-0001, Multidisciplinary Center for Earthquake Engineering Research*, Buffalo, New York.

Hays, W. W. (1981). Facing Geologic and Hydrologic- Hazards Earth Science Considerations, *Geological Survey Professional Paper 1240-B*, U.S. Government Printing Office, Washington, D.C.

Hetenyi, M. (1946). Beams on Elastic Foundations. University of Michigan Press, Ann Arbor, Michigan.

Hou, Z., Cai, J., and Liu, X. (1990). Response Calculation of Oil Pipeline Subjected to Permanent Ground Movement Induced by Soil Liquefaction, *Proceedings of the China-Japan Symposium on Lifeline Earthquake Engineering*, Beijing, China, pp. 107-114.

Jafarzadeh F., Jahromi H.F., Yoosefi S., Sehizadeh M. and Joshaghani M., Alavi M. (2012). Dynamic Response of Buried Gas Pipelines Due to Earthquake Induced Landslides by Nonlinear Numerical Modeling

Jibson, R.W. and Keefer, D.K. (1993). Analysis of the Seismic Origin of Landslides:Examples from the New Madrid Seismic Zone, *Geological Society of America Bulletin*, April, ***Vol. 105***, pp. 521-536.

Jibson, R.W., Harp, E.L., Michael, J.A. (1998). A method for producing digital probabilistic seismic landslide hazard maps: An example from the Los Angeles California area. *US Geol. Surv. Open-File Rep*. ***98-113***. 17 pp.

Karamitros, D. K., Bouckovalas, G. D. and Kouretzis, G. P. (2007). Stress analysis of buried steel pipelines at strike-slip fault crossings, *Soil Dynamics and Earthquake Engineering*, ***27/3***, 200–211.

Keefer, D. K. (1984). Landslides caused by earthquakes, Geological Society of America Bulletin, USA.

Kobayashi, T., Nakane, H., Suzuki, N., and Ishikawa, M. (1989). Parametric Study on Flexibility of Buried Pipeline Subject to Large Ground Displacement, Proceedings of the Second U.S.-Japan Workshop on Liquefaction, Large Ground Deformation and Their Effects on Lifelines, Buffalo, New York, Technical Report NCEER-89-0032, Multidisciplinary Center for Earthquake Engineering Research, Buffalo, New York, pp. 348-362.

Kramer, S. L. (1996). Geotechnical Earthquake Engineering, Prentice Hall International Series in Civil Engineering and Engineering Mechanics, New Jersey.

Lee H. (2010). Finite element analysis of a buried pipeline. *A dissertation submitted to The University of Manchester for the degree of Master of Science. School of Mechanical*, Aerospace and Civil Engineering.

Lim, Y., Kim, M., Kim, T., and Jang, J. (2001). The Behavior Analysis of Buried Pipeline: Considering Longitudinal Permanent Ground Deformation. Pipelines 2001: pp. 1-11.

Liu, X. and O'Rourke, M. (1997b). Behavior of Continuous Pipeline Subject to Transverse PGD, *Journal of Earthquake Engineering and Structural Dynamics*, ***Vol. 26***, pp. 989-1003.

Lo, S. H., Wu, D. and SZE, K. Y. (2010). Adaptive meshing and analysis using transitional quadrilateral and hexahedral elements. *Finite Element in Analysis and Design*, ***46***, 2-16.

Makdisi F, Seed H. (1978). Simplified procedure for estimating dam and embankment earthquake-induced deformations. *Journal of Geotechnical Engineering* ***104(7)*****:** 849–867

Matsumoto, H., Sasaki, Y., and Kondo, M. (1987). Coefficient of Subgrade Reaction on Pile in Liquefied Ground, *Proceedings of the Second National Conference on Soil Mechanics and Foundation Engineering*, pp. 827-828 (in Japanese).

Meyersohn, W.D. (1991). Analytical and Design Considerations for the Seismic Responseof Buried Pipelines, *Thesis*, Graduate School of Cornell University, January

Miyajima, M. and Kitaura, M. (1989). Effects of Liquefaction-Induced Ground Movement on Pipeline, Proceedings of the Second U.S.-Japan Workshop on Liquefaction, Large Ground Deformation and Their Effects on Lifelines, Buffalo, New York, *Technical Report NCEER-89-0032, Multidisciplinary Center for Earthquake Engineering Research*, Buffalo, New York, pp. 386-400.

Newmark, N.M. and Hall, W.J. (1975). Pipeline Design to Resist Large Fault Displacement, *Proceedings of the 1975 U.S. National Conference on Earthquake Engineering*, Ann Arbor, Michigan, pp. 416-425.

O'Rourke, M.J. (1989). Approximate Analysis Procedures for Permanent Ground Deformation Effects on Buried Pipelines, *Proceedings of the Second U.S.-Japan Workshop on Liquefaction, Large Ground Deformation and Their Effects on Lifelines*, Buffalo, New York, Technical Report NCEER-89-0032, Multidisciplinary Center for Earthquake Engineering Research, Buffalo, New York, pp. 336-347.

O'Rourke, M.J., Liu, X. (1999). Response Of Buried Pipelines Subject To Earthquake Effects, *Multidisciplinary Center for Earthquake Engineering Research*, University at Buffalo, Buffalo, New York, p.13.

O'Rourke, M. J., Gadicherla, V., and Abdoun, T. (2003). Centrifuge modeling of buried pipelines, Sixth U.S. *Conference and Workshop on Lifeline Earthquake Engineering*, Long Beach, California.

O'Rourke, T.D. and Tawfik, M.S. (1983). Effects of Lateral Spreading on Buried Pipelines During the 1971 San Fernando Earthquake, Earthquake Behavior and Safety of Oil and Gas Storage Facilities, *Buried Pipelines and Equipment, PVP-77, ASME*, New York, June, pp. 124-132.

O'Rourke, T.D. (1988). Critical Aspects of Soil-Pipeline Interaction for Large Ground Deformation, *Proceedings of the First Japan-U.S. Workshop on Liquefaction, Large Ground Deformation and Their Effects on Lifeline Facilities*, Tokyo, Japan, November, pp. 118-126.

O'Rourke, T.D., Lane, P. A. (1989). Liquefaction hazards and their effects on buried pipelines, *Technical Report NCEER-89-0007, National Center for Earthquake Engineering Research*, Buffalo, New York

O'Rourke, T.D. and Meyersohn, W.D., Shiba, Y., and Chaudhuri, D. (1994), Evaluation of Pile Response to Liquefaction-Induced Lateral Spread, *Proceedings of the Fifth U.S.-Japan Workshop on Earthquake Resistant Design of Lifeline Facilities and Countermeasures Against Soil Liquefaction*, Snowbird, Utah, Technical Report NCEER-94-0026, Multidisciplinary Center for Earthquake Engineering Research, Buffalo, New York, pp. 457-479.

O'Rourke, T.D., Palmer, M.C. (1996). Earthquake performance of gas transmission pipelines, *Earthquake Spectra **20(3)***, 493-527.

Prakash, S. (1981). Soil Dynamics, McGraw-Hill Book Company, USA.

Ramberg W., and Osgood W. R. (1943). Description of stress-strain curves by three parameters. *Technical Note No.902, National Advisory Committee For Aeronautics*, Washington DC.

Suzuki, N. and Masuda, N. (1991). Idealization of Permanent Ground Movement and Strain Estimation of Buried Pipes, *Proceedings of the Third Japan-U.S. Workshop on Earthquake Resistant Design of Lifeline Facilities and Countermeasures for Soil Liquefaction, San Francisco, California, NCEER Report Number 91-0001*, Multidisciplinary Center for Earthquake Engineering Research, Buffalo, New York, pp. 455-469.

Suzuki, H. (1988). Damage to Buried Pipes Caused by Large Ground Displacement, *Proceedings of the First Japan-U.S. Workshop on Liquefaction, Large Ground Deformation and Their Effects on Lifeline Facilities*, Tokyo, Japan, pp. 127-132.

Takada, S., Tanabe, K., Yamajyo, K., and Katagiri, S., (1987). Liquefaction Analysis for Buried Pipelines, *Proceedings of the Third International Conference on Soil Dynamics and Earthquake Engineering*.

Takada, S. (1991). Lifeline Earthquake Engineering, (In Japanese), 241p.

Takada, S., Hassani, N., and Fukudu, K. (2001). A new proposal for simplified design of buried steel pipes crossing active faults, *Earthquake Engineering & Structural Dynamics* ***30(8)***, 1243–1257.

Tanabe, K. (1988). Fundamental Study on Seismic Assessment and Design of Buried Pipelines Subjected to Ground Failure During Earthquake, *Doctoral Dissertation*, Kobe University, 1988 (in Japanese).

Trautmann, C.H. and O'Rourke, T.D. (1983). Load-Displacement Characteristics of a Buried Pipe Affected by Permanent Earthquake Ground Movements, *Earthquake Behavior and Safety of Oil and Gas Storage Facilities, Buried Pipelines and Equipment, PVP-77, ASME*, New York, June, pp. 254-262.

Vazouras, P., Karamanos, S. A. and Dakoulas, P. (2010). Finite element analysis of buried steel pipelines under strike-slip fault displacements. *Soil Dyn. Earthqu. Eng.* ***30:11***, 1361-1376.

Vazouras, P., Karamanos, S. A., and Dakoulas, P. (2012). Mechanical behavior of buried steel pipes crossing active strike-slip faults, *Soil Dynamics and Earthquake Engineering*, ***Vol. 41***, pp. 164–180.

Vesic, A. B. (1961). Beams on an Elastic Subgrade and Winkler's Hypothesis, Proc. 5th Int. Conf. On Soil Mechanic and Foundation Engineering, Paris, pp. 845-850.

Vlasov, V. Z. And Leontiev U. N. (1966). Beams, Plates and Shells on Elastic Foundation. Israel Program for Scientific Translations, Jerusalem.

Wells, D. L., and K. J. Coppersmith (1994). New empirical relationships among magnitude, rupture length, rupture width, rupture area, and surface displacement, *Bull. Seism. Soc. Am.* ***84***, 974-1002.

Wilson, R.C. and Keefer, D.K. (1983). Dynamic Analysis of a Slope Failure from the 6 August 1979 Coyote Lake, California Earthquake, *Bulletin of the Seismological Society of America*, ***Vol. 73***, No. 3, pp. 863-877.

Xie, X., Symans, M.D., O'Rourke, M.J., Abdoun T.H., O'Rourke, T.D., Palmer, M.C., Stewart, H.E. (2011). Numerical Modeling of Buried HDPE

Pipelines Subjected to Strike-Slip Faulting, *Journal of Earthquake Engineering*, ***15:8***, 1273-1296.

Yasuda, S., Saito, K., and Suzuki, N. (1987). Soil Spring Constant on Pipe in Liquefied Ground, *Proceedings of the 19th JSCE Conference on Earthquake Engineering*, pp. 189-192 (in Japanese).

Yeh, Y.H. and Wang, L.R.L. (1985). Combined Effects of Soil Liquefaction and Ground Displacement to Buried Pipelines, *Proceedings of the 1985 Pressure Vessels and Piping Conference - Seismic Performance of Pipelines and Storage Tanks*, PVP-98-4, ASME, pp. 43-52.

Yiğit, A. (2007). Gömülü Boru Hatlarının Deprem Etkilerine Karşı Davranışı, Master Thesis, İstanbul Technical University, June.

Yoshida, T. and Uematsu, M. (1978). Dynamic Behavior of a Pile in Liquefaction Sand, *Proceedings of the Fifth Japan Earthquake Engineering Symposium*, pp. 657-663 (in Japanese).

Yoshizaki, K. and Oguchi, N. (1998). Effect of Strain Rate on Stress/Strain Properties of Gas Pipeline Steel, *Proceedings, 10th Japan Earthquake Engineering Symposium*, Yokohama, Japan, pp. 3171-3174, (in Japanese).

Yoshizaki, K., O'Rourke, T. D. and Hamada, M. (2001). Large Deformation Behavior of Buried Pipelines with Low-angle Elbows Subjected to Permanent Ground Deformation, *Journal of Structural Mechanics and Earthquake Engineering*, ***I-2130***, pp. 41-52.

Yoshizaki and Sakanoue (2004). A Study on Eartquake-Resistant Design for Buried Pipeline Using Lightweight Backfill. *13th World Conference on Earthquake Engineering*, Vancouver, B.C., Canada, August 1-6, 2004, Paper No.2389

Youd, T.L. & Perkins, D.M. (1987). Mapping of liquefaction severity index. *Journal of Geotechnical Engineering, ASCE*, ***113 (11)***, 1374-1392.

CURRICULUM VITAE

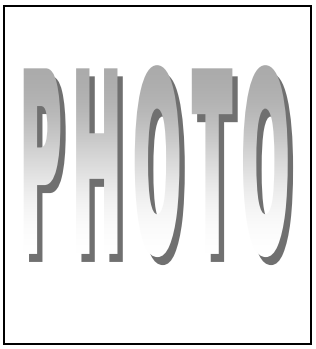

Name Surname: Hasan Emre Demirci

Place and Date of Birth: İzmir, 29.06.1989

Address: Yeşilova Mahallesi 4006 Sokak No:33, Bornova/İzmir

E-Mail: hasandemirci@iyte.edu.tr

B.Sc.: Dokuz Eylül University

List of Publications and Patents:

- **Demirci HE**, Lav MA (2013). Deprem Kaynaklı Şev Deplasmanlarını Hesaplayan Basitleştirilmiş Yöntemlerin İncelenmesi, *Taşkın ve Heyelan Sempozyumu*, Trabzon
- Bakunowicz P, **Demirci HE**, Egeli I. (2014). FEM Analysis with special focus on Soil-Structure Interaction of Floating Slab Track Infrastructure in High Speed Railway Embankments, *3rd International Conference on Road and Rail Infrastructure*, Split, Crotia.
- **Demirci HE**, Lav MA, Gedikli A, Yiğit A. (2014). Yanal Kalıcı Zemin Deformasyonuna Maruz Gömülü Boru Davranışının Sonlu Elemanlar Yöntemi ile İncelenmesi, *Zemin Mekaniği ve Temel Mühendisliği 2. Özel Konulu Sempozyumu*, Antalya.
- Ecemis N, **Demirci HE**, Karaman M (2014). Effects of relative density and coefficient of consolidation on re-liquefaction potential of sand, Second European Conference on Earthquake Engineering and Seismology, Istanbul.